# Development of Pre-Vascularized Tissues Containing Aligned and Perfusable Microvessels

A Dissertation
SUBMITTED TO THE FACULTY OF
UNIVERSITY OF MINNESOTA
BY

Sonja Belgrade Riemenschneider

IN PARTIAL FULFILLMENT OF THE REQUIREMENTS
FOR THE DEGREE OF
DOCTOR OF PHILOSOPHY

Robert T. Tranquillo, Advisor

May 2016

# Acknowledgements

I am humbled by the outpouring of support, guidance, and encouragement I have received in the pursuit of my PhD. To those that have offered words of encouragement, commiseration, and the occasional dose of reality, I want you to know how important our conversations were. You kept my spirits up when I felt the odds against me.

This PhD research would not have been possible without the guidance and support of my advisor, Bob Tranquillo. Thank you for giving me the opportunity to work on such a novel and exciting project. I greatly appreciate all that you have taught me over the past several years and I am humbled by your unwavering optimism for the next experiment even when everything is going wrong.

I would also like to thank my funding sources for providing the resources needed to accomplish this goal. Thank you to the National Institute of Health for the R01 used to fund the majority of this work. Also, thanks to the Chemical Engineering and Materials Science Department for two years of graduate fellowships and the Biotechnology Training Grant for two years of trainee funding and educational opportunities.

A huge thank you is owed to all of the senior Tranquillo lab members who have taught me everything from cell culture to immunohistochemistry to bioreactor design. I would especially like to thank Krissy Morin, the previous microvascular tissue guru, for all that she taught me and all that she did to ensure I was prepared to tackle this project.

Not one experiment in my PhD research was an individual effort. I owe all of my fellow lab members a big thank you for their help in the completion if this PhD research. I would especially like to thank Jackie Wendel and Jeremy Schaefer, my fellow “heart patch” teammates, for all of their hard work with the microvascular implant study. I still cannot believe how many forms you must have filled out to keep my experiments by-the-book, or how many times you had to administer meds to keep my animals pain-free and healthy. We won’t even talk about how many “last surgery” days we had. Thank you to the excellent surgeons I had the chance to work with, Lei Ye and Pilar Guzman. I truly could not have done it all without your help and you deserve all of the thanks I can give. A big thanks also goes out to Zeeshan Syedain for all of the times I went to him with a problem and he always had a solution. You are a true engineer, and I know you’ll do great things.

Thank you to all of the support staff in the lab. Naomi Ferguson, thank you for keeping the lab running smoothly and for helping with cell culture as my

experiments became too complicated to handle by myself. Pat Schaeffer and Susan Saunders, thank you for the hundreds (thousands?) of sections and slides and your help with staining all of those hearts. Sandy Johnson, thank you for your technical expertise and guidance in helping me troubleshoot my experiments over the years.

I have been lucky enough to work with and mentor several talented and dedicated undergraduate students, and without their help, I would not be where I am today. Paul Carlson, Ian Pierson, and Abi Field, it was my pleasure working with you I truly appreciate all of your hard work. Jake Siebert deserves special thanks for taking on one of the most daunting image quantification jobs out there during his first month, and as a freshman in the lab, and tackling it with skill and ease. You've come so far and learned so much this past year, from learning to make microvascular tissues to designing your own perfusion bioreactor. I have no doubt you will make an excellent researcher and I thank you for all of your hard work and contributions to this research. Special thanks also goes out to Donald Mattia, who worked alongside me for two years and whose efforts led to a pre-clinical study and a co-authored paper found in this manuscript (Chapter 2). I feel incredibly lucky to have had the opportunity to work with you and I cannot thank you enough for all of your contributions, many of which have found their way into this dissertation in a not-so-small way.

To my pups, Lily, Char Bar, Hali, and Little Bear, thank you for your companionship and the reminder that sometimes there are more important things in life, like food, walks, snuggles, and ice cream.

To my mom, dad, and sister, I cannot thank you enough for all of the support and encouragement, the phone calls, the dinners, and the much-needed wine deliveries. You have given me the strength and confidence I needed to achieve this goal. Thank you is not enough, and I could never have done it without you.

To my husband, Garren, you have been there by my side through it all. From helping me work up the courage to hit “send” on my grad school applications, to helping me practice my prelims presentation, to helping me operate my perfusion pump on the weekends when I didn’t have enough hands, all the way through reading every last word of this dissertation - you have been there for me every step of the way. Thank you for being my champion in times of celebration and for being my support in times of hardship. Your unwavering support has meant the world to me.

# Dedication

This thesis is dedicated to my husband, my family, and my friends who have supported me in this endeavor. Thank you for believing in me.

# Abstract

The single greatest restraint in tissue engineering is the inability to create and perfuse functional microvasculature in dense engineered tissues of physiological stiffness. Without active delivery of nutrients and oxygen, tissue size is diffusion-limited to thicknesses of around 400 μm, or much less for highly metabolic tissues. Thus, the creation of pre-vascularized tissues that have a high density of organized microvessels that could be perfused is a major goal of tissue engineering. The present work makes significant advances toward this goal. Tissue patches containing a high density of human microvessels that were either randomly oriented or aligned were placed acutely on rat hearts post-infarction and in both cases, inosculation occurred and perfusion of the transplanted human microvessels was maintained, proving the *in vivo* vascularization potential of these engineered tissues. *In vitro*, a high-throughput assay was developed to investigate optimal conditions for angiogenic sprouting, vasculogenic microvascular network formation, and inosculation of the sprouts and microvessels in 3D fibrin gels. Samples loaded with vascular endothelial growth factor and fibroblast growth factor exhibited enhanced angiogenic sprouting, and a hybrid medium culture regimen resulted in enhanced sprouting, well-developed microvascular networks, and inosculation of the microvessels and sprouts. These results showed potential for the *in vitro* perfusion of larger-scale microvascular

tissues. An engineering strategy was developed to perfuse endothelialized microchannels that could form sprouts into fibrin gels containing a microvascular network. An *in vitro* perfusion bioreactor was designed and tested that enabled these microvascular tissues to be cultured, compacted, and aligned to form a dense network of microvessels that also contained perfusable microchannels with sprouts. Different microchannel seeding regimens and perfusion regimens were applied and it was determined which conditions ultimately led to microchannel endothelialization, sprouting, perfusion, and maintenance during gel compaction. While inosculation and perfusion of the microvessels has yet to be achieved, this work presents the building blocks for a potential strategy that could ultimately enable the perfusion of a dense, aligned microvascular network through anastomoses of sprouts and microvessels. Achievement of this goal would unlock a number of tissue engineering opportunities in the development of large engineered tissues for regenerative therapies.

# Table of Contents

# List of Tables

# List of Figures

# Chapter 1. Introduction

The largest restraint in the field of tissue engineering is the complete lack of robust methods for developing functional microvasculature that can be perfused *in vitro* and support transplanted tissue survival *in vivo*.[1–4] Non-vascularized engineered tissues are restricted by oxygen diffusion limits that cannot keep up with consumption rates of highly metabolic cells. This limits the development of functional native-like tissues to thicknesses of approximately 400 µm or less, restricting clinical tissue engineering applications to skin and other very thin tissues.[5] Native myocardium, the most oxygen-demanding tissue in the body, is supplied by approximately 2,000 capillaries per square millimeter in humans with a distance between capillaries of around 20 µm.[6] These capillaries supply all of the oxygen and nutrients needed for survival by the cardiomyocytes and other cells found in the myocardium.[7] For an engineered tissue to meet the demands of cardiac or other highly metabolic tissues, the incorporation of a microvascular network to deliver oxygen and nutrients will be critical, and unless the microvascular network can be perfused *in vitro,* the potential for engineered tissues such as these is severely limited.

### 1.1 Microvascular network formation

The formation of microvascular networks has been studied to great length.[8–14] When endothelial cells (ECs) are entrapped in a 3D extra-cellular matrix (ECM), ECs will self-assemble into a network and intracellular vacuole formation and coalescence will result in the formation of a continuous lumen.[8,12,15] This occurs without need to pattern or direct the network morphology, though network properties can be tuned by altering the chemical or physical stimuli presented to the cells.[16–18] Capillary-like microvascular networks can be self-assembled *in vitro* in a variety of 3D matrices.

#### 1.1.1 Microvessel assembly in vitro

There are three basic approaches to creating microvessels *in vitro*. The first is via the patterning of ECM to create microchannels that can be lined with ECs to create endothelialized microchannels. This method is relatively simple in execution, allows for geometric control over the network morphology, and enables easy connection to flow circuits. However, it does not allow for the creation of capillary-sized microvessels. These microchannels are on the order of 100 - 500 µm in diameter,[19,20] and are thus, not considered true capillary networks, which have capillary diameters on the order of 10 µm.[6]

The second approach to creating microvessels involves angiogenic sprouting from an endothelialized surface. Angiogenesis is the sprouting of a new

vessel from an existing one. In the angiogenic approach, new capillaries are formed via sprouting from an existing vessel or channel that is lined with ECs. With this approach, the network morphology is not patterned or fabricated (with the exception of the larger-diameter parent vessel), but instead it is determined by the self-assembly of the ECs, with the resulting sprouts and microvessels having capillary-like diameters.[17]

The third approach to creating *in vitro* microvessels involves vasculogenic tubulogenesis. Vasculogenesis is the de novo formation of microvessels from randomly dispersed ECs. With this method, ECs are entrapped in a 3D matrix and the cells spread and connect, forming a network.[17] The cells then form vacuoles that merge and span across multiple cells to form a continuous tubular network.[15]

### 1.1.2 Endothelial cell sources

In choosing an EC type for the development of engineered microvascular networks for potential therapies, it is important to consider autologous sources, when possible, and critical to use human cells. However, many studies are still using human umbilical vein endothelial cells (HUVECs),[21–23] a non-autologous source, as they are a readily available and well-characterized EC. There are several potential autologous EC sources including embryonic derived stem cell endothelial cells (which have ethical issues to consider and are rarely used in

microvascular tissue engineering), induced pluripotent stem cell endothelial cells (iPS ECs), adipose-derived stem cell endothelial cells[24], endothelial progenitor cells (EPCs)[9], and blood outgrowth endothelial cells (BOECs)[25], to name a few. While other labs have had success with iPS ECs[26], this work will focus on BOECs for the formation of microvascular networks due to their high proliferative potential, autologous nature, and availability. Although both BOECs and EPCs are derived from circulating cells, BOECs, unlike EPCs, exhibit a late-stage phenotype, and are characterized by expression of VE-cadherin, flk-1, vWF, CD36, and CD14 (negative), all markers for mature endothelial cell phenotype. BOECs are isolated and expanded through collaboration with Robert Hebbel from the University of Minnesota.[25]

### 1.1.3 Support cells

Capillaries, *in vivo,* are supported by pericytes (PCs), a perivascular cell type that extends cytoplasmic processes along the outer surface of capillaries.[27] PCs are known to play a role in vascular stability, and interactions between ECs and PCs play a role in maturation, remodeling, and maintenance of the microvasculature.[28,29] These functions involve the secretion of growth factors and remodeling of the surrounding ECM.[27] Not surprisingly, PCs do an excellent job of stabilizing engineered microvessels *in vitro* as well, by encouraging basement membrane deposition and preventing regression of the microvessels over

time.[30–32] PCs also have the potential to be an autologous source, as they can be harvested from the skin.[33]

Some studies have also shown success using non-pericyte cells such as bone marrow-derived mesenchymal stem cells,[21,34,35] adipose-derived stem cells,[34–36] and fibroblasts[37,38] as support cells for engineered microvascular networks, but the work presented here will focus on pericytes, obtained from the laboratory of George Davis (University of Missouri).[12]

### 1.1.4 Matrices for engineered microvasculature

Matrices used for EC tube formation include collagen I, fibrin, Matrigel™, and a variety of poly(ethylene) glycol or poly(L-lactic acid)/poly(DL-lactic-co-glycolic acid) hydrogels.[1] Collagen I and fibrin are known to be pro-morphogenic stimulators for vasculogenesis in 3D matrices.[8] Collagen I gels have been used in a variety of vasculogenic studies.[13,39,40]

Fibrin has been established as one of the primary matrices used for the construction of microvascular tissues.[8,17] Fibrin gel is used extensively in the Tranquillo lab for engineered tissues[41–47] and is known to stimulate tissue growth, encourage collagen deposition (more so than in collagen gels), and can be compacted by cellular traction forces to increase the density of engineered tissues.[30] It is known to retain growth factors added into the gel formulation, and release them over a several day period.[48] The work presented here will use fibrin

for its greater potential in the creation of dense, cell-remodeled tissues and it's pro-vasculogenic properties.

### 1.2 Microvascular tissue engineering

Microvascular tissue engineering is a rapidly growing field, with many researchers creating microvessels and microvascular networks in 3D matrices in the lab for the study of disease, the testing of drugs, and the development of engineered tissues for regenerative therapies.

#### 1.2.1 Engineered microvascular networks in vitro

Current techniques in the development of engineered microvasculature generally follow one of two paths. The first path involves lining pre-fabricated channels with endothelial cells (ECs).[49,50] Advantages to this method are that it is simple to connect the channels to fluid flow, and that many pre-determined channel patterns can be used. However, it is impossible to fabricate channels at physiologically relevant dimensions for capillaries, and the appropriate microvascular patterning must be determined.

The second path involves exposing cells to stimuli and inducing EC morphogenesis to form a capillary network. While this method is physiologically complex, the technical aspects are relatively straightforward because the microvascular network morphology is entirely determined by the cells. The two

main approaches for inducing capillary network formation use either angiogenic or vasculogenic engineering strategies. When an angiogenic approach is used for *in vitro* formation of engineered microvasculature, ECs sprout into a gel from either an EC monolayer on the surface of the gel or from entrapped endothelialized beads. In the gel (typically collagen or fibrin), they proliferate, migrate, and form capillary networks.[16,37,51–56] With vasculogenic strategies ECs and, often, support cells such as pericytes or fibroblasts, are entrapped in collagen or fibrin gels and the cells self-assemble into a microvascular network.[5,30–32,57–60] In this proposed work, a combination of all of the described techniques will be employed.

### 1.2.2 Pre-vascularized engineered tissues in vivo

There is a great need for engineered vascular tissue that can be rapidly perfused following implantation and can sustain a high density of metabolically active cells. Applications, such as for engineered cardiac or liver tissue, especially depend on a dense network of perfusable microvessels for survival. While recruitment of host vessels via angiogenesis to the transplanted patch is a common method for vascularizing state-of-the-art cardiac patches,[41,46] this method only works for thin tissues that are already within the diffusion limits. For thicker, more functionally relevant tissues to survive transplantation, a perfusable microvascular network must be co-transplanted with the cardiomyocytes.

A few groups have made initial advances in the implantation of pre-vascularized engineered tissues in animals.[21,38,40,61–63] These tissues all contain self-assembled microvessels cultured *in vitro*, and then implanted *in vivo* to determine their potential to be perfused. An example of such advances is the implantation of pre-cultured human microvessels into the subcutaneous space of immune-compromised mice.[38] These microvessels inosculated with the host and were perfused as early as 1 day. A more recent study implanted pre-vasularized tissues into dorsal window chambers in mice and visualized anastomosis with host vessels after 2-6 days with subsequent thrombosis, and then later, re-perfusion of some of the microvessels.[40]

While these results demonstrate the advances and challenges in the field, their applications are limited. In order to truly test the vascularization potential of microvascular engineered tissues, they must be transplanted into the target environment, which is often infarcted or diseased, rather than the highly vascularized subcutaneous environment used in previous studies. Only then, can the results indicate the potential for future tissue engineering therapies.

### 1.2.3 Need for in vitro perfusion

While the *in vivo* perfusion of microvascular tissues is critical to the viability of transplanted engineered tissues, their *in vitro* perfusion is, perhaps, even more crucial. In order to create dense, highly metabolic engineered tissues

in the lab, they will need to begin as large-volume gels that are later compacted and remodeled to form a dense, organized, functional tissue. This requires both engineering manipulations as well as time to allow cells to remodel the ECM. In order to keep the cells alive during *in vitro* culture, they will need a microcirculation to perfuse the culture medium and growth factors necessary for tissue development.

While larger diameter vessels or endothelialized channels may suffice for low-density tissues, the presence of a microvascular network will become more and more important as these tissues compact. This is because capillaries have a larger surface area to blood-volume ratio, and are able to be packed more densely and deliver nutrients more efficiently. Ideally, microvascular tissues would integrate higher-order vessels and capillary-like microvessels for efficient perfusion and ease of connection to flow of blood or culture medium.

*In vitro* perfusion of tissues containing microvascular networks would also help prime the microvessels for flow prior to implantation. By having a functional, perfusable network at the time of implantation, the time between inosculation and complete tissue perfusion could be greatly reduced. It is even possible that early thrombosis, which has been shown to occur with transplanted pre-vascularized tissues[40], could be avoided by *in vitro* perfusion prior to implantation.

### 1.2.4 Microfluidic perfusion of engineered microvessels

Despite the urgent need for large-scale, perfusable microvascular tissues, no one has been able to achieve *in vitro* perfusion of microvascular engineered tissues. Perfusion of microvascular networks in low-density hydrogels, however, has been accomplished using microfluidic devices. Microvessel perfusion in microfluidic devices has been motivated by a need for more efficient drug screening as well as the need for more accurate vasculogenesis models for the study of microcirculatory diseases and cancer.

Microfluidics have the advantage of enabling the establishment of complex microenvironments by precisely regulating both chemical and mechanical stimuli. These platforms typically seed ECs in microfluidic channels containing pores leading to 3D micro-tissues, where ECs and a support cell type are entrapped and self-assemble into a microvascular network. Interstitial flow through the micro-tissue encourages sprouting from the endothelialized channel through the pore and anastomosis with the microvascular network in the 3D micro-tissue.[5,18,23,26,64–68]

The laboratory of Steven George (University of Washington, St. Louis) has reported *in vitro* perfusion of engineered microvascular networks[5] and their efforts have continued to demonstrate the consistency of these systems for their ability to create perfusable microvascular tissues.[59,64,69] This research platform,

with collaboration from Chris Hughes (University of California, Irvine), is using these techniques for the development of organ-on-a-chip models and studies of tumor microvasculature perfusion, and recently demonstrating the ability to perfuse these 3D microvessel networks without leakage between the endothelialized channel and the microvascular network.[66]

Other groups, such as the laboratory of Roger Kamm (Massachusetts Institute of Technology) are also making major strides in the *in vitro* perfusion of microvascular tissues, also using microfluidic platforms. Their design of a modular microfluidic system used alginate beads to serve as carriers for potential co-culture cell-types and demonstrated perfusion of microvessels by directing angiogenic sprouting and subsequent inosculation.[18] Their recent studies have validated the use of human iPS ECs for their ability to be perfused in microfluidic platforms.[26]

### 1.2.5 Scale up from microfluidic devices to perfusing microvascular engineered tissues

Although significant advances have been made in the field of microvascular tissue engineering, they have many limitations. Most of the methods for creating self-assembled engineered microvasculature use very small volumes of highly porous gel. Without increasing the tissue density, these constructs lack the necessary stiffness to be implanted *in vivo*.[70] They also fall

short of obtaining capillary densities comparable to native tissues.[6] Successful *in vitro* perfusion of engineered microvessels has exclusively been in microfluidic platforms rather than an environment suitable for culturing engineered tissues of a clinically relevant size and stiffness.[5] These shortcomings of the current state-of-the-art strategies limit their use in tissue engineering.

The ability to create perfusable microvessels in engineered tissue would revolutionize the field, unlocking opportunities for the design and fabrication of much larger tissues or organs. In this work, engineered microvascular tissues were designed, developed, and tested for their ability to function as pre-vascularized tissues that could be perfused *in vitro* or implanted and perfused *in vivo*. These studies evaluate the potential of tissue engineering strategies to create dense, functional microvascular tissues that could ultimately support the culture and transplantation of other highly metabolic cell types, such as cardiomyocytes, with cell densities similar to native myocardium.

# Chapter 2. Inosculation and Perfusion of Pre-Vascularized Tissue Patches Containing Aligned Human Microvessels after Myocardial Infarction

Reprinted with permission: Riemenschneider et al. *Biomaterials,* 97**,** 2016.

## 2.1 Introduction

The creation of engineered tissues containing microvascular networks that can be rapidly perfused within a few days following implantation remains a major goal of tissue engineering.[1,3] Applications that involve highly metabolic tissues, such as myocardium and liver, are especially dependent on the presence of a rapidly perfusable microvascular network to prevent the formation of a necrotic core beyond the diffusion limit in the implanted tissue.[4,71,72] Recruitment of vasculature via angiogenesis is a common method for vascularizing tissue engineered constructs *in vivo*, but this vascularization strategy is too slow to permit the survival of thick, highly metabolic tissues.[3] Implantation of tissues with pre-formed microvascular networks could enable rapid perfusion of thick engineered tissues by inosculation of the implanted microvessels with adjacent host blood vessels.

Many examples of creating “engineered microvessels” exist,[5,13,14,16,43,73] and many groups are striving to create functional microvessel patches in

macroscopic, implantable materials.[9,21,38,43,61,74–76] The most impressive of these studies demonstrate that implantation of pre-cultured human microvessels in immune-compromised mice can result in inosculation with the host vasculature and perfusion of the human microvessels.[21,38,61] However, these studies were carried out in the healthy subcutaneous environment, and no study has implanted pre-cultured human microvessels in the especially challenging myocardial infarct environment. With the ultimate goal of treating myocardial infarctions and heart disease with a perfusable, beating cardiac patch containing both microvessels and cardiomyocytes, the only fair way to assess the vascularization potential of a precursor patch containing only microvessels would be to implant it at the site of a myocardial infarction. This way, the insights gained from such a study could be leveraged in the future development of a patch that also contained cardiomyocytes.

Many studies in rodents have administered tissue-engineered heart patches onto myocardial infarcts containing various cell types,[41,46,77] but implantation of human microvessels has not yet been reported. The Okano Group has shown that thin microvascular cardiac patches made from neonatal rat cardiomyocytes and rat endothelial cells can be perfused by the host and result in improved cardiac function after 4 weeks.[62] In our lab's prior studies we have implanted heart patches made from either neonatal rat heart isolates or

human induced pluripotent stem cell derived cardiomyocytes co-entrapped with human pericytes. These heart patches were made in fibrin gel and cultured for 1-2 weeks to align the cells and fibrin. In both studies, the patches had no microvessels at the time of implantation, yet we observed perfused host-derived capillaries invading the patch as early as 1 week.[41,46] These results suggest the possibility that a similar patch that contained pre-formed human microvessels could rapidly inosculate with the invading host vessels and be perfused within 1 week.

The microvessel density and organization also needs to be addressed. In tissues that require efficient perfusion, the capillaries are generally highly organized in microvascular beds, with many capillaries spanning across the same arteriole and venule. In myocardium, the capillaries are not only very dense, but they are also aligned.[6,78,79] Therefore, emulating these two features in the engineered microvessels of a heart patch is highly desirable. Previous studies of pre-vascularized engineered tissues do not control microvessel alignment, nor do they achieve lumen densities within the same order of magnitude as native adult myocardium (2,000 lumens/mm$^2$)[6,78]. To date, reports of pre-implant cross-sectional lumen density range from fewer than 200 lumens/mm$^2$ up to 650 lumens/mm$^2$, the latter of which was reported by our lab.[43,54,80–82]

A necessity for a heart patch that would aim to restore mechanical function would be rapid connection to blood flow to maintain viability of the large number and high density of transplanted cardiomyocytes in a thick tissue-like patch. Ideally, this would be achieved by implanting a cardiomyocyte patch containing a pre-formed, perfusable microvascular network that could rapidly anastomose with the host and maintain perfusion. As a step toward that goal, the present study sought to determine the rapid vascularization potential of a remodeled fibrin patch containing either an aligned or randomly oriented microvascular network, but no cardiomyocytes, implanted onto a myocardial infarction for 6 days.

In this study we investigated the rapid *in vivo* vascularization potential of tissue patches pre-vascularized with either aligned or non-aligned human microvessels and implanted over myocardial infarcts. Patches containing human microvessels, were made by entrapping human blood outgrowth endothelial cells (BOECs)[25] and human pericytes (PCs) in fibrin gel, and allowing self-assembly of a microvascular network of tubules. Patches with aligned human BOEC/PC microvessels ("aligned microvessel patches") were anchored at both ends by porous plastic spacers, and aligned via cell-induced gel compaction, as previously described.[74] Briefly, as the samples compact laterally and remain constrained in the longitudinal direction by the spacers, the fibrils, cells, and the

formed microvessels become aligned in the longitudinal direction. To investigate the effects of a patch lacking microvessels, patches made in a similar manner with only aligned PCs (“aligned PC patches”) were also investigated. Patches with non-aligned microvessels (“isotropic microvessel patches”) were made by maintaining gel adhesion to the bottom surface of the culture plate and preventing lateral compaction and longitudinal alignment.

The patches were sutured onto the infarcted region of the heart of nude rats immediately following LAD ligation, as we previously described for heart patches containing cardiomyocytes,[41,46] and were implanted for 6 days. Perfusion of the patches was evaluated with species-specific endothelial-binding fluorescent labels injected into the left ventricle to circulate throughout the bloodstream prior to sacrifice. Immunohistochemistry on histological sections from explanted hearts was used to quantify the total number of human vessels in the patches. Aligned microvessel patches were predicted to have a greater number of perfused vessels after 6 days and isotropic microvessel patches were predicted to have some perfused vessels, but less than the aligned microvessel patches. Aligned PC patches were expected to recruit some host-derived microvessels by 6 days, but the total number of perfused microvessels (human + rat) was expected to be much lower than in the pre-vascularized patches.

While we did not expect these patches to have an effect on cardiac function or infarct size, as they were lacking cardiomyocytes, ejection fraction and fractional shortening were measured before implantation and at sacrifice to ensure any changes were recorded. The infarct was characterized by measuring the percent of the left ventricular wall occupied by scar as well as the left ventricular wall thickness.

## 2.2 Methods

### 2.2.1 Culture of human blood outgrowth endothelial cells and human pericytes

Human BOECs were isolated from adult peripheral blood by the lab of Dr. Robert Hebbel at the University of Minnesota – Twin Cities[25]. Briefly, BOECs were screened for VE-cadherin, flk-1, vWF, CD36, and CD14 (negative). Passage 5 BOECs were thawed and plated on 0.05 mg/ml collagen I – coated flasks in BOEC medium (EGM-2 bulletkit medium (Lonza) supplemented with 10% FBS, 1% penicillin/streptomycin (Gibco)). Medium was changed every other day and BOECs were passaged after 4 days, then plated and cultured for 4 more days prior to harvest.

Human brain vascular PCs (ScienCell, fetal, characterized by immunofluorescence with antibody specific to α-smooth muscle actin) were transduced to express GFP and obtained from the lab of Dr. George Davis at the

University of Missouri. Passage 6 PCs were thawed and plated on 1 mg/ml gelatin-coated flasks in PC medium (13% FBS, 1% penicillin/streptomycin (Gibco), 10 ng/ml gentamicin (Gibco) in low-glucose DMEM (Lonza)). Medium was changed every 2-3 days and PCs were harvested after 10 days.

### 2.2.2 Creation of aligned microvessel patches

Rectangular molds (18.4 mm x 5 mm) were created by melting ridges into the bottom of a 6 well tissue culture plate. Porous polyethylene spacers (5 mm x 5 mm) were placed on top of a dollop of sterile vacuum grease at both ends of the rectangular mold leaving a central rectangular well (8.4 mm x 5 mm). Droplets of fibrin gel solution containing BOECs and PCs were pipetted onto the edge of the two spacers and dragged toward the center to fill the central rectangular well (Figure 2-1A). This ensures that the gel is integrated with the porous spacers and is anchored in place. The gel solution was made up of 2.55 mg/ml fibrinogen (Sigma), 200 ng/ml of stem cell factor (SCF), interleukin-3 (IL-3), and stromal derived factor 1α (SDF-1α) (R&D Systems), $2x10^6$ BOECs per mL and $0.4x10^6$ PCs per mL, 1.25 U/ml thrombin (Sigma) and Medium 199 basal medium (Gibco) (M199). The total volume of each gel was 112 µl. Samples were incubated at 37°C, 5% $CO_2$ for 20 min before adding BOEC medium. Medium was replaced after 1, 3, 5, and 7 days. In these samples, a microvascular network of tubules self-assembles and PCs are recruited to the abluminal side of

the vessels after 5 days of *in vitro* culture.[43] We will hereafter refer to these structures as microvessels and microvascular networks.

After 5 days of culture, samples were detached from the bottom surface of the tissue culture plastic by sliding the spacers along the bottom back and forth. To re-anchor the spacers, samples suspended between the two spacers were carefully transferred to a new well by picking up the spacers and placing them on fresh droplets of sterile vacuum grease. Spacers were re-anchored the same distance apart to maintain a constant sample length. The samples were then free to compact laterally via cell-induced compaction (Figure 2-1B). It has been shown that lateral compaction causes alignment of the microvessels and fibrin fibrils in the longitudinal direction.[74] Aligned microvessel patches were harvested after 8 or 9 days for implantation.

### 2.2.3 Creation of aligned PC patches

Aligned PC patches were created identically to the aligned microvessel patches with the exception that the BOEC cell suspension volume was replaced by M199 (Gibco). PC density was identical to BOEC/PC patches to maintain similar levels of paracrine factors released by the PCs in the patch.

### 2.2.4 Creation of isotropic microvessel patches

Isotropic microvessel patches were included in the study to assess the importance of vessel alignment in achieving perfusion of pre-formed vessels *in vivo*. Isotropic patches were designed to maintain similar size and identical cell loading as aligned microvessel tissue patches. Maintaining the same length (8.4 mm) ensured that the patches spanned the infarct region. Isotropic patches were implanted as a single patch, while aligned patches were implanted as three parallel strips, thus the isotropic patches were made to contain 3 times the cell number as the aligned patches. The minimum width that would hold the required volume without spilling the gel-forming solution was 7 mm. In this way the cell content was identical between the isotropic and aligned microvessel patch groups, while the patch area was marginally different (50.4 $mm^2$ for three aligned microvessel patches vs 58.8 $mm^2$ for a single isotropic microvessel patch).

Rectangular wells (8.4 mm x 7 mm) were created by melting ridges into the bottom of a 6 well tissue culture plate (Figure 2-1C). Fibrin gel-forming solution identical to the aligned microvessel patch formulation (but triple the volume - 336 µl) was pipetted carefully to fill the rectangular well without spilling outside the ridges. Samples were left to gel in the cell culture hood untouched for 15 min due to their precariously high liquid height, then transferred to the incubator at 37°C, 5% $CO_2$ for 15 min to complete the gelation process. Once

gelation was complete, BOEC medium was added to cover the samples. Medium was replaced after 1, 3, 5, and 7 days. Samples remained adhered to the bottom culture surface throughout the culture period to prevent compaction-induced alignment. The resulting isotropic microvessel patches were harvested after 8 or 9 days for implantation.

### 2.2.5 Patch Characterization

Patches not implanted (at least 6 per group) were harvested after 8 or 9 days of *in vitro* culture and fixed with 4% paraformaldehyde (PFA) (Electron Microscopy Sciences) for 10 min at room temperature, then rinsed in phosphate buffered saline (PBS) (Corning). Samples were cut in half longitudinally and one half was reserved for histology and the other was saved for whole-tissue immunofluorescence staining.

Whole-tissue samples were blocked in 5% Normal Donkey Serum (Jackson Immunoresearch) for 2 hours, then incubated in 1:40 antibody to human CD31 (hCD31) (Dako) in blocking serum for one hour. Three 5 min PBS rinses were performed, then the samples were incubated in 1:200 donkey anti-mouse secondary antibody conjugated with Alexa Fluor® 594 (Jackson Immunoresearch) in PBS for 1 hour. After secondary antibody incubation, samples were incubated in 1:10,000 Hoescht 33342 (Invitrogen) in PBS for 10 min, followed by two 5 min rinses in PBS. All steps were performed at room

temperature on an orbital shaker. Whole-stained patches were visualized with confocal microscopy (Zeiss LSM 510) and three random fields of view from were captured for each sample to assess microvessel alignment, microvascular network length, network connectivity, and PC recruitment and alignment.

For each image, the angle and length of each microvessel segment was measured in Fiji and exported to Excel. Total network length was calculated by taking the sum of all vessel segment lengths for each image and dividing by the area in the field of view. Microvessel alignment was verified by calculating an anisotropy index. The x and y components of each vessel segment were calculated according to the angle and segment length, with x being the longitudinal direction. The anisotropy index was calculated by dividing the sum of the x components by the sum of the y components for each image. Alignment of the PC patches was quantified using a similar method, except rather than measuring microvessel segments, individual PCs were measured by drawing line segments along the major axis of each cell. An anisotropy index of 1 indicated random orientations of cells or microvessels and values increasing from 1 indicated vessels and PCs that were more strongly aligned in the longitudinal direction.

Samples reserved for histology were placed in infiltration solution 1 (30% w/V sucrose in PBS) at 4°C overnight and then transferred to infiltration solution

2 (50% infiltration solution 1, 50% embedding medium (Tissue-Tek OCT)) at room temperature for 4 hours. Samples were then frozen in embedding medium and cross sections were cut by cryosectioning 9 µm thick cross-sections for immunohistochemical staining, as is common-practice for measuring lumen density in aligned tissues. Sections were stained for hCD31 similarly to the whole-tissue samples except incubation steps were not performed on an orbital shaker. hCD31 stained cross-sections were viewed with confocal fluorescence microscopy and three random fields of view were captured for each sample. Lumen density was assessed by manual counting and lumen diameters were measured manually in ImageJ based on hCD31 staining. PC recruitment was assessed by counting the number of PCs in contact with hCD31+ cells and dividing by the total number of PCs in each image.

Patch width was determined from photographs taken prior to harvesting the samples and thickness was measured from histological sections. The fibrin concentration at harvest was estimated by simplifying the patch shape to be two side-by-side trapezoids with constant thickness and calculating the fibrin concentration based on the volume reduction from the initial gel formulation. This estimate assumes no degradation of fibrin occurred over the 8-9 days of *in vitro* culture.

### 2.2.6 Experimental Design

Four groups were evaluated in this study: 1. MI + aligned microvessel patch (n=6), 2. MI + isotropic microvessel patch (n=6), 3. MI + aligned PC patch (n=5), and 4. MI only (n=6). Patches were applied on the left ventricle below the ligation suture immediately after ligation in patch groups, while MI only received no other treatment. The aligned microvessel patch contained a dense network of aligned microvessels to serve as the predicted optimal treatment group. The isotropic microvessel patch functioned to evaluate the importance of microvessel alignment in a pre-vascularized heart patch. The aligned PC patch functioned as a non-vascularized control patch. Since cell-mediated gel contraction is essential for remodeling the fibrin gels during *in vitro* culture, an acellular control patch was not tested because a cell-free fibrin patch could not be made with physical properties similar to cell-containing gels.

### 2.2.7 Implantation of patches into an acute nude rat infarct model

Procedures used in this study were reviewed and approved by the Institutional Animal Care and Use Committee (Protocol ID:1501-32275A) and Research Animal Resources at the University of Minnesota and conform to NIH guidelines for care and use of laboratory animals.

Twenty-three female Foxn1rnu nude rats (Harlan Sprague-Dawley) were used in this study, aged 6-8 weeks old and weighing 150-200 g. Isofluorane was

administered for anesthesia, and rats were intubated prior to surgery. Depth of anesthesia was monitored throughout the surgery by pinching the toe and tail of the animals. The chest wall and pericardium was opened to expose the heart, and the LAD was permanently ligated to achieve an MI. Once an MI was established, either an aligned microvessel patch, an isotropic microvessel patch, or an aligned PC patch was applied for the three treatment groups. Aligned patches were cut free from the porous polyethylene spacers and three patches were sutured parallel to each other over the epicardial surface of the left ventricle below the ligation suture, approximately parallel to the alignment of the surface myocardium and covering the width of the infarct (Figure 2-1D), similar to our previous studies.[41,46] Isotropic patches were detached by sliding a spatula between the tissue and the bottom culture surface to free the tissue. A single isotropic patch was placed over the epicardial surface in the same location as the aligned patches. Once the patch was sutured in place, the chest was closed and the animal was allowed to recover. Ketoprofen (2.5mg/kg, Pfizer) and Enrofloxacin (15mg/kg, Bayer) were administered to the rats daily for 3 days.

### 2.2.8 Cardiac Functional Measurements and Perfusion Assessment

Both prior to the initial surgery and 6 days post-implantation, echocardiography (Vevo2100) was performed on the animals to assess left ventricular ejection fraction and fractional shortening. During each session, at

least two measurements were recorded for both short and long axis views. After echocardiography was performed on day 6, isofluorane was administered for anesthesia, and the chest was re-opened. Immediately prior to sacrifice, rhodamine-conjugated ulex europaeus agglutinin – I (UEA-I) (Vector Laboratories) and fluorescein conjugated griffonia simplicifolia lectin I, isolectin B4 (IB4) (Vector Laboratories), endothelial labels for human and rodent, respectively, were injected directly into the chamber of the left ventricle at a dose of 1.2 µg/g body weight. Blood was allowed to circulate for 1-2 min, then the animal was euthanized via a potassium chloride intracardiac injection and the heart was removed for characterization.

### 2.2.9 Histological Assessment

Upon explant, hearts were rinsed in PBS for 5-15 min, then cut in two pieces by making a transverse cut below the ligation suture. The two pieces were transferred to 4% PFA for overnight fixation at 4°C on an orbital shaker. After fixing, the hearts were rinsed 3 times for 15 min in PBS on an orbital shaker. Then another parallel cut was made half-way between the apex and the first cut, resulting in three total transverse sections from each heart. Sections were placed in infiltration solution 1 for 24 hours, then infiltration solution 2 for 48 hours at 4°C on an orbital shaker. Heart pieces were then frozen in embedding medium and

cryosectioned in 9 µm sections for immunohistochemistry and histological analysis.

### 2.2.10 Infarct Assessment

Masson's trichrome stain was applied to transverse heart cryosections to evaluate infarct size and left ventricular (LV) wall thickness for three different regions of the heart. The three regions were approximately: below the ligation suture, half-way between the ligation suture and the apex, and near the apex. Infarct size was calculated by averaging the percentage of the LV free wall area occupied by scar. LV wall thickness was calculated by averaging three measurements of the thickness of the LV wall in infarcted regions of three sections from different regions of the heart. When all three trichrome-stained heart sections showed no evidence of infarction, the animal was excluded from the study.

### 2.2.11 Perfusion Analysis

Heart cryosections were stained for hCD31 to visualize human vessels in the explanted patches. Images of the patch region were captured with confocal fluorescence microscopy using sequential excitation to avoid crossover from multiple wavelength excitation. Nuclei (labeled with Hoescht 33342, 405 nm excitation), PCs (expressing GFP, 488 nm excitation), perfused rat vessels (labeled *in vivo* with IB4, 488 nm excitation**)**, perfused human vessels (labeled *in*

*vivo* with UEA-I, 561 nm excitation), and all human vessels, perfused and non-perfused (labeled with hCD31, 633 nm excitation), were visualized. The number of UEA-I positive vessels and hCD31 positive vessels were counted manually from 40x images captured from at least 10 random locations within the patch. GFP PCs and IB4+ rat vessels (both viewed in the green channel) were differentiated by morphology. When looking at cross sections, a PC that was wrapped fully around a human vessel sometimes looked like a lumen, so green lumen-like structures were considered recruited PCs if the interior of the green lumen contained hCD31 positive staining and all other green lumens were considered rat vessels. Green structures that did not contain a lumen were considered PCs. Lumen diameters were also measured from these images, as described previously. Sections were also stained with hematoxylin and eosin (H&E) and separately, an antibody for rat red blood cells (RBC) (Rockland) to confirm perfusion of human vessels in the patches.

### 2.2.12 Statistical Analysis

Data are represented as a mean ± standard deviation. Students t-tests were performed in Excel. Multiple groups were compared with 1-way analysis of variance (ANOVA) with Games-Howell post-hoc tests in Minitab. P-values $< 0.05$ were considered significant.

## 2.3 Results

### 2.3.1 In Vitro Characterization of Patches

Aligned patches compacted vertically throughout the culture period and compacted laterally once they were detached from the bottom culture surface after 5 days of culture. Isotropic patches were left constrained by the bottom culture surface throughout the culture period, thus they only underwent vertical compaction (Figure 2-1C). The final patch dimensions and their estimated fibrin concentrations are summarized in Table 1.

Aligned microvessel patches contained a dense network of longitudinally aligned microvessels with PCs recruited to the abluminal side of the microvessels (Figure 2-2). Isotropic microvessel patches formed a network of microvessels with recruited PCs, but showed no alignment. Aligned PC patches contained elongated PCs aligned in the longitudinal direction.

Image analysis of CD31 stained non-implanted tissue patches (Figure 2-2) revealed that the aligned microvessel patches contained 940±240 lumens/mm$^2$. In comparison, isotropic microvessel patches had a reduced lumen density of 420±140 lumens/mm$^2$. Similarly, network length for the aligned microvessel patches was higher at 33±6 mm/mm$^2$ versus 16±4 mm/mm$^2$ for the isotropic patches. The percent of PCs recruited to the abluminal side of the vessels was not different, at 77±10% versus 75±9%. The anisotropy index, a measure of the

alignment of the microvessels or PCs (random = 1, aligned > 1), was different for each group. The anisotropy index for aligned microvessel, isotropic microvessel, and aligned PC patches was 3.1±0.8, 1.0±0.2, and 5.0±2.0, respectively.

### 2.3.2 Patch Engraftment and Alignment

All patches remained located on the epicardial surface of the left ventricle after the 6 day implantation period, covering all or a portion of the infarct (Figure 2-3D). No evidence of a necrotic core was found in any of the patch groups, which all showed uniform cell density throughout the patch thickness (Figure 2-3A-C). Generally, human vessels near the edges of the patch appeared to have a higher prevalence of perfusion, from visual inspection, but perfusion also occurred in the center region. The thickness of the explanted patches were 410 ± 120 μm for aligned microvessel, 400 ± 140 μm for isotropic microvessel, and 360 ± 90 μm for aligned PC. Trichrome staining showed a mix of fibrin (red) and collagen (blue), and a cell-dense, collagenous interface between the patch and the myocardium (Figure 2-3E). Subsequent immunohistochemical analysis revealed many rat vessels spanning this interface between the patch and myocardium. Aligned patches maintained their alignment after 6 days implantation, while isotropic patches remained isotropic (Figure 2-3F-H).

### 2.3.3 Microvessel Characterization and Perfusion Assessment

Total human vessels remaining in the patch after 6 days implantation were counted from hCD31 stained sections (Figure 2-4). Aligned microvessel patches contained 435 ± 98 human vessel lumens/mm$^2$ and isotropic microvessel patches contained 374 ± 98 human vessel lumens/mm$^2$. Due to the oblique sectioning angle with respect to the alignment of the patch microvessels (a necessity for obtaining transverse heart sections), the apparent lumen density of the aligned microvessel patches was reduced compared to *in vitro* sectioning and characterization (Figure 2-5). Also, explanted patches could not be distinguished by eye from the surrounding tissues, thus the precise position of the patch at explant was uncertain, and oblique sectioning would have been unavoidable in any case.

The perfused human and rat endothelial labels, UEA-I and IB4, were used to quantify perfused human and rat vessels in the patch. Aligned microvessel patches contained 173 ± 97 perfused human vessel lumens/mm$^2$, meaning 40 ± 23% of the human vessels were perfused. Isotropic microvessel patches contained 111 ± 75 perfused human vessel lumens/mm$^2$, meaning 30 ± 18% of the human vessels were perfused. No differences in total vessel density, perfused vessel density, or perfused fraction were found between aligned and isotropic microvessel patches. Aligned PC patches were perfused by invading rat

vessels (92 ± 80 rat vessels/mm$^2$), as were the other two patch groups to a similar extent.

Inosculation of the human microvessels with rat vessels was visualized in several histological sections as lumens stained for UEA-I that connected with lumens stained for IB4, primarily near the patch-heart interface (Figure 2-4B). Sections stained for rat RBCs (Figure 2-4C) as well as H&E (Figure 2-4D) confirmed perfusion by visualizing RBCs in lumens, providing further evidence of patch microvessel perfusion and inosculation with the host.

Lumen diameters for aligned and isotropic microvessel patches were found to be in the 5-10 µm range of normal human capillaries[6,78,79] both before and after implantation with a small increase in mean diameter from 6 µm to 8 µm observed for aligned patches (Figure 2-6)**.**

### 2.3.4 Infarct Histology Assessment

Infarct size, defined as the percentage of the LV free wall area occupied by scar (averaged from three different regions of the heart), was evaluated for each patch group as well as the MI only control (Figure 2-7D). Infarct sizes for the three treatment groups were, on average, smaller than the MI only control, but none of the comparisons were statistically different. Similarly, the LV wall thickness for the treatment groups were not statistically different from the MI only

control, except for the isotropic microvessel group, which showed less thinning of the LV wall compared to the MI only control (Figure 2-7E).

### 2.3.5 Cardiac Function Measurements

Ejection fraction and fractional shortening measurements from baseline and day 6 echocardiography showed a decrease in ejection fraction and fractional shortening at 6 days compared to baseline measurements prior to MI (Figure 2-7B,C). While the average ejection fraction and fractional shortening values were approximately 10% higher for the three treatment groups, no statistical differences were observed.

## 2.4 Discussion

This is the first report of pre-formed human microvessels being implanted and perfused in a myocardial infarct model. This is a challenging environment for cell survival, but despite the challenging infarct environment, both the aligned and isotropic microvessel patches demonstrated a high degree of perfusion of human microvessels after 6 days of implantation. The results from these precursor microvessel patches highlight the potential for future pre-vascularized cardiomyocyte patches to be rapidly perfused after implantation onto a myocardial infarct.

To the best of our knowledge,[18,43,61] the aligned microvessel patches used in this study contained the highest reported density of microvessel lumens achieved for engineered tissues *in vitro* (940±240 lumens/mm$^2$). Perfused lumen densities at explant were comparable to high reports for pre-formed engineered microvessels[23,38,83], yet they are the highest among aligned pre-formed microvessels. With a lumen density well above that of human skeletal muscle[84] and half the density of human adult cardiac muscle, the most capillary-dense tissue in the body, these pre-vascularized tissue patches could be translated to a wide variety of clinical applications with the addition of therapeutic cells. Our ability to create either aligned or isotropic microvascular networks and tune the alignment of these microvessel patches (shown in previous studies[74]) makes them especially versatile.

Explanted patches maintained a high density of human vessels with physiological lumen diameters. The high degree of PC recruitment to the vessels *in vitro* likely helped maintain them for 6 days *in vivo*, as PCs enhance microvessel stability.[28] The vessel alignment in the aligned patches was also preserved *in vivo*, indicating these patches presented a robust template to maintain alignment upon remodeling. It should be noted that lumen densities for explanted aligned microvessel patches are lower than the pre-implant measurements, while the isotropic microvessel patches had no change in lumen

density pre- and post-implantation. It is likely that most, if not all, of the reduction seen in the aligned patches is an artifact of sectioning at an oblique angle, rather than orthogonal to the alignment direction, as was done for *in vitro* characterization and as is common-practice in the field. This would cause fewer vessels with wider-appearing lumens to be presented per unit area for the aligned patches, but would cause no change for the isotropic patches due to the random orientation of the microvessels (Figure 2-5). In addition to the reduction due to oblique sectioning, it is possible that some lumens collapsed or vessels regressed during the implantation period.

The majority of vessels present in the patches after 6 days implantation were human, with a small fraction of them being from the host (Figure 2-4E). None of the patches had formed a necrotic core after 6 days of implantation, including the aligned PC patches, which were also invaded by vessels from the host. It is not entirely surprising that the aligned PC patches lacked a necrotic core, as the patches used in this study were relatively thin and they did not contain a highly metabolic cell type such as cardiomyocytes, which would likely have had greater oxygen and nutrient demands. Human vessels, evidenced by hCD31 staining, were found to be uniform in density for both the aligned and isotropic patches. Perfusion of the human vessels, on the other hand, was more pronounced near the patch-host interface. This suggests that there were

disconnected vessel networks present in the patches, and only those that inosculated with the host vessels were perfused. Greater perfusion efficiency could potentially be achieved with longer implantation time or by pre-conditioning these patches with flow[43] to promote greater network connectivity.

While no perfusion benefit was observed for aligned microvessel patches, it is possible that a longer implant duration would reveal differences in remodeling and perfusion efficiency. It is also possible that with the high density of microvessels in both aligned and isotropic patches, the improved efficiency that might come from an aligned microvessel network was unnecessary for meeting the metabolic demands of the patch and therefore, was not observed. If this was the case, the benefits of alignment could be elucidated with the addition of a highly metabolic cell type, such as cardiomyocytes.

The implantation of a microvascular patch for 6 days had no effect on the ejection fraction, fractional shortening, or infarct size, confirming our expectation that a microvessel patch lacking cardiomyocytes would not be efficacious itself. Several studies have shown that the transplantation of cardiomyocyte patches can improve cardiac function after a myocardial infarction.[22,41,62] Rather than serving a therapeutic role, the microvessel patches in the present study could be combined with a cardiomyocyte patch to provide rapid blood flow to the

implanted heart patch. This could allow for the implantation of larger patches and higher numbers of cardiomyocytes.

The perfusion of these engineered tissue patches containing aligned human microvessels is promising for the future of tissue engineering, especially in the creation of highly metabolic tissue constructs. The next step would be to integrate these aligned patches with a third cell type, such as cardiomyocytes, to create pre-vascularized heart patches. Even more, these patches would greatly benefit from the development of a hierarchical vascular network containing microvessels, such as those created in this study, connected to larger diameter arteriole and venule-like engineered vessels. The addition of larger diameter vessels integrated within the microvessel patches would allow for direct microsurgical attachment to host vasculature and therefore, immediate perfusion.

These pre-vascularized aligned tissue patches, which contained the highest reported density of engineered microvessels at implantation, inosculated with host vessels and were perfused within 6 days of implantation on the epicardial surface post-infarction. In this study we report the highest perfused lumen density of aligned pre-vascularized microvessels, with no difference in the percentage of human microvessels that were perfused for the aligned versus isotropic patches at this early time point. The rapid inosculation and perfusion of these aligned, pre-vascularized tissue patches containing capillary-size

microvessels is a major step forward toward the goal of creating a thick, beating heart patch that mimics native anatomical structure and can sustain high metabolic demand.

## 2.5 Tables

| Patch | Length (mm) | Width (mm) | Thickness (mm) | Est. [Fibrin] (mg/ml) |
|---|---|---|---|---|
| Aligned Microvessel | 8.4* | 1.6 ± 0.4 | 0.31 ± 0.08 | 33 |
| Aligned PC | 8.4* | 2.2 ± 0.3 | 0.38 ± 0.12 | 24 |
| Isotropic Microvessel | 8.4* | 7* | 0.39 ± 0.12 | 36 |

*These dimensions were constrained

**Table 2-1.** Patch dimensions before implant, and their estimated fibrin concentration.

* indicates a constrained direction. Data represented as mean ± standard deviation. Student's t-test comparing aligned microvessel and aligned PC patches revealed no difference in width (aligned microvessel patch n = 31, aligned PC patch n = 40), 1-way ANOVA among all patch groups revealed no differences in thickness ($p > 0.05$) (aligned microvessel patch n = 18, isotropic microvessel patch n = 9, aligned PC patch n = 14).

## 2.6 Figures

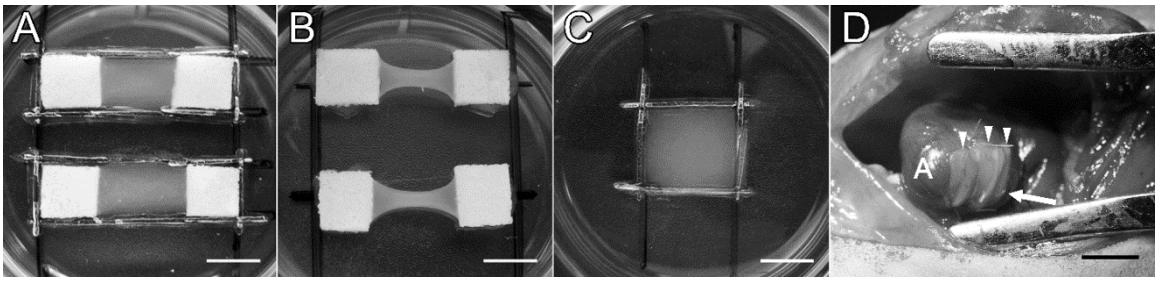


**Figure 2-1.** Patch Alignment and Implantation.

A. Aligned patch before compaction and alignment and B. after compaction and alignment. C. An isotropic patch that was restricted from compacting laterally. D. Implantation of aligned patches onto the infarcted region of the left ventricle. Arrow = LAD ligation suture, arrowheads = patch, A = apex. Scale bar = 5 mm.

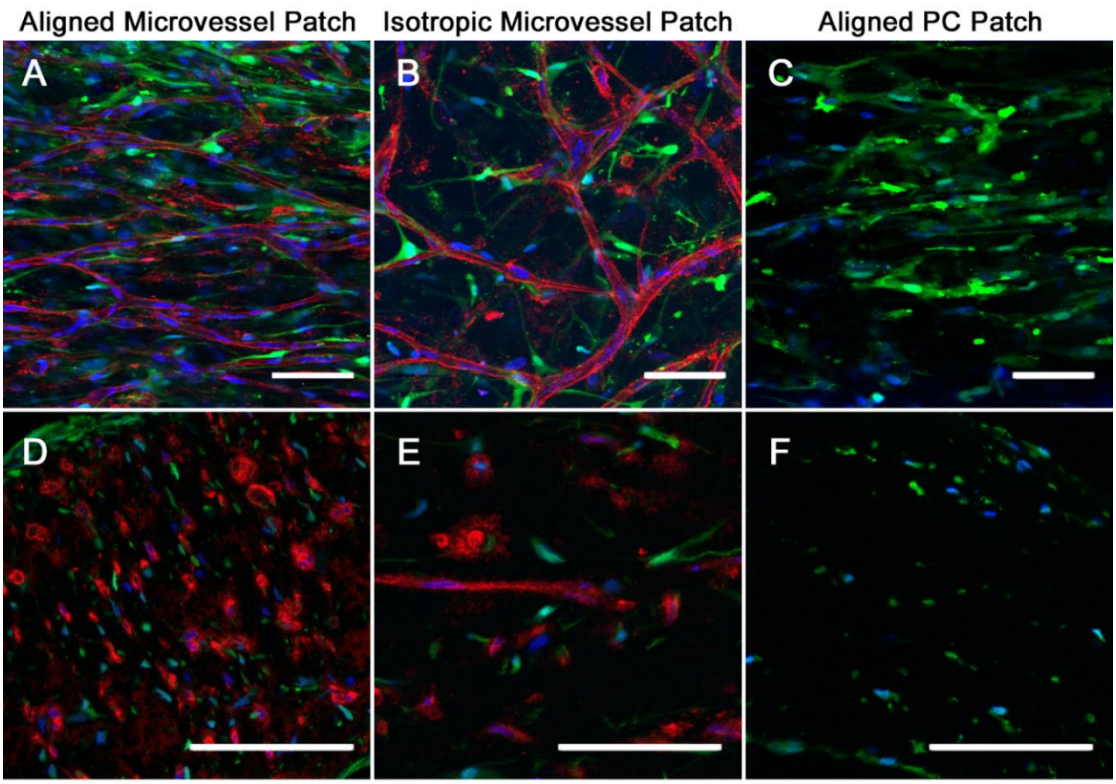
Aligned Microvessel Patch
Isotropic Microvessel Patch
Aligned PC Patch
A
B
C
D
E
F

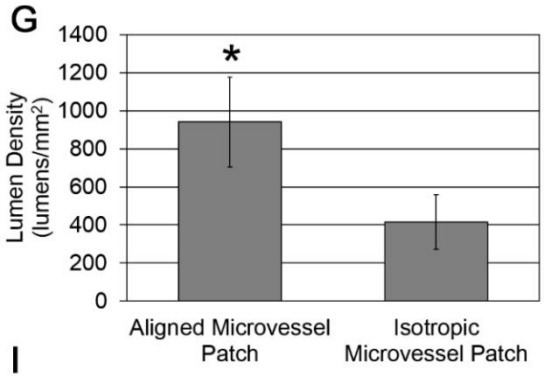
G
Lumen Density (lumens/mm²)
1400
1200
1000
800
600
400
200
0
*
Aligned Microvessel Patch
Isotropic Microvessel Patch

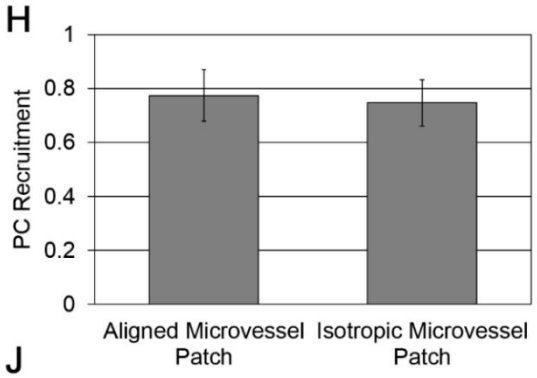
H
PC Recruitment
1
0.8
0.6
0.4
0.2
0
Aligned Microvessel Patch
Isotropic Microvessel Patch

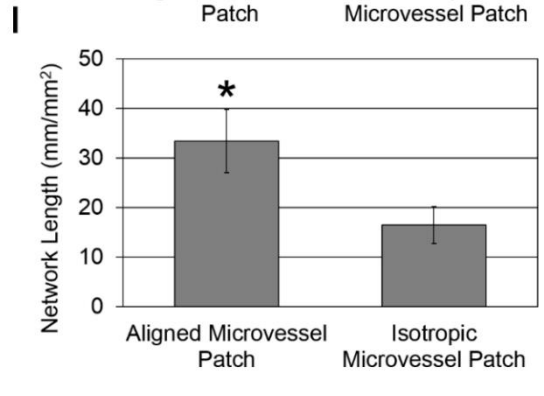
I
Network Length (mm/mm²)
50
40
30
20
10
0
*
Aligned Microvessel Patch
Isotropic Microvessel Patch

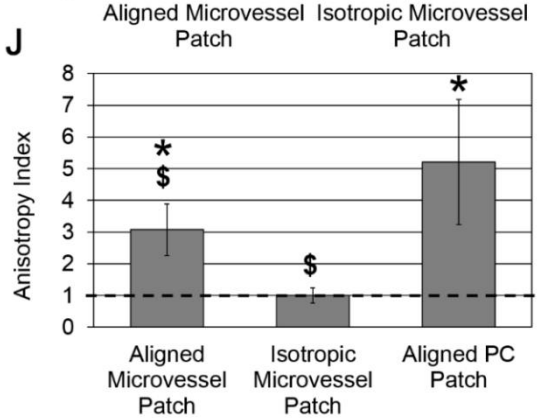
J
Anisotropy Index
8
7
6
5
4
3
2
1
0
*
$
$
*
Aligned Microvessel Patch
Isotropic Microvessel Patch
Aligned PC Patch

**Figure 2-2.** Pre-Implant Patch Characterization.

Top-down view of an A. aligned microvessel patch (n=14), B. isotropic microvessel patch (n=6), and C. aligned PC patch (n=12) via confocal microscopy. D. Cryosection orthogonal to the longitudinal direction for an aligned microvessel patch, E. isotropic microvessel patch, F. aligned PC patch. Red-hCD31, green-GFP transduced PCs, blue-Hoescht-labelled nuclei, scale bar = 100 µm. G. Lumen density of patches measured from histological cross-sections, H. PC Recruitment, or fraction of PCs in contact with vessels, I. Network length, or the sum of the vessel lengths per $mm^2$, J. Anisotropy index, a measure of the degree of alignment with a value of 1 being isotropic (dashed line). Data represented as the mean ± standard deviation. * indicates a difference from isotropic microvessel patch, $ indicates a difference from aligned PC patch, $p<0.05$, student's t-test (G-I), 1-way ANOVA + Games-Howell post hoc test (J).

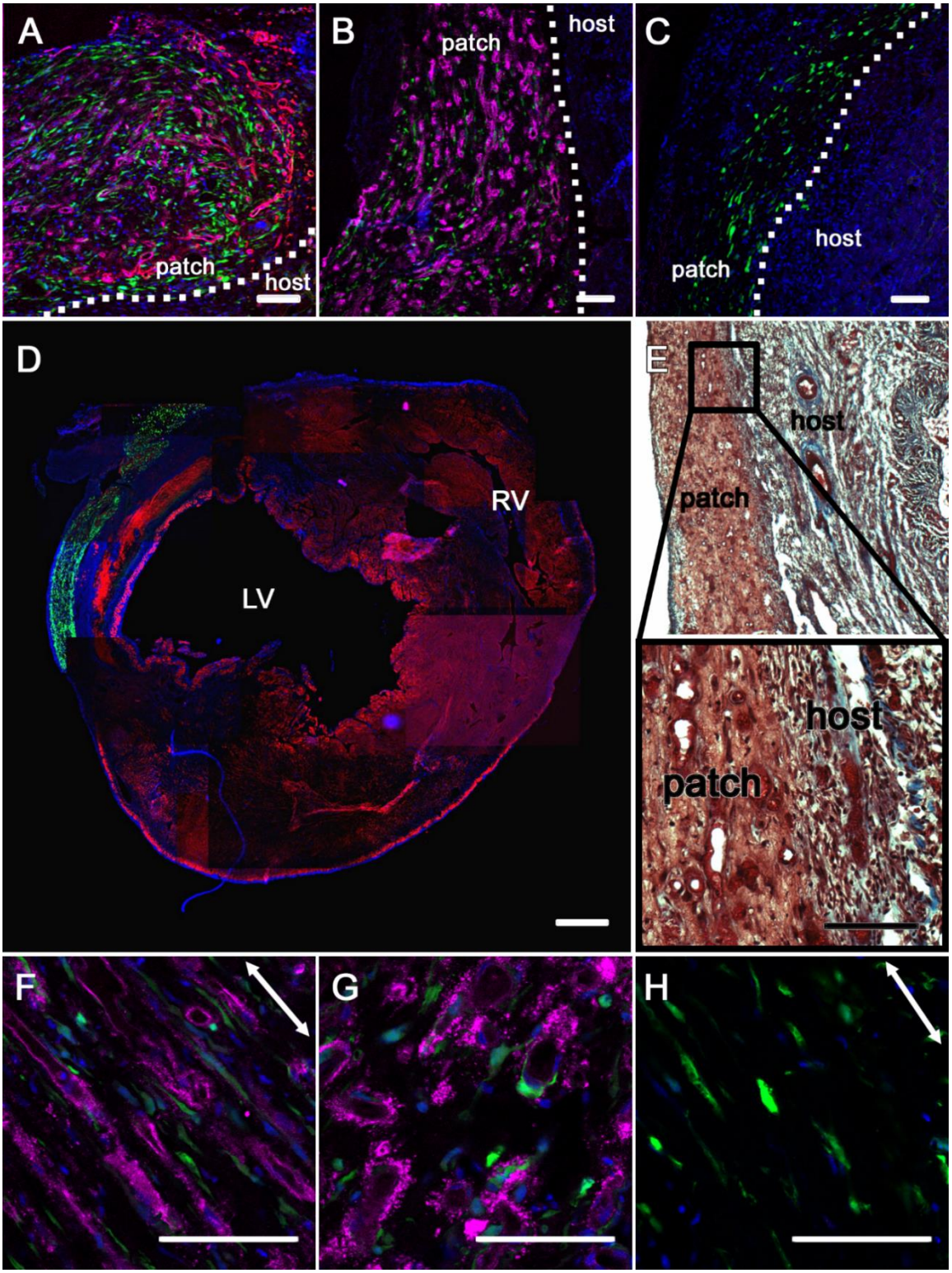
A
patch
host
B
patch
host
C
host
patch
D
RV
LV
E
host
patch
host
patch
F
G
H

**Figure 2-3.** Patch Cellularity and Organization.

Patches engrafted with the host and maintained a high density of human microvessels and PCs throughout the patch thickness for all treatment groups. A. An aligned microvessel patch (n=6), B. an isotropic microvessel patch (n=6), and C. an aligned PC patch (n=5) all showing uniform cell density throughout the patches. A. shows increased perfusion of human microvessels near the edge of the patch. Red-UEA-1 human perfusion label, magenta-hCD31, green-GFP-PCs or IB4 rat perfusion label, blue-Hoescht, scale bar = 100 µm. D. A heart section stained for cardiac troponin T (red), imaged and stitched together. GFP-PCs mark the patch location. LV = left ventricle, RV = right ventricle, scale bar = 500 µm. E. Trichrome stain showing an isotropic microvessel patch and the cell-dense collagenous interface between the patch and the myocardium. F. Patch alignment 6 days post-implant for aligned microvessel patch, G. isotropic microvessel patch, and H. aligned PC patch. Double arrows indicate alignment direction, scale bar = 100 µm.

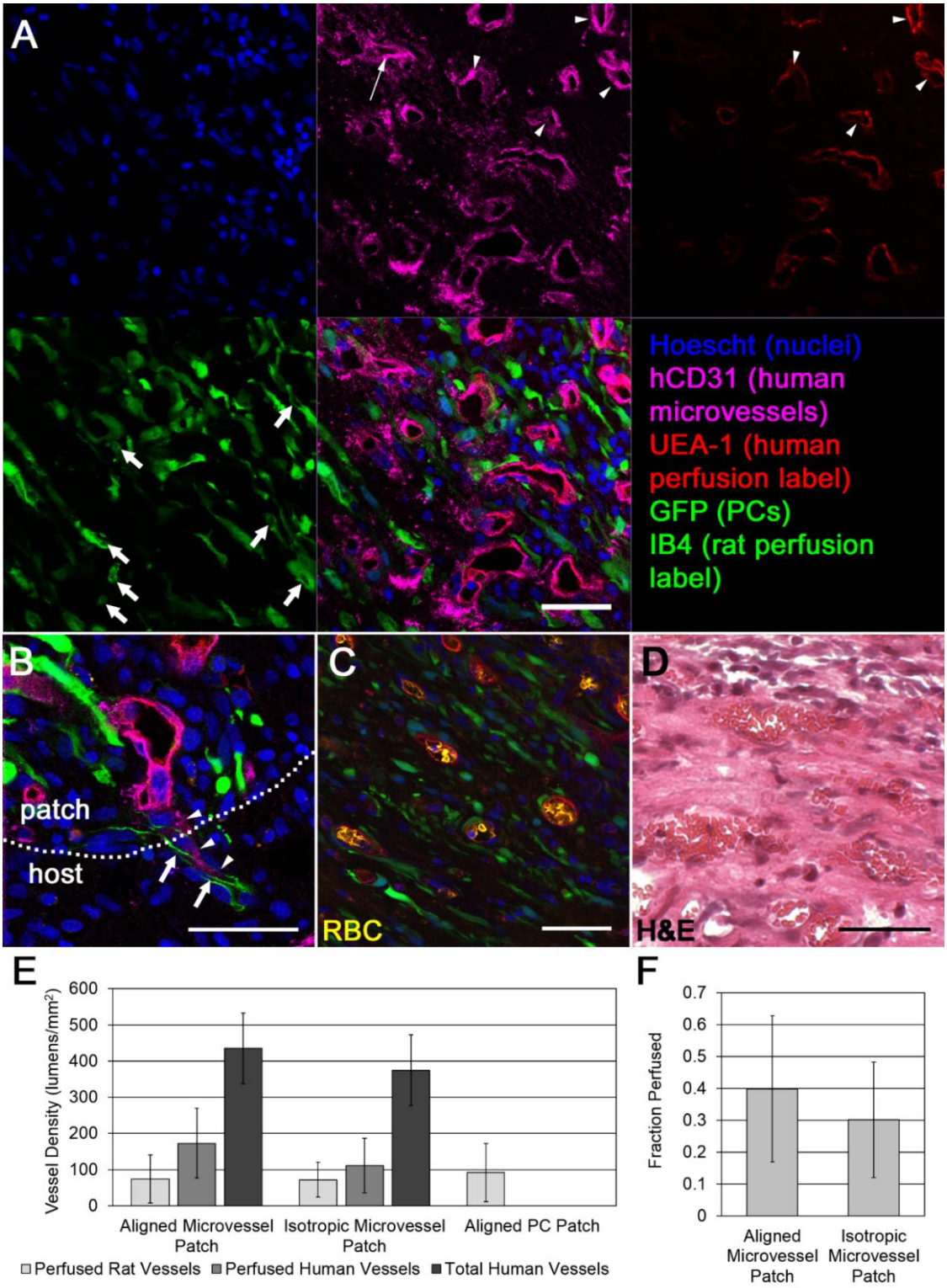
A
Hoescht (nuclei)
hCD31 (human microvessels)
UEA-1 (human perfusion label)
GFP (PCs)
IB4 (rat perfusion label)
B
patch
host
C
RBC
D
H&E
E
Vessel Density (lumens/mm²)
600
500
400
300
200
100
0
Aligned Microvessel Patch
Isotropic Microvessel Patch
Aligned PC Patch
Perfused Rat Vessels
Perfused Human Vessels
Total Human Vessels
F
Fraction Perfused
0.7
0.6
0.5
0.4
0.3
0.2
0.1
0
Aligned Microvessel Patch
Isotropic Microvessel Patch

**Figure 2-4.** Patch Perfusion.

A. Confocal micrograph displaying an area of an isotropic microvessel patch that had both perfused and non-perfused vessels. A few perfused human vessels (hCD31-magenta and UEA-1-red) are marked by white arrowheads and an example of a non-perfused vessel (magenta only) is marked by a thin white arrow. The bold white arrows mark rat vessel lumens (IB4-green) among the transplanted PCs (GFP-green). B. An example of inosculation of a perfused human vessel (magenta and red) with a rat vessel (green). Arrow heads point at the human vessel and bold arrows point at the inosculating rat vessel. C. Rat RBC stain (yellow) showing many RBCs inside perfused human microvessels (UEA-I-red) D. H&E stain showing an aligned microvessel patch with many lumens containing RBCs. E. Vessel density of perfused rat, perfused human, and total human vessels in the patch for aligned microvessel patch (n=6), isotropic microvessel patch (n=6), and aligned PC patch (n=5). F. Fraction of human vessels that were perfused in the patch. Scale bar = 50 μm. Data represented as mean ± standard deviation. 1-way ANOVA (E) and student's t-test (F) revealed no differences among the groups ($p > 0.05$).

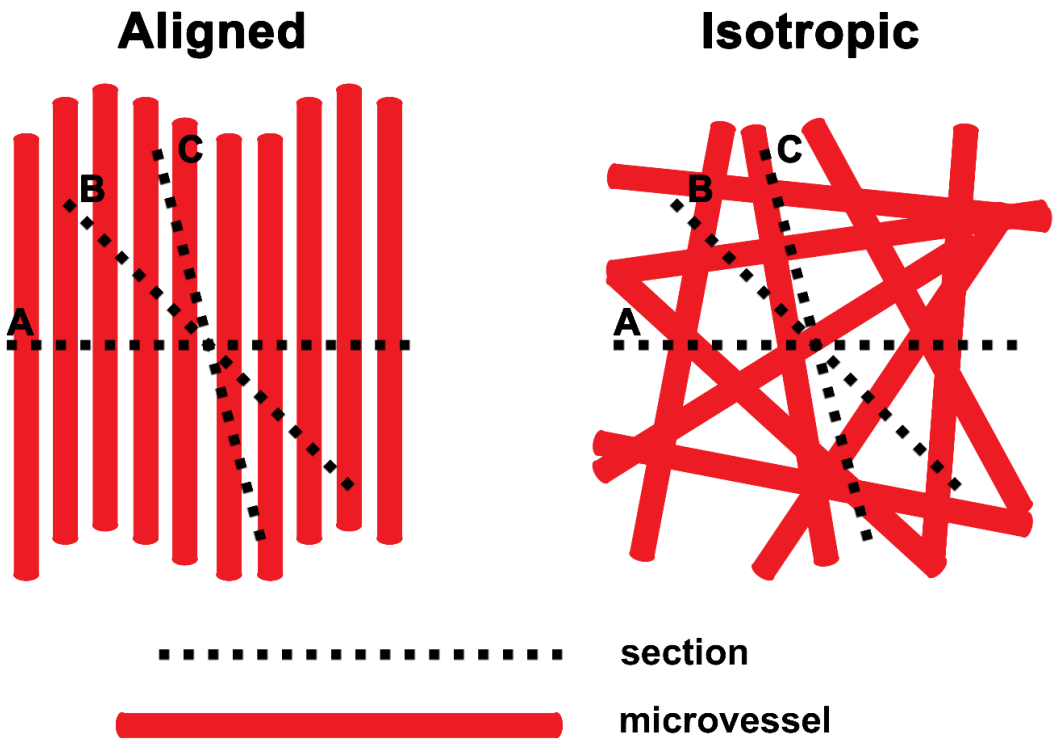


**Figure 2-5.** Lumen Density Dependence on Section Angle.

As the sectioning angle approaches the direction of alignment (A→C), the probability of a lumen being intersected by the section becomes lower and lower for aligned microvessel patches, but remains unchanged for isotropic microvessel patches due to the random orientation of the microvessels. This causes the aligned microvessel patch lumen density to appear lower for explanted sections, which were generally cut at an oblique angle (B or C) than if they were cut orthogonal to the alignment direction (A), as they were for *in vitro*

characterization. Explanted patches could not be sectioned orthogonally due to the need for transverse heart sections in determining infarct size. Also, the inability to distinguish the patch from surrounding tissue by macroscopic analysis at explant would have made oblique sectioning unavoidable in any case.

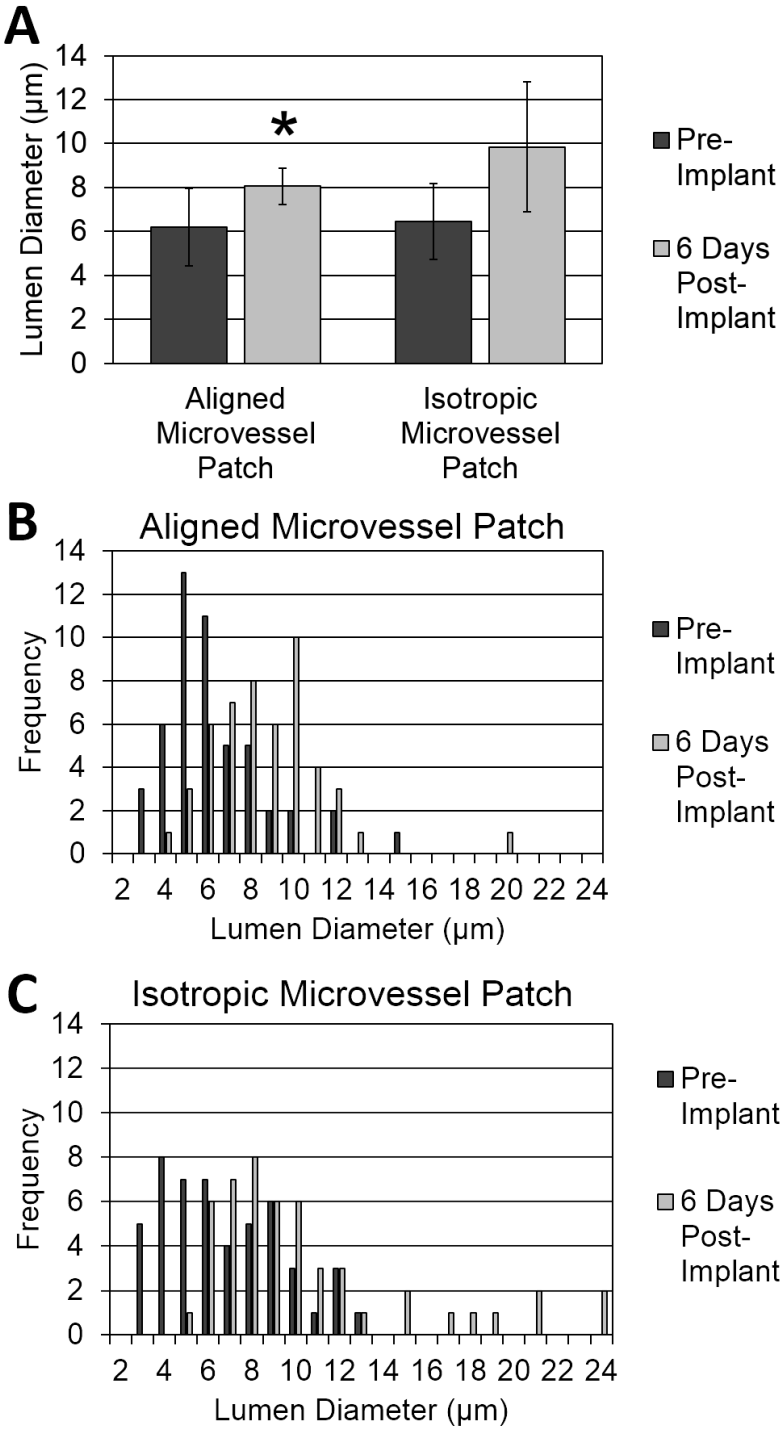
A
Lumen Diameter (μm)
14
12
10
8
6
4
2
0
*
Aligned Microvessel Patch
Isotropic Microvessel Patch
Pre-Implant
6 Days Post-Implant
B
Aligned Microvessel Patch
Frequency
2 4 6 8 10 12 14 16 18 20 22 24
Lumen Diameter (μm)
Pre-Implant
6 Days Post-Implant
C
Isotropic Microvessel Patch
Frequency
2 4 6 8 10 12 14 16 18 20 22 24
Lumen Diameter (μm)
Pre-Implant
6 Days Post-Implant

**Figure 2-6.** Lumen Diameters.

A. Summary of lumen diameters for Aligned and Isotropic microvessel patches pre-implant (n=14 aligned, n=6 isotropic) and 6 days post-implant (n=6 aligned, n=6 isotropic). B. Histogram of lumen diameters for aligned microvessel patches and C. isotropic microvessel patches to show the variation in lumen diameter pre- and post-implant. * indicates a difference from pre-implant lumen diameter by student's t-test, $p < 0.05$.

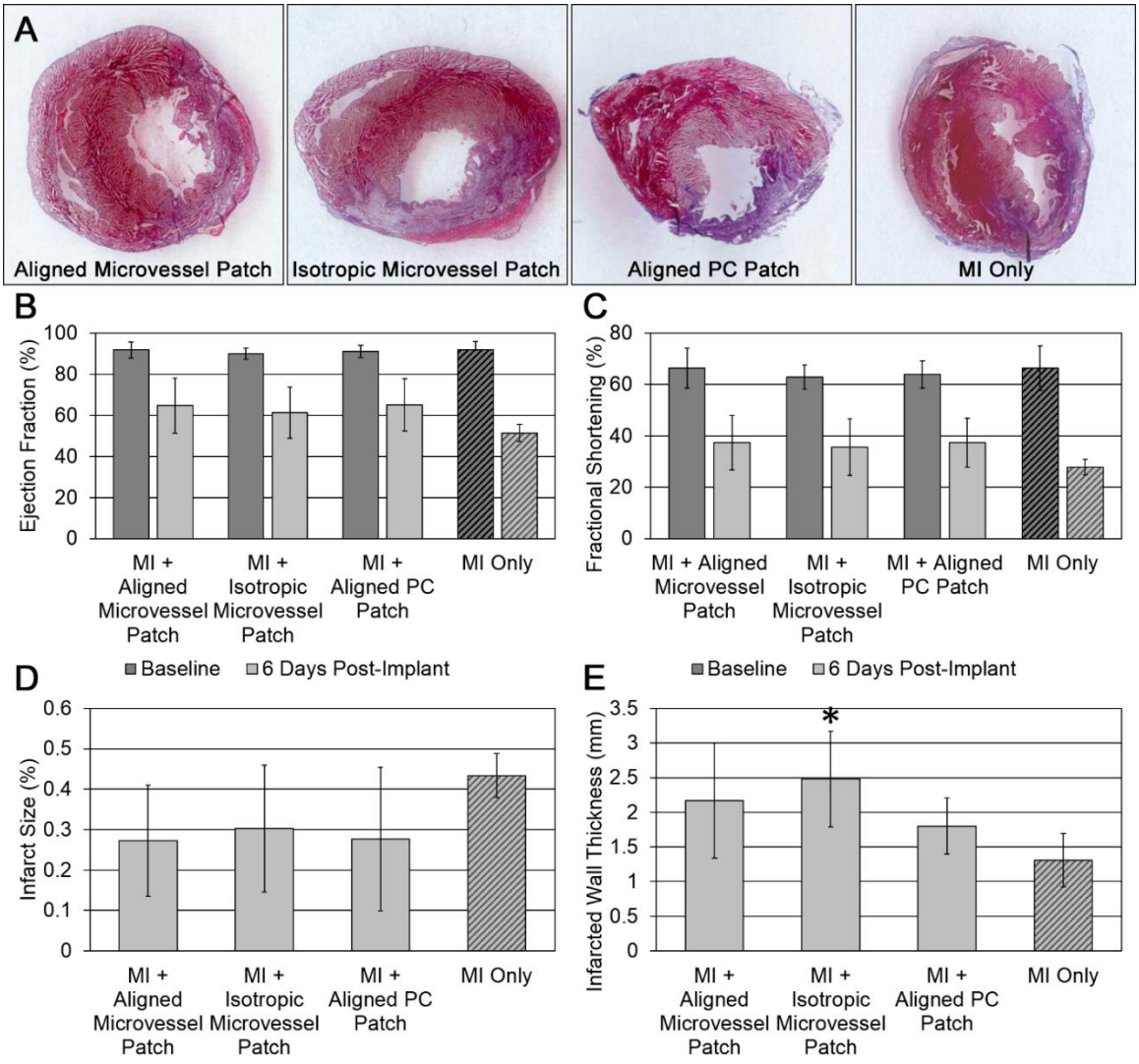


**Figure 2-7.** Infarct and Heart Function Assessment.

A. Trichrome stained heart sections taken from below the ligation suture. Infarct indicated by collagen presence (blue). B. Ejection Fraction and C. Fractional Shortening for animals prior to surgery and again after 6 days implantation, measured by echocardiography. D. Infarct size measured by the percent of the

left ventricular anterior wall occupied by scar and E. thickness of infarcted left ventricular wall measured from trichrome stained sections. Data represented as the mean ± standard deviation. Groups are MI + aligned microvessel patch (n=6), MI + isotropic microvessel patch (n=6), MI + aligned PC patch (n=5), MI Only (n=6). * indicates a difference from MI only, by 1-way ANOVA + Games-Howell post hoc test, $p < 0.05$.

# Chapter 3. Sprouting Assays

## 3.1 Introduction

### 3.1.1 Motivation for connecting microvessels to flow

Pre-vascularized tissues containing engineered microvessels were shown to be perfusable when implanted for 6 days *in vivo* (Chapter 2).[47] However, only 40% of the vessels were perfused. Greater perfusion efficiency could potentially be achieved by pre-conditioning microvessels with flow to promote greater network connectivity. *In vitro* perfusion of microvascular networks would also enable larger and denser tissues to be grown in the lab if they had a supporting, perfusable microvascular network to provide sufficient nutrients to meet their metabolic demand. Current tissue engineering strategies are severely limited to low density, thin tissues that are nourished by diffusion alone.

*In vitro* perfusion, however, presents many challenges. In order to perfuse the lumens of engineered microvessels *in vitro*, the microvessels must be connected to flow. While many microfluidic perfusion strategies exist, they do not allow for the creation of thick, dense tissues that could be implanted for regenerative therapies. We have previously developed a strategy for conditioning large, dense, and aligned microvascular tissues with flow, but the flow was

limited to the interstitial space between the microvessels, and the lumens were not perfused.[43]

### 3.1.2 Strategy for connecting microvessels to flow

Our strategy for connecting tissue engineered microvessels to flow involves encouraging sprouting from an endothelialized channel and encouraging the sprouts to anastomose with the microvessels in the bulk of the sample (Figure 3-1). This would enable flow to travel throughout the lumens of the microvascular network, which were previously closed to flow. Angiogenic sprouting from an endothelial monolayer and anastomosis with self-assembled microvessels in a fibrin gel was a critical feature for the design of a microvascular heart patch that could be perfused *in vitro*. Therefore, the conditions that favored sprouting, inosculation, and microvessel self-assembly had to be determined.

### 3.1.3 Sprouting conditions for testing

Our lab has had success creating lumen-containing microvessels in 3D fibrin gels containing stem cell factor (SCF), interleukin-3 (IL-3), and stromal-derived factor-1α (SDF) under a variety of conditions[43,47,74] and these growth factors have also been shown to enhance angiogenic sprouting in 3D collagen assays[16]. Vascular endothelial growth factor (VEGF) and fibroblast growth factor (FGF) are also known to promote angiogenesis.[85,86] Studies have shown

angiogenic sprouting to occur in collagen and fibrin gels containing these growth factors,[16,87] but they had not yet been tested in our system.

The cell culture medium used in 2D cell culture can greatly affect the angiogenic and vasculogenic potential of ECs. Studies have also shown that priming ECs in 2D culture with “supermedium” comprised of M199, reduced serum II supplement (RSII)[39], VEGF, and FGF 16-20 hours prior to casting in 3D gels can prepare them for angiogenesis and enhance microvessel formation.[16] While our lab had previously only used BOEC medium for 2D cell culture of BOECs prior to casting, supermedium priming could potentially enhance the angiogenic or vasculogenic potential of the BOECs and increase sprouting or tubulogenesis.

The culture medium for 3D gel culture can also greatly affect sprouting and tubulogenesis. The Davis lab has shown enhanced sprouting and tubule formation with medium containing only RSII, ascorbic acid, FGF at 40 ng/ml, and antibiotics (hereafter referred to as “defined medium”).[16,39] Although our lab has had success with vasculogenic tubulogenesis using BOEC medium, it’s potential for encouraging angiogenic sprouting had yet to be determined.

In this study, culture of BOECs prior to casting was primarily with BOEC medium, with some groups being primed with supermedium 16-20 hours before casting. All fibrin gels contained the growth factors SCF, IL-3, and SDF, while

some also contained VEGF and FGF. Once the gels had formed, both BOEC medium and defined medium were tested for sprouting efficiency.

### 3.1.4 High-throughput assay for testing sprouting conditions

Perfusion bioreactor tissue culture consumes a large amount of culture medium and time preparing and manipulating the sample. Thus, for preliminary studies it is beneficial to work with a smaller scale system that is higher throughput, simpler to culture, and uses less material. Therefore, initial experiments were carried out with gels that were cast in half-area 96-well plates (A/2 gels).

A novel assay was developed to investigate tubulogenesis and sprouting in a combined vasculogenic and angiogenic assay (Figure 3-2). In the assay, BOECs and PCs could be entrapped in a 3D fibrin gel with a variety of possible growth factors. BOECs could also be seeded as a monolayer on the gel surface to simulate angiogenic sprouting from an endothelialized channel. The vasculogenic assay contained only entrapped BOECs and PCs without the BOEC surface-monolayer, the angiogenic assay had a cell-free fibrin gel with only the BOEC surface-monolayer, and the combined vasculogenic/angiogenic assay had both entrapped cells and a surface-monolayer with cells pre-labeled with a cell-tracking dye. The combination assay was novel in that it expanded upon the simultaneous study of vasculogenesis and angiogenesis, described in

Koh et al.[39], and also allowed for easy tracking of inosculation of surface angiogenic sprouts and vasculogenic tubules through the use of the cell-tracking dye.

Samples were cultured statically to elucidate the desirable conditions that led to sprouting from the monolayer, microvessel formation in the bulk gel, and inosculation of the resulting sprouts and microvessels. This format enabled the study of these three key processes under a wide variety of conditions in a high throughput manner.

## 3.2 Materials and Methods

### 3.2.1 Culture of human blood outgrowth endothelial cells and human pericytes

Human BOECs were isolated by the lab of Dr. Robert Hebbel at the University of Minnesota – Twin Cities[25]. Passage 5 BOECs were thawed and plated on 0.05 mg/ml collagen I – coated flasks in BOEC medium (EGM-2 bulletkit medium (Lonza) supplemented with 10% FBS, 1% penicillin/streptomycin (Gibco)). Medium was changed every other day and BOECs were passaged after 4 days, then plated and cultured for 3 more days prior to harvest. Some experiments tested priming the BOECs with "supermedium"[16] (Medium 199 basal medium (Gibco) (M199), 0.4% RSII, 40 ng/ml VEGF (R&D Systems), 40 ng/ml FGF (R&D Systems)). In these cases,

BOEC medium was completely replaced with supermedium 16-20 hours prior to harvest while all other samples had BOEC medium replaced with fresh BOEC medium.

GFP-labeled PCs were obtained from the lab of Dr. George Davis at the University of Missouri. Passage 6 PCs were thawed and plated on 1 mg/ml gelatin-coated flasks in PC medium (13% FBS, 1% penicillin/streptomycin (Gibco), 10 ng/ml gentamicin (Gibco) in low-glucose DMEM (Lonza)). Medium was changed every 2-3 days and PCs were harvested after 10 days.

### 3.2.2 Labeling BOECs with Qtracker for surface-seeding

BOECs reserved for surface-seeding were stained with Qtracker 705 Cell Labeling Kit (ThermoFisher Scientific) by incubating a T175 flask in the Qtracker labeling solution at 37°C, 5% $CO_2$ for 65 min. Prior to harvest, cells were washed twice with BOEC medium, then harvested as usual.

### 3.2.3 Creation of fibrin gels for sprouting assays

Fibrin gel-forming solution was pipetted into 96-well half-area plates. The gel solution was made up of 2.55 mg/ml fibrinogen (Sigma), $2x10^6$ BOECs per mL and $0.4x10^6$ PCs per mL, 200 ng/ml of stem cell factor (SCF), interleukin-3 (IL-3), and stromal derived factor 1α (SDF-1α) (R&D Systems), and 1.25 U/ml thrombin (Sigma) in M199. Some gels also contained vascular endothelial growth

factor (VEGF) and fibroblast growth factor (FGF) (200 ng/ml, R&D Systems) for testing their effects on sprouting, vasculogenesis, and inosculation. Cell-free gels (gels without entrapped BOECs or PCs, but still seeded with a BOEC monolayer later) replaced BOECs and PCs with equal volumes of M199. Table 3-1 details each of the different conditions evaluated.

The gel solution was quickly made up in 180 µl aliquots, one at a time, mixed well, and 28 µl of gel solution was pipetted into each of 6 wells in a 96-well half-area plate (Corning). Samples were incubated at 37°C, 5% $CO_2$ for 20 min before adding 100 µl of either BOEC medium or defined medium (0.4% RSII[39], 50 µg/ml Ascorbic Acid (Sigma), 40 ng/ml FGF (R&D Systems) in M199). Medium was replaced (with either BOEC or defined) by removing and replenishing 60 µl per well daily.

### 3.2.4 Seeding the BOEC surface-monolayer

For surface-seeded gels, BOECs were added to the culture medium above the gels at a concentration of $8x10^4$ cells/mL for a seeding density of 50,000 cells/$cm^2$. Seeding was done during the initial addition of culture medium, 20 min after casting.

### 3.2.5 Harvest of fibrin gels

After 5 days of culture, samples were fixed in 4% paraformaldehyde (Electron Microscopy Sciences) for 10 min at room temperature, rinsed in PBS 3x5 min, then detached from the bottom surface of the 96 well plate by sliding a sharp forceps around the perimeter of each gel and underneath the gel between the bottom surface and the tissue culture plastic. Gels were transferred to separate wells in PBS and saved for whole-tissue immunofluorescence staining.

### 3.2.6 Immunohistochemical characterization

Whole-tissue samples were blocked in 5% Normal Donkey Serum (Jackson Immunoresearch) for 2 hours, then incubated in an antibody specific to human CD31 (hCD31, 1:40 dilution) (Dako) in blocking serum for one hour. Three 5 min PBS rinses were performed, then the samples were incubated in 1:200 donkey anti-mouse secondary antibody conjugated with Alexa Fluor® 594 (Jackson Immunoresearch) in PBS for 1 hour. After secondary antibody incubation, samples were incubated in 1:10,000 Hoescht 33342 (Invitrogen) in PBS for 10 min, followed by two 5 min rinses in PBS. All steps were performed at room temperature on an orbital shaker.

### 3.2.7 Confocal imaging and analysis

Whole-stained samples were visualized with confocal microscopy (Zeiss LSM 510). Images were acquired near the top and bottom surfaces of each sample and z-stacks were acquired starting at the top surface and continuing in 1µm slices approximately 20 µm deep into the sample to track sprouts from the surface-monolayer. Long sprouts were tracked by manually adjusting the focus up to 100 µm deep and recording the maximum depth of the sprouts. Images were assessed to evaluate sprouting from the monolayer, assess the morphology of the microvascular network, and check for inosculation of Q-tracker-labeled sprouts with the hCD31 labeled microvessels.

## 3.3 Results

### 3.3.1 Assessment of microvessel self-assembly in vasculogenic assays

Priming BOECs with supermedium 16-20 hours prior to casting resulted in reduced microvessel formation compared to gels cast with cells cultured in BOEC medium prior to casting (Figure 3-3). This was independent of the type of culture medium used after casting. Priming conditions were removed from further testing and all other samples were cast with cells that had been cultured in BOEC medium prior to harvest. Further testing of culture medium conditions refers to the medium used during 3D gel culture rather than 2D cell culture.

Vasculogenic assays without VEGF/FGF and cultured with BOEC medium formed a network of lumen-containing microvessels throughout the gel with PCs recruited to the abluminal side of the microvessels (Figure 3-4A). VEGF and FGF did not affect microvessel formation or network properties (Figure 3-4D) when cultured in BOEC medium.

When defined medium was used to culture BOEC/PC gels, very few intact microvessels were found (Figure 3-4B,E). It was observed during culture that tubules would initially form in the bulk of the gel when cultured with defined medium, but they would begin to regress and disorganize by the second day of culture, and were mostly degraded by day 5. The addition of VEGF and FGF did not recover vasculogenic tubule formation in these gels.

A hybrid medium approach, with 1 day of defined medium and 4 days of BOEC medium was tested to attempt to attain the benefits of defined medium[31,39,74] without the microvessel regression that was observed after 24 hours. The hybrid medium approach resulted in the formation of a network of lumen-containing microvessels with recruited PCs (Figure 3-4C,F), a great improvement compared to samples cultured in defined medium alone, and similar to samples cultured in BOEC medium alone. There were no differences between samples cultured with or without VEGF and FGF in vasculogenic assays.

### 3.3.2 Sprouting assessment in angiogenic assays

Angiogenic assays (gels cast without entrapped BOECs or PCs, and seeded with a monolayer of BOECs) were evaluated for their sprouting potential under each testing condition. Samples cultured in BOEC medium without VEGF/FGF contained a surface monolayer of BOECs with few to no sprouts (Figure 3-5 A,C). When VEGF/FGF were added, sprouting increased, but the sprouts were less frequent and short, only extending 10-20 µm (Figure 3-5 E,H). Samples without VEGF/FGF and cultured in defined medium, also contained few to no sprouts, and failed to maintain a monolayer of BOECs on the surface (Figure 3-5 B,D). When VEGF/FGF was added to defined medium cultured samples, however, the result was a surface-network of microvessels rather than a continuous monolayer of BOECs, and there were many lumen-containing sprouts extending into the gel 30-120 µm (Figure 3-5 F,I).

Hybrid medium culture was tested with the angiogenic assays as well. When the hybrid medium protocol (1 day defined medium, 4 days BOEC medium) was used on the angiogenic assays containing VEGF/FGF, a surface monolayer of BOECs formed and was maintained over 5 days. Additionally, extensive sprouts were found in the gels, with no reduction in sprouting compared with gels cultured in defined medium alone (Figure 3-5 G,J). The hybrid medium protocol applied to gels containing VEGF/FGF was the only

condition that yielded both a complete endothelial monolayer on the gel surface and many long, angiogenic sprouts.

### 3.3.3 Inosculation of sprouts and microvessels in combined assays

Combined vasculogenic/angiogenic assays with samples containing both entrapped BOECs and PCs and a monolayer of surface-seeded BOECs were evaluated for the inosculation potential of sprouts and microvessels. The assay was carried out for the conditions deemed most favorable during the vasculogenic and angiogenic assay testing (+VEGF/+FGF gels cultured under a hybrid medium protocol, and no priming of the BOECs). A control group without VEGF/FGF, cultured with BOEC medium was tested as well. Sprouts from the BOEC monolayer (labeled with Qtracker) were observed with confocal microscopy and traced into the gel thickness to check for inosculation with non-labeled microvessels. Samples containing VEGF/FGF and cultured with the hybrid medium protocol contained several Q-tracker-labeled sprouts that anastomosed with non-labeled microvessels at least 60μm deep (Figure 3-6). Control gels cultured with BOEC medium did not contain any Qtracker labeled sprouts, and thus, did not show any evidence of inosculation.

## 3.4 Discussion

While several conditions led to sprouting and microvessel formation individually, only one set of conditions led to all three events needed to connect

microvessels to an endothelialized surface: sprouting from a monolayer, microvessel formation in the gel, and inosculation of sprouts and microvessels. The single set of conditions that led to these events was hybrid medium culture, +VEGF/+FGF, -primed cells.

Priming of BOECs in 2D culture did not enhance vasculogenic tubulogenesis, thus it was quickly eliminated from testing. This could be attributed to inherent differences in BOECs, a late-outgrowth cell type derived from adult peripheral blood, and HUVECs, human umbilical vein endothelial cells, which were used in studies showing the benefits of priming ECs.[16]

In angiogenic assays, an endothelial monolayer was only observed in samples cultured in BOEC medium or the hybrid medium protocol. Defined medium samples did not support the formation of a continuous endothelium. Rather, +VEGF/+FGF samples cultured in defined medium contained a surface network of microvessels that sprouted into the gel thickness. While interesting, the formation of a surface network rather than a monolayer would not be useful in the development of a perfusable microvascular tissue, because the endothelialized channel needs to act as a barrier and direct flow through the lumens of sprouts that come out from the endothelium. Only a surface monolayer of ECs could achieve this, thus the BOEC medium or hybrid medium approach

are better suited for continued efforts in development of a perfusable microvascular tissue.

The addition of VEGF and FGF enhanced sprouting, which is unsurprising, as several studies[16,53,56,88] have shown these growth factors to have positive effects on angiogenesis. In vasculogenic assays, however, VEGF and FGF did not affect microvessel formation. It is possible that the VEGF and FGF present in BOEC medium saturated the cells' response, so additional growth factors showed no effect. Defined medium, which contained fewer growth factors and reduced serum, may have elucidated a response with addition of VEGF and FGF, but vasculogenic assays showed poor tubule formation with defined medium culture, so it was difficult to measure improvements in response to VEGF and FG addition. In the combined angiogenic + vasculogenic assay, sprouting was driven by culturing the samples in defined medium for the first 24 hours, during which the presence of VEGF and FGF in the fibrin gel formulation could act as chemoattractants and encourage the initiation of angiogenic sprouting. Here, extensive angiogenic sprouting was observed, with many sprouts that had anastomosed with the microvessels in the gel.

While defined medium culture yielded excellent angiogenic sprouting, these conditions were poorly suited for microvessel formation in the bulk gel. Conditions well-suited for microvessel formation (BOEC medium) yielded poor

sprouting. It was only after observing the initial microvessel formation and then later, regression, in vasculogenic assays cultured with defined medium that led to the formulation of a hybrid medium culture approach. Culturing gels for the first 24 hours in defined medium allowed for the necessary conditions to initiate angiogenic sprouting from the monolayer while enabling the early stages of microvessel formation in the bulk gel. Then later culture with BOEC medium helped complete microvessel formation and allowed for stable microvessels to develop without affecting the angiogenic sprouting potential.

This hybrid medium approach with 1 day of defined medium and 4 days of BOEC medium resulted in angiogenic sprouting of BOECs from a monolayer, excellent vasculogenic network formation within the fibrin gel, and inosculation of the sprouts with the network microvessels. These results are promising for the use of combined angiogenic and vasculogenic methods to develop perfusable microvessels in tissues for regenerative therapies, and it is the first step toward creating a perfusable microvascular network with BOECs and PCs in fibrin gel. The next step would be to move from this high-throughput platform to a system that allows for perfusion of endothelialized flow channels.

### 3.5 Tables

| Entrapped BOECs/PCs | Surface-Seeded | Primed Cells | VEGF/FGF | Culture Medium |
|---|---|---|---|---|
| X | | X | | BOEC |
| X | | X | X | BOEC |
| X | | X | | Hybrid |
| X | | X | X | Hybrid |
| X | | | | BOEC |
| X | | | X | BOEC |
| X | | | | Defined |
| X | | | X | Defined |
| X | | | | Hybrid |
| X | | | X | Hybrid |
| | X | | | BOEC |
| | X | | X | BOEC |
| | X | | | Defined |
| | X | | X | Defined |
| | X | | X | Hybrid |
| X | X | | | BOEC |
| X | X | | X | Hybrid |

**Table 3-1.** Vasculogenic, Angiogenic, and Combined Assay Testing Conditions.

Table showing vasculogenic assays (colored in blue, all have entrapped BOEC/PCs and no surface-seeded BOECs), angiogenic assays (colored in yellow, no entrapped BOECs/PS, all have surface-seeded BOECs), and combined vasculogenic + angiogenic assays (colored in pink, all have entrapped BOECs/PCs and surface-seeded BOECs). Primed cells refers to replacing the culture medium with supermedium in 2D cell culture 16-20 hours prior to harvest. VEGF/FGF refers to the addition of 200 ng/ml of VEGF and FGF to the gel formulation. Culture medium refers to the type of medium used during 3D gel culture (BOEC, defined, or hybrid).

### 3.6 Figures

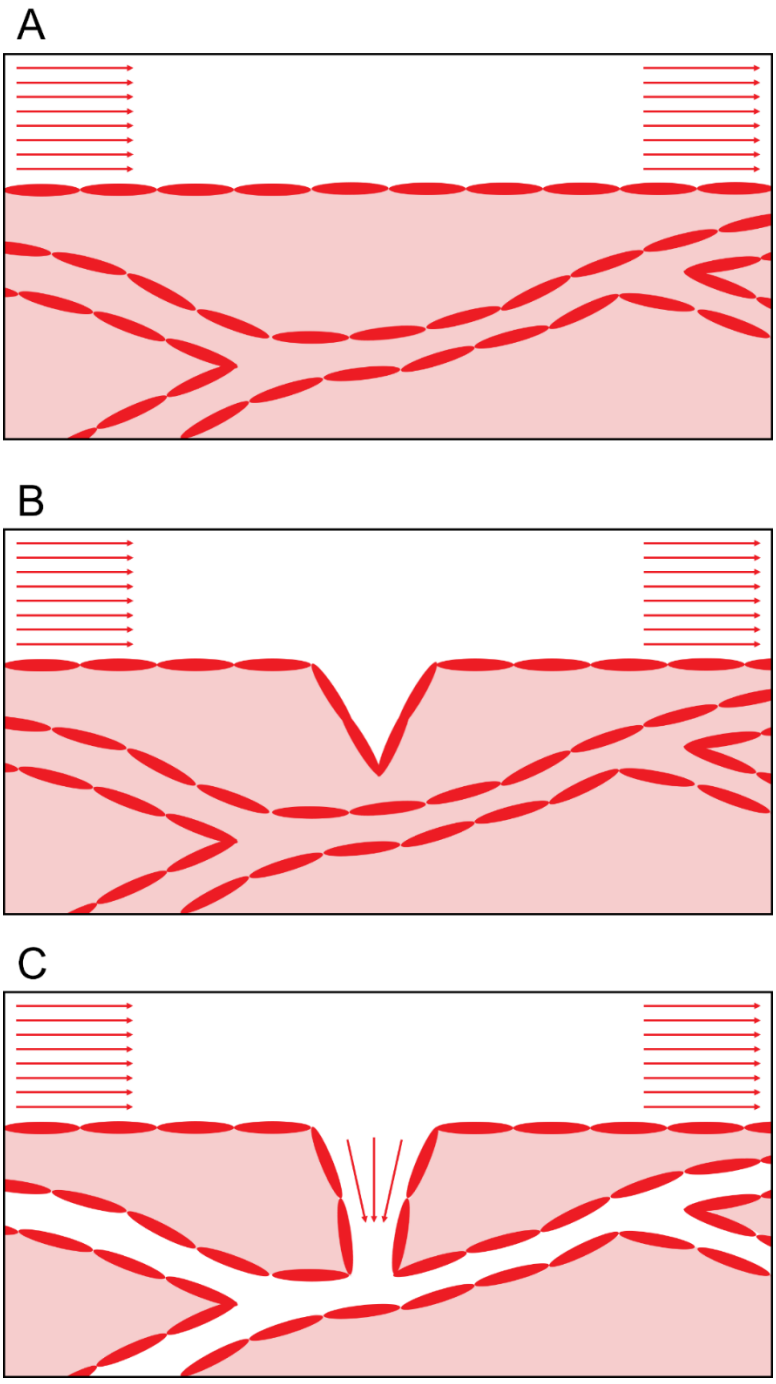

**Figure 3-1.** Strategy for Connecting Microvessels to Flow.

A. A flow channel (arrows) could be lined with endothelial cells (red). The flow channel would be surrounded by a fibrin gel (pink) containing a microvascular network made up of endothelial cells (red). B. By encouraging sprouting from the endothelial monolayer of the flow channel, sprouts would grow into the fibrin gel. C. By encouraging anastomosis of angiogenic sprouts with the microvessels in the fibrin gel, flow could enter the lumens of the microvessels, enabling perfusion of the microvascular network.

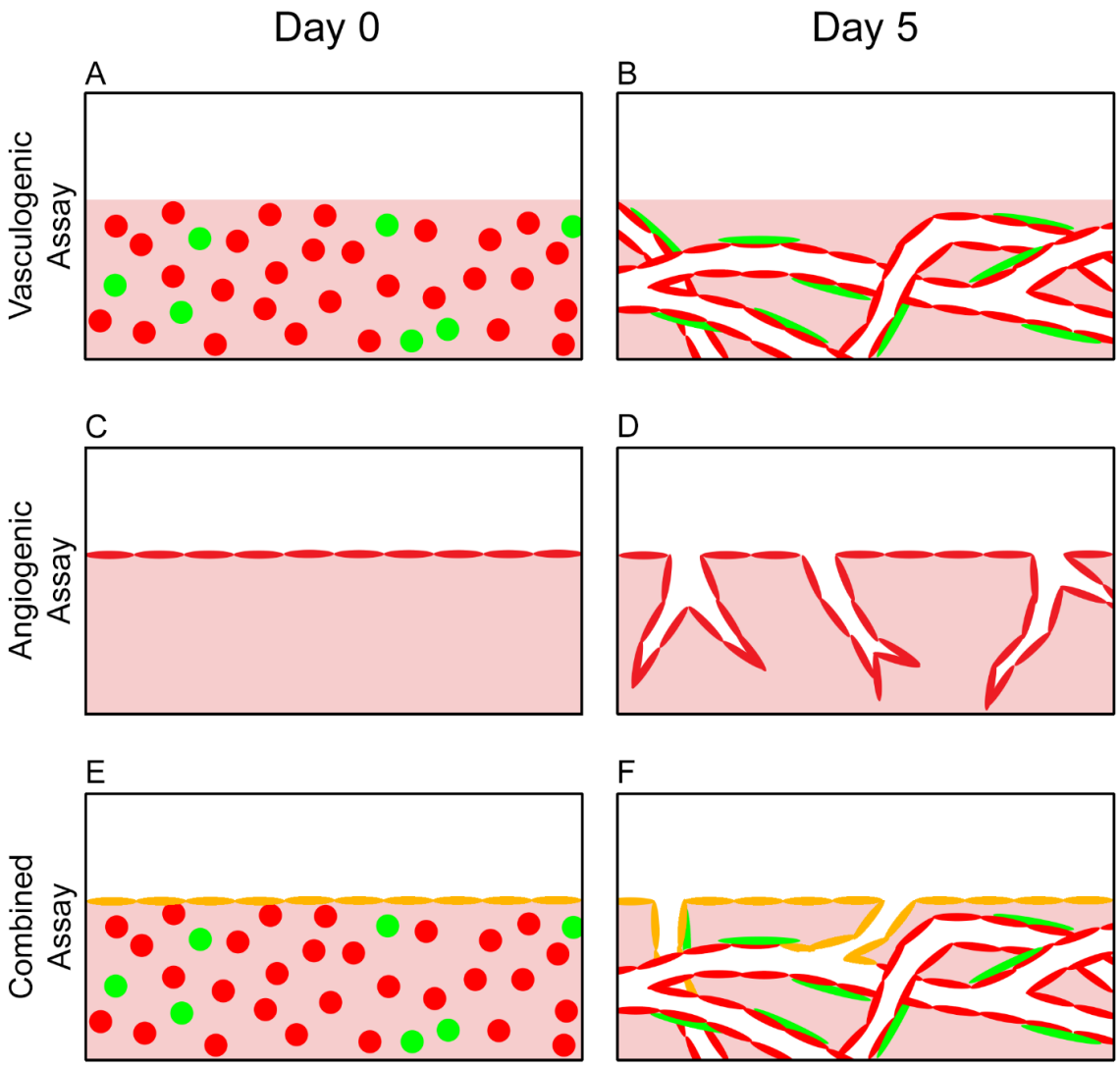


**Figure 3-2.** Angiogenic/Vasculogenic/Combined Sprouting Assay Format.

Fibrin gels are cast in half-area 96 well plates. A. In the vasculogenic assay, BOECs (red) and PCs (green) are entrapped in fibrin gels (pink) without surface-seeding. B. Under the right conditions, entrapped BOECs and PCs self-assemble

into a microvascular network. C. In the angiogenic assay, cell-free fibrin gels are surface-seeded with BOECs. D. Under the right conditions, BOECs form angiogenic sprouts into the fibrin gel. E. In the combined vasculogenic/angiogenic assay, BOECs and PCs are entrapped in fibrin gels and are surface-seeded with pre-labeled BOECs (yellow). F. Under the right conditions, pre-labeled BOECs form angiogenic sprouts that anastomose with the microvascular network.

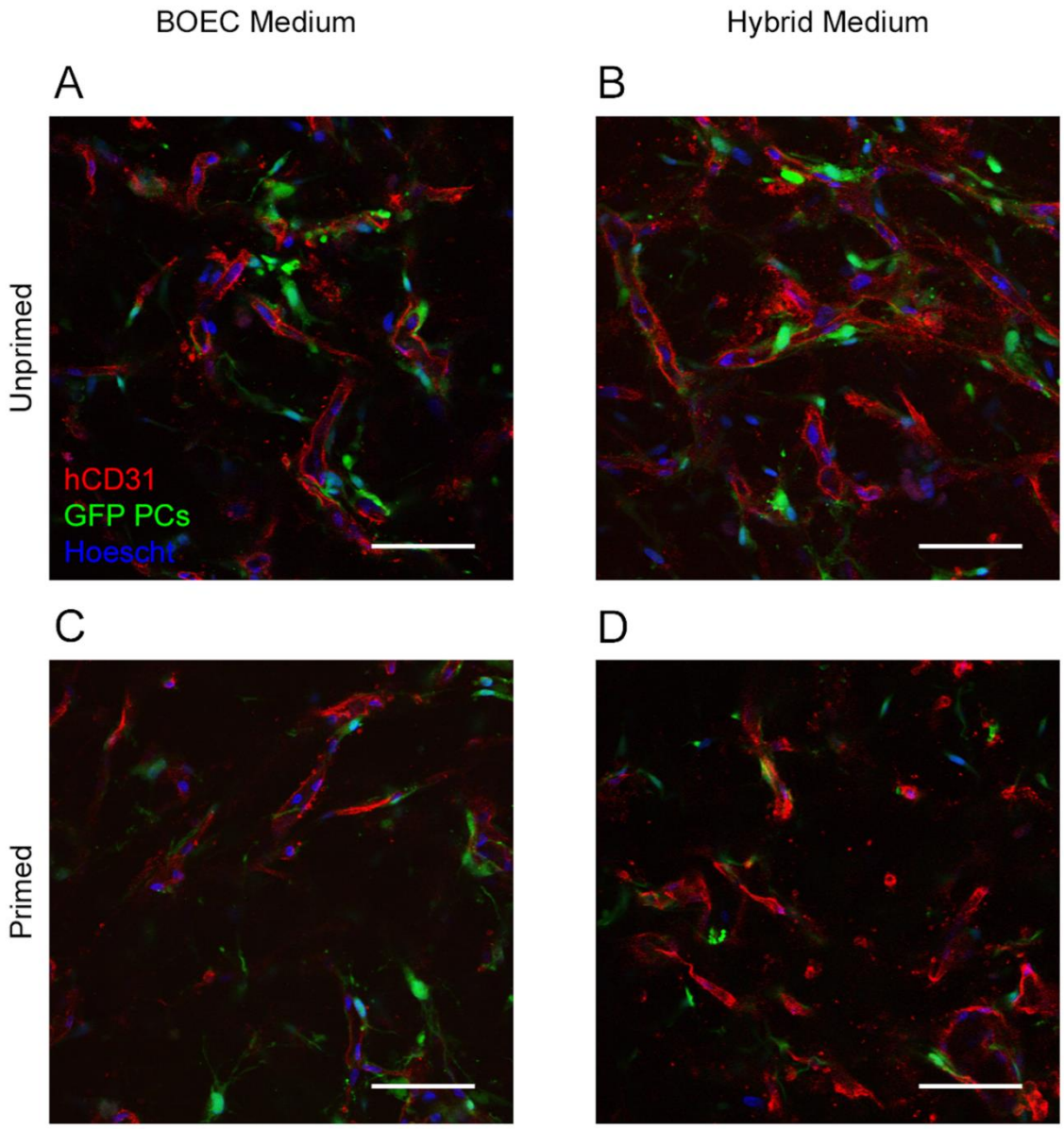


**Figure 3-3.** Priming Experiment.

Representative images of vasculogenic assay that tested gels cast with primed or unprimed BOECs, with better microvessel formation achieved in gels cast with

unprimed cells. All images were taken from gels lacking VEGF and FGF and lacking a surface-seeded BOEC monolayer. A. Unprimed, cultured with BOEC medium, B. Unprimed, cultured with Hybrid medium, C. Primed, cultured with BOEC medium, D. Primed, cultured with Hybrid medium. Scale bar = 100 µm.

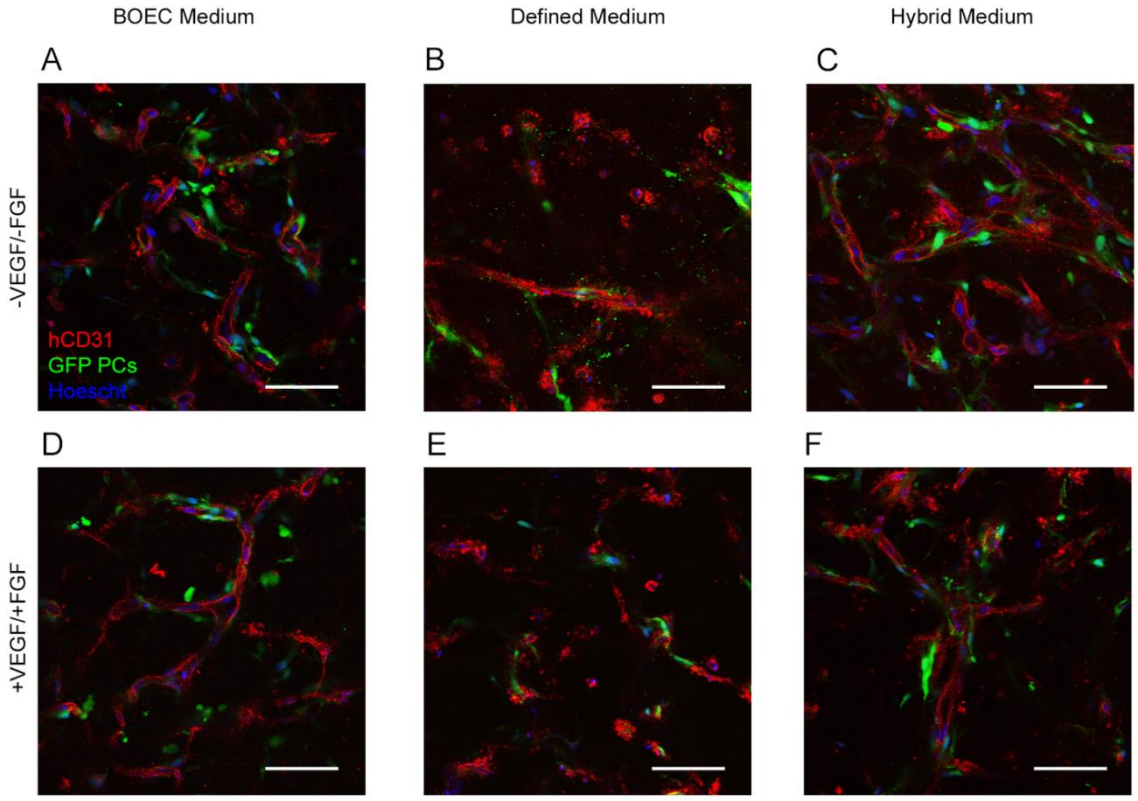


**Figure 3-4.** Vasculogenic Assay Results.

Representative images are displayed for each condition tested: A. BOEC medium, -VEGF/-FGF, B. Defined medium, -VEGF/-FGF, C. Hybrid medium, -VEGF/-FGF, D. BOEC medium, +VEGF/+FGF, E. Defined medium, +VEGF/+FGF, F. Hybrid medium, +VEGF/+FGF. Scale bar = 100 µm.

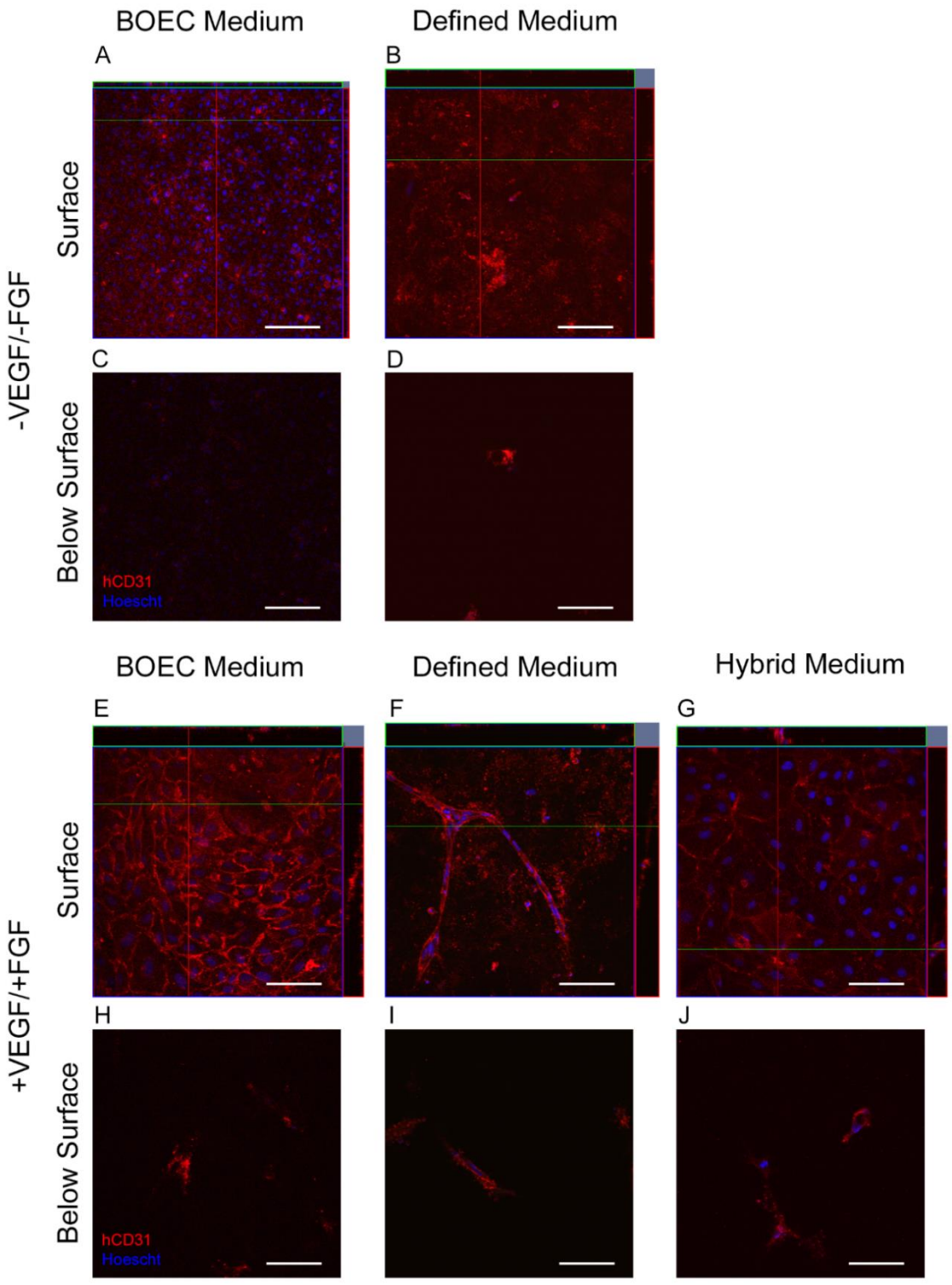
BOEC Medium
Defined Medium
A
B
Surface
-VEGF/-FGF
C
D
Below Surface
hCD31
Hoescht
BOEC Medium
Defined Medium
Hybrid Medium
E
F
G
Surface
+VEGF/+FGF
H
I
J
Below Surface
hCD31
Hoescht

**Figure 3-5.** Angiogenic Assay Results.

A-B and E-G show an image of the BOEC-seeded top surface with panels on the top and right sides showing cross-sectional views constructed from confocal z-stacks. C-D and H-J show an image several microns below the gel surface to demonstrate the presence of sprouts (in some cases) with lumens. A, C. BOEC medium, -VEGF/-FGF, B, D. Defined medium, -VEGF/-FGF, E, H. BOEC medium, +VEGF/+FGF, F, I. Defined medium, +VEGF/+FGF, G, J. Hybrid medium, +VEGF/+FGF. Scale bar = 100 µm.

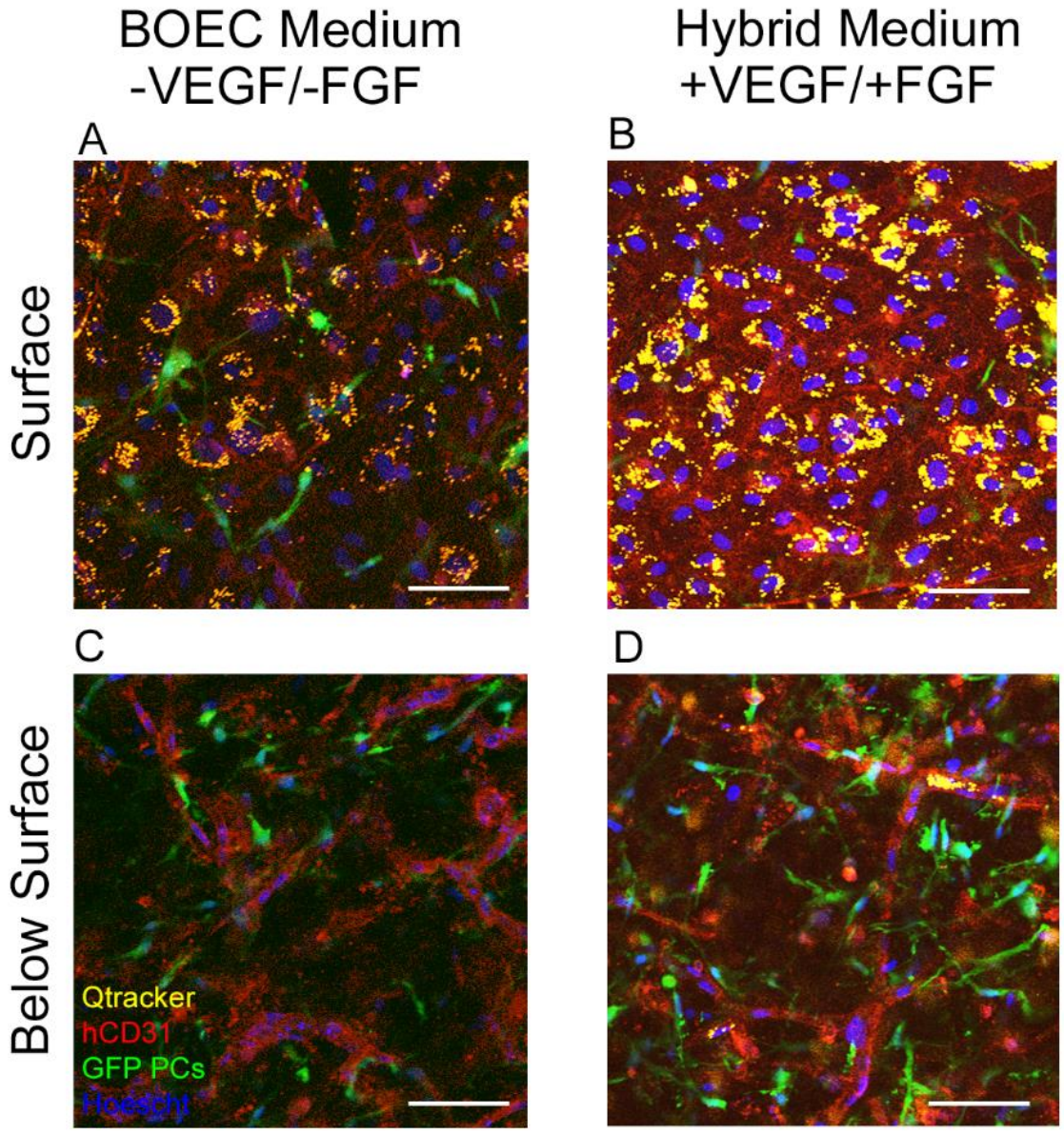


**Figure 3-6.** Combined Vasculogenic + Angiogenic Assay Results.

Top surface, seeded with Qtracker (yellow) labeled BOECs for A. BOEC medium, -VEGF/-FGF and B. Hybrid medium, +VEGF/+FGF. Microvascular

network below the surface for C. BOEC medium, -VEGF/-FGF and D. Hybrid medium, +VEGF/+FGF with sprouts (yellow, labeled with Qtracker) integrated with the microvascular network. Scale bar = 100 µm.

# Chapter 4. Bioreactor Strategy for In Vitro Microvascular Tissue Perfusion

## 4.1 Introduction

### 4.1.1 Why is in vitro perfusion important?

In vitro perfusion of microvascular networks is a rapidly growing field and more and more groups are attempting to mimic the microcirculation in a lab environment. In vitro perfusion of microvessels has a wide range of applications, starting with diagnostics and drug testing and ranging to the culture of implantable engineered tissues for regenerative medicine. Over the past few years, many groups have been creating microvascular networks in the lab and a few are even successfully perfusing them in microfluidic systems.[5,23,26,64–68] These groups are developing perfusable microvasculature for organ-on-a-chip applications that can function as a model system to be used for drug screening or for the study of various diseases of the microcirculatory system. These advances are groundbreaking for the field of microvascular engineering, and they can help guide the scale-up to implantable engineered tissues for regenerative therapies.

Pre-vascularized engineered tissues are becoming essential to the continued development of the field of tissue engineering. Without pre-vascularization, engineered tissues are limited in size, thickness, and cell density

due to diffusion limitations and high metabolic demand of certain cell types.[2,3,89] In vivo, native tissue is supplied with nutrients by an extensive microcirculatory system of capillaries that can be as dense as 2,000 capillaries/mm$^2$ in human adult cardiac tissue. Attempts to develop engineered tissues that can mimic or replace native tissue will require integration of a network of microvessels that can supply the necessary nutrients to meet the metabolic demands of the cells.

Having a functional engineered microvascular network that is perfusable prior to implantation could reduce the time needed to achieve complete tissue perfusion following implantation. With an engineered microvascular network that is perfusable prior to implantation, anastomosis with the host vessels would be the only limitation in providing complete blood perfusion of the donor tissue. This would help deliver nutrients to implanted cells quickly and efficiently and would enable the delivery of larger, denser engineered tissues with high metabolic demands that would, otherwise, not have survived implantation.

In vitro perfusion of microvascular tissues would also enable the creation of much larger and denser tissues containing highly metabolic cells in the lab, because nutrients could be delivered more efficiently and would not be limited by diffusion. Perfusion culture of pre-vascularized tissues that contained other cell types, such as cardiomyocytes or hepatocytes, would open up a myriad of engineering possibilities for the creation of regenerative therapies. Despite the

urgent need and consensus in the field,[3,89] perfusion of pre-vascularized tissues has yet to be accomplished. This is, in part, due to the challenge of flow connectivity to the microvascular network.

### 4.1.2 What are current in vitro perfusion methods missing?

Current reports[5,23,26,64–67] of perfusable 3D microvascular networks utilize microfluidic technology and are designed for drug screening platforms or study of diseases. The microfluidic platform technology is excellent for small-scale, high-throughput flow studies, or lab-on-a-chip technology, but it is not suitable for growing large engineered tissues to be implanted for regenerative therapies. Microfluidic samples are typically on the millimeter scale, while engineered tissues typically require significant size and thickness, on the centimeter scale or larger.

In microfluidic studies, ECs are typically entrapped in low-density collagen gels, fibrin gels, or Matrigel™ which lack the mechanical strength and robustness to survive implantation and mimic native function, in most cases. These samples are constrained on all sides, which prevents cell-induced gel compaction and remodeling of the extracellular matrix. This further limits their utility in regenerative medicine, as this matrix remodeling is critical to the creation of a dense, native-like tissue.[42,43] It is through selective constraints and guided cell-

induced compaction and remodeling that cell-loaded gels can become robust engineered tissues with finely tuned cell and matrix alignment.[43,74,90]

3D printing technology is another approach that has been studied in attempts to solve the perfusion problem. The Chen lab has shown success in printing and perfusing EC-lined channels in printed poly(ethylene glycol) hydrogels. Perfusion of channels like these enhanced survival of the cells surrounding the perfused channels, but more distant cells do not survive (Chen Miller 2012, Chen cords for implantation, Schuller-ravoo 2014).[20,91,92] While this approach improves nutrient delivery compared to samples without perfusable channels, 3D printing technology does not have the resolution to print at the capillary-level (10 μm).[93] With diffusion distances typically on the order of 150-200 μm[94], any tissue created using this approach would require approximately 50% of its volume to be occupied by flow channels. Not only is this not physiologically accurate, it would also disrupt important cell:cell contact in tissues such as myocardium, and would hinder the mechanical properties of the tissue. Capillaries are more efficient for nutrient delivery as they have a greater surface area for a given blood volume, enhancing their potential for supplying nutrients throughout a tissue. A hierarchical network consisting of arteries, arterioles, capillaries, venules, and veins that could be patterned and 3D printed would be incredibly promising, but unfortunately, 3D printing technology cannot match the

resolution required for a capillary network. This prevents this approach from meeting the nutrient demands of dense, highly metabolic tissues.

### 4.1.3 Tissue engineering approaches for microvessel perfusion

Current microvessel perfusion technologies have major limitations, and the scaling up from microfluidics to large-scale culture poses many challenges. Engineered tissues for regenerative medicine applications have a demanding set of requirements and the creation of thick, dense, implantable tissues requires engineering manipulations not possible in microfluidic devices. In our lab, we use uniaxial constraints and allow our samples to undergo cell-induced gel compaction to create a dense and aligned tissue. In a microfluidic device, such manipulation of the tissue would not be possible. We use bioreactors and large volumes of culture medium to condition our tissues and sustain the high density of cells that we can achieve in these bioreactors. Microfluidic systems would not allow for such conditioning and would not be able to sustain the high metabolic demand required for a large, densely compacted tissue.

But with added flexibility comes greater challenges. The transition from microfluidics to bioreactors makes perfusion much more difficult. The idea of flow connectivity, or the necessity to connect tissues to flow paths and direct the flow through the tissue, becomes a major design challenge. Flow will take the path of least resistance, and any gap between the flow path and the tissue will result in a

leak. Steps must be taken to ensure that the path of least resistance is the desired path through the tissue, and ultimately through the microvessel lumens, while still ensuring the tissue is getting the culture medium it needs to survive.

Major advances have already been made toward the creation of an aligned microvascular tissues with the highest reported density of engineered microvessels that can be perfused in vivo (Chapter 2). These tissues, however, have yet to be perfused in vitro. A bioreactor for perfusion culture of similarly prepared microvascular tissues was developed by Krissy Morin and was shown to enhance microvessel density under low flow conditions, though the microvessels were found to be closed to flow, and the tissues were only perfused interstitially through the matrix rather than through the microvessel lumens.[43]

### 4.1.4 Bioreactor design and strategy for a perfusing microvascular tissues

Optimal design criteria for an engineered microvasculature are that it is perfusable, aligned, stable, and contains enough microvessels to meet oxygen and nutrient demands of the tissue. Perfusion of the tissue must occur through the lumens of the microvascular network in order for the tissue to perform its function. This means that either the microvessels must be open at the ends of the tissue, or they must anastomose with a larger channel that is open to flow. Anisotropic alignment of microvessels is highly desirable because it provides a natural inlet and outlet for perfusion and would match the natural alignment of

native myocardium, as well as many other aligned tissues. Stability is important for any engineered tissue, but it is especially important for engineered microvasculature to remain intact and not collapse or regress, otherwise the supply of oxygen and nutrients to cells in the tissue would be compromised.

In this work, an engineering strategy was developed to connect microvessels to flow and enable perfusion of their lumens. Fibrin gels with entrapped BOECs and PCs were formed with 150 μm diameter microchannels inside them that connected to the inlet and outlet flow tubes. (Figure 4-1) These microchannels could be endothelialized with BOECs, and then perfused. Perfusion of these microchannels would force interstitial flow across the BOEC-lined walls. Interstitial flow across an endothelial monolayer has been shown to induce angiogenic sprouting in several studies.[51,52,57,58,95] This, combined with the conditions deemed favorable for sprouting, vasculogenesis, and inosculation in Chapter 3, could promote sprouting from the BOEC-lined microchannels and anastomosis with the microvessels in the fibrin gel. If successful, flow would be directed from the BOEC-lined microchannels, through the sprouts, and into the lumens of the microvessels, thus perfusing the microvascular network (Figure 4-1D).

## 4.2 Materials and Methods

### 4.2.1 Cell Culture

Human BOECs were isolated from adult peripheral blood by the lab of Dr. Robert Hebbel at the University of Minnesota – Twin Cities[25]. Briefly, BOECs were screened for VE-cadherin, flk-1, vWF, CD36, and CD14 (negative). Passage 5 BOECs were thawed and plated on 0.05 mg/ml collagen I – coated flasks in BOEC medium (EGM-2 bulletkit medium (Lonza) supplemented with 10% FBS, 1% penicillin/streptomycin (Gibco)). Medium was changed every other day and BOECs were passaged after 4 days, then plated and cultured for 4 more days prior to harvest.

Human brain vascular PCs (ScienCell, fetal, characterized by immunofluorescence with antibody specific to α-smooth muscle actin) were transduced to express GFP and obtained from the lab of Dr. George Davis at the University of Missouri. Passage 6 PCs were thawed and plated on 1 mg/ml gelatin-coated flasks in PC medium (13% FBS, 1% penicillin/streptomycin (Gibco), 10 ng/ml gentamicin (Gibco) in low-glucose DMEM (Lonza)). Medium was changed every 2-3 days and PCs were harvested after 10 days.

### 4.2.2 Assembly of perfusion chambers

Perfusion gels are cast in perfusion chambers (Figure 4-2), which are assembled as follows. For each perfusion chamber, a custom ultem mold (consisting of a main piece and a removable bottom), 4 polycarbonate screws and nuts, 2 silicon o-rings, 2 glass capillary tubes flared at one end, and 2 PTFE coated wires are autoclaved along with a plastic culture jar that can hold up to 6 perfusion gels, a 0.5x0.5x1.5cm piece of scrap Teflon, and a blunt forceps.

Once autoclaved, the screws, bolts, wires, and culture jars were set aside for later use and the remaining materials were layed out on a sterile drape or the inside of the large autoclave package in the cell culture hood. Using sterile gloves, perfusion chambers were assembled and placed in a large sterile petri dish for later use.

### 4.2.3 Casting perfusion gels

Immediately prior to casting, warm BOEC medium was pipetted into each glass capillary tube to remove air from the system. Next, PTFE-coated wires were threaded through the glass capillary tubes so that each wire protruded approximately 15 mm into the well space (Figure 4-2). In some cases, only a single wire was used. An anti-static gun was used to dissipate static charge on the wires when both wires were present in order to prevent the two wires from touching.

Droplets of fibrin gel solution containing BOECs and PCs were pipetted into the well space of each perfusion mold, making sure the gel solution covered the flare of each glass capillary tube. The gel solution was made up of 2.55 mg/ml fibrinogen (Sigma), 200 ng/ml of stem cell factor (SCF), interleukin-3 (IL-3), and stromal derived factor 1α (SDF-1α) (R&D Systems), $2x10^6$ BOECs per mL, $0.4x10^6$ PCs per mL, 1.25 U/ml thrombin (Sigma) and Medium 199 basal medium (Gibco) (M199). The total volume of each gel was 400 µl. Samples were incubated at 37°C, 5% $CO_2$ for 20 min to allow for gelation to complete.

After gelation was complete, samples were removed from the incubator and, using sterile gloves, a sterile razor blade was used to pry apart the bottom ultem piece from the rest of the chamber and to carefully detach the gel from the bottom ultem surface. Then autoclaved screws were inserted from the top through each of the four holes in the perfusion chamber, and nuts were loosely threaded onto each screw. A few drops of BOEC medium was pipetted onto the top of the gel surface, then the perfusion chamber was inverted and placed in a culture jar containing 70 ml of BOEC medium, or just enough to cover the top of the perfusion chamber. Medium was replaced every 2-3 days. In these samples, microvessels self-assemble and PCs are recruited to the abluminal side of the vessels after 5 days of *in vitro* culture.

### 4.2.4 Microchannel formation and seeding

Microchannels were created in the fibrin gels by quickly pulling out the PTFE-coated wires while the chambers were submerged, leaving behind 150µm channels. At this point, the microchannels could be seeded with BOECs, if desired. A suspension of $0.1x10^6$ – $10x10^6$ BOECs/mL (depending on the experiment) in M199 was used for seeding the microchannels.

A variety of methods for microchannel seeding were evaluated. In early experiments, a 1 cm segment of silastic tubing was connected to the glass capillary tube and 20 µl of $10x10^6$ cells/ml EC suspension was pipetted into the tubing and pushed into the capillary tube and microchannel ("pipet + tubing" method). The "direct pipet" method involved directly pipetting the cell suspension into the end of the glass capillary tube using a 0.1-10 µl pipet tip and slowly dispensing 10 µl of cell suspension over the course of 30 seconds with the receiving glass capillary tube pointing straight up. Dispensed liquid was wicked down the glass capillary tube. A second dose of 10 µl of either cell-suspension or M199 followed.

The "perfusion seeding" method used the syringe pump, a 1ml syringe, and 1mm silastic tubing into which the cell suspension was injected using a syringe needle. The cell suspension was then pushed downstream into the microchannels using the syringe pump at a flow rate of 10 – 60 µl/min, depending

on the experiment. With this seeding method, both channels could be seeded simultaneously if both glass capillary tubes were connected to perfusion tubing, or they could be seeded sequentially by connecting one glass capillary tube and then the other to the perfusion tubing.

The timing of the wire-removal and method of microchannel seeding was varied in order to determine ideal conditions for endothelialization and maintenance of the microchannels. Several static culture experiments were conducted both separately and in parallel with perfusion studies to better understand microchannel formation, maintenance, endothelialization, and sprouting.

### 4.2.5 Perfusion gel compaction and alignment

Alignment of the microvascular network and tissue fibrils was achieved by detaching the gel from the chamber walls and allowing cell-induced compaction to remodel the gel while constrained in the longitudinal direction. Compaction was initiated after 5 days of culture, at which point samples were detached from the walls of the perfusion chambers by sliding a dental pick between the gel and the chamber wall on all sides. The gel was not detached from the flare of the glass capillary tubes. The samples were then free to compact uniaxially via cell-induced compaction while the gel remained anchored at a fixed length by the two glass capillary flares (Figure 4-2C). It has been shown that lateral compaction

causes alignment of the microvessels and fibrin fibrils in the longitudinal direction.[74]

### 4.2.6 Perfusion bioreactor design

A perfusion bioreactor was designed and built to culture and perfuse these microvascular tissues in vitro (Figure 4-3). The lid of a shallow glass Pyrex™ baking dish was modified to contain 13 air-tight flow ports with female-female luer connectors on either side for the connection of perfusion tubing and a syringe filter to allow for air transfer through a 0.22 µm filter. For each flow loop, a 1 ml syringe connected to a segment of 3/16" silastic tubing, which connected to the flow port in the lid, which connected to another segment of 3/16" silastic tubing, which was slipped onto the glass capillary tube of the perfusion chamber. The outlet of the perfusion chamber could either be connected to a second flow loop or remain open to the culture medium in the dish. If the outlet was connected to a second flow loop, care was taken to ensure the outlet was not higher or lower than the perfusion gel and that the syringe was not connected to ensure the outlet was at zero pressure.

The perfusion bioreactor was designed to perfuse 6 samples simultaneously with the ability to alternate the flow direction by alternating the flow loop that was connected to the syringe pump. Perfusion samples were not embedded in agarose, but rather, they were immersed in 170 ml of medium,

enough to cover the samples in the bioreactor. This was to ensure sufficient nutrient availability, as the flow rates selected for experimentation were chosen based on mechanical stimuli and were too low to provide sufficient nutrients to the tissue.

Perfusing a tissue immersed in medium required extra care to ensure that flow was guided through the tissue. Fluid would take the path of least resistance, and thus, the microchannels provided the least-resistance pathway for flow. The presence of microchannels in the gel directed flow from the inlet flare down the inlet microchannel, across the gel toward the outlet microchannel, and then down the outlet microchannel and into the outlet glass capillary tube (Figure 4-1C). Without microchannels, the flow would have quickly channeled to the nearest tissue edge.

Perfusion bioreactor components were assembled and autoclaved, and the perfusion lines were primed with warm culture medium and stored in a 37°C incubator at least several hours prior to the start of perfusion. This ensured bubbles formed from reduced oxygen solubility at warmer temperatures could be flushed prior to connection of the perfusion samples.

### 4.2.7 Perfusion regimens

A target superficial velocity of 10 μm/min across the microchannel wall was selected based on literature reports of enhanced angiogenic sprouting under

these conditions[51,52]. For the microchannel geometry used in these studies, this translated to a perfusion flow rate of 0.072 µl/min.

Perfusion of microvascular tissues of this scale, however, was unchartered territory, thus a variety of perfusion regimens were tested while maintaining the same flow rate for each condition. The first “early perfusion” approach involved perfusion of uncompacted gels in the first five days of culture. (Figure 4-4) In these experiments, samples were connected to the bioreactor and perfusion was begun anywhere from 50 minutes to 24 hours after microchannel seeding. Perfusion culture was continued until day 5, at which point samples were harvested for analysis.

The second “compaction perfusion” approach involved initiating perfusion immediately after gels were detached from the walls of the perfusion chambers (Figure 4-4). In these experiments, samples were cultured statically for 5 days, transferred to the perfusion bioreactor, detached (as described above) to allow cell-induced gel compaction and alignment to take place, and perfused. Perfusion was continued as the gels compacted and aligned over several days, and were harvested after 3-6 days of perfusion, or 8-11 days of total culture.

The third “late perfusion” approach delayed perfusion until after compaction had begun (Figure 4-4). In these experiments, samples were cultured statically for 5 days, then detached and allowed to compact in static

culture. Perfusion was initiated anywhere from 1 to 3 days after detachment (days 6 to day 8 of culture).

### 4.2.8 Microbead perfusion

At the time of harvest, perfusion chambers were disconnected from the perfusion tubing and a suspension of 1 µm yellow-green fluorescent microbeads in M199 was loaded into the perfusion tubing and then reconnected to the perfusion chambers. The microbead suspension was then perfused into the tissue at a rate of 10 µl/min for 2-10 minutes. The microbead suspension functioned as a perfusion tracer that would aid in evaluating whether the microvessels and microchannels were open to flow and had been perfused. Non-perfused control samples could also be perfused with the microbead suspension by connecting them to the perfusion bioreactor flow loops at the time of harvest.

### 4.2.9 Tissue harvest and characterization

After microbead perfusion, the inlet of each tissue was marked with a droplet of verhoeff's stain and samples were harvested and fixed with 4% paraformaldehyde (PFA) (Electron Microscopy Sciences) for 10 min at room temperature, then rinsed in phosphate buffered saline (PBS) (Corning).

To prepare for freezing and histological sectioning, samples were placed in infiltration solution 1 (30% w/V sucrose in PBS) at 4°C overnight and then

transferred to infiltration solution 2 (50% infiltration solution 1, 50% embedding medium (Tissue-Tek OCT)) at room temperature for 4 hours. Samples were then frozen in embedding medium and cross sections were cut by cryosectioning 9 µm thick cross-sections for immunohistochemical staining. Sections were stained for hCD31 to visualize the microvascular network and microchannel endothelialization. For hCD31 staining, sections were blocked in 5% Normal Donkey Serum (Jackson Immunoresearch) for 2 hours, then incubated in 1:40 antibody to human CD31 (hCD31) (Dako) in blocking serum for one hour at room temp or overnight at 4°C. Three 5 min PBS rinses were performed, then the samples were incubated in 1:200 donkey anti-mouse secondary antibody conjugated with Alexa Fluor® 594 (Jackson Immunoresearch) in PBS for 1 hour at room temp or overnight at 4°C. After secondary antibody incubation, samples were incubated in 1:10,000 Hoescht 33342 (Invitrogen) in PBS for 10 min, followed by two 5 min rinses in PBS. Fluorescent mounting medium (Dako) was applied to slides prior to adding coverslips, and once dry, hCD31 stained cross-sections were viewed and imaged with either confocal or fluorescence microscopy.

## 4.3 Results

### 4.3.1 Microchannels can be seeded with BOECs, endothelialized, and form sprouts in static culture

Gels were cast without any cells in the gel formulation, wires were removed, and the microchannels were seeded with a pipet connected to silastic tubing delivering 20 µl of 10M/ml HUVEC suspension (BOECs were unavailable) over about 5 seconds (240 µl/min). Cell-free gels were used in this experiment to better visualize endothelial coverage of seeded microchannels. With 2 days of static culture, this seeding method resulted in complete endothelialization of the microchannels with some angiogenic sprouting observed (Figure 4-5A). However, it also appeared to cause distortions to the microchannel, perhaps due to the irregular and fast seeding flow rate.

When BOEC/PC gels with microchannels seeded with BOECs using the perfusion seeding method (120 µl/min or 60 µl/min) were cultured with 5 days of static culture, microchannels were endothelialized and maintained throughout the culture period, and many sprouts were observed extending from the microchannels (Figure 4-5B,C). The microchannels were still, somewhat distorted, with segments of varying diameters appearing in histological sections. Interestingly, unseeded microchannels also had endothelialized microchannels (Figure 4-5D).

### 4.3.2 Early perfusion culture supports microchannel endothelialization and sprouting, but does not result in microvessel perfusion.

Even when microchannels were perfusion seeded at ultra-low flow rates (0.043µl/min) from day 0, the microchannels were endothelialized and sprouting was seen from the microchannels. (Figure 4-6) Samples with microchannels seeded at 60 µl/min on day 0 then perfused for 5 days at 0.043 µl/min showed complete endothelialization of the microchannels and many sprouts (Figure 4-6B), but no microbeads were present in the microvessels. Control samples containing unseeded microchannels cultured statically also had endothelialized microchannels with sprouts (Figure 4-6C).

To attempt to prevent distortion of the microchannels, seeding was delayed to day 1 to give the samples a day to deposit matrix and strengthen the tissue. Microchannels perfusion seeded on day 1 at 60 µl/min then perfused through day 5 at 0.072 µl/min also contained endothelialized microchannels, but again, the microchannel diameter varied widely and appeared to have been distorted by flow (Figure 4-6D). These samples were perfused with microbeads at the time of harvest to check for perfusion of the microchannels, sprouts, and microvessels. Microbeads were found in the endothelialized microchannels, but not in any sprouts or microvessel lumens.

### 4.3.3 Compaction presented new perfusion challenges

None of the early-perfused samples contained microbeads inside the lumens of the microvessels and the microvessels appeared to be distorted with flow, so different perfusion regimens were tested. Samples were cultured for 5 days with the wires left in place, gels were detached to allow for compaction, and then the wires were removed on day 6 just prior to seeding and perfusion. However, removal of the wires became difficult once the gels had compacted, and many samples were destroyed in the wire-removal process. Surviving samples were seeded and perfused and controls were cultured statically. This method led to mostly-endothelialized microchannels with sprouts (Figure 4-7A) in perfused samples while non-perfused controls had BOEC-filled microchannels (Figure 4-7B).

Earlier seeding was tested to give the microchannels more time to be endothelialized before compaction. Microchannels were seeded on day 0, detached and perfused on day 5 and harvested on day 10. These samples, however, did not compact as much as they typically do, and they had fewer microvessels present in the gel at harvest. Partially endothelialized microchannels were present, however, with sprouts extending from the endothelium (Figure 4-7G,H). These microchannels did not exhibit signs of distension from flow, though some histological sections showed microchannels

filled with aggregated BOECs. No microbeads were found in the microchannels or the microvessel lumens for any samples. A second attempt at this perfusion regimen, with perfusion delayed to day 6, again allowed for the survival of the microchannels without distension, although microchannels were again occluded with aggregated BOECs (Figure 4-7I,J). These samples did show normal tubule formation, with many lumen-containing microvessels present, but microbeads perfused at harvest were not found in any lumens or microchannels.

### 4.3.4 Unseeded microchannels were not maintained

To attempt to prevent aggregation of BOECs in the microchannels and determine whether microchannel seeding was necessary, experiments were conducted with unseeded microchannels. When wires were removed just prior to detachment, but not seeded, and gels were perfused from day 5 through day 10, the microchannels could not be found in the resulting histological sections. Microbead perfusion at harvest showed no microbeads in the gel. Indentations were observed on the outer surface of the gel that suggested the wires may have been too close to the surface of the gel, resulting in a loss of the microchannel during compaction and a distorted, yet attractive, sample shape. (Figure 4-7C,D) When the experiment was repeated with similar conditions, except perfusion was delayed to day 6, microchannels could not be found in any histological sections (Figure 4-7E,F).

### 4.3.5 Further perfusion studies were hindered by catastrophic cell death unrelated to perfusion

None of the previous culture conditions led to perfusion of the microvessel lumens. Results from all other testing of perfusion regimens and microchannel seeding methods were impeded by catastrophic cell death in recent experiments. Microchannel formation, seeding, and perfusion were tested in over 35 separate experiments conducted over the course of 3 years. Of those experiments, 15 resulted in gels with widespread cell death and failure of the cells to attach and spread in the matrix, 8 of these experiments occurring in the past 12 months. The cause for this failure was tested in 15 different experiments investigating material toxicity, fibrin gelation in other geometries, mechanical manipulations, and environmental factors, but a conclusive solution or cause was never determined.

## 4.4 Discussion

This work investigated methods for connecting microvessels to flow in large-scale tissues. The general approach taken for achieving this aim was to create endothelialized microchannels in microvascular fibrin gels, induce sprouting from the microchannels, and encourage anastomoses to form between the sprouts and the microvessels in the rest of the tissue, all while perfusing the microchannels with culture medium.

In static culture experiments, microchannels were successfully formed and maintained over 5 days of culture, with complete endothelialization and sprouting under a variety of conditions and seeding methods, validating this method as a potential perfusion strategy. Distortions were present in many of the microchannels for all seeding methods, which could be attributed to the flow rate being too high for the freshly cast fibrin. Microchannel distention could also have occurred as a result of irregularities in the flow rate delivered to the microchannels, especially during connection of perfusion tubing and manipulation of the samples, when some pressure fluctuations are unavoidable.

Early perfusion of seeded microchannels also supported maintenance and endothelialization of the microchannels, with many sprouts extending from the BOEC-lined channels. The resulting microchannels did have a wide variety of shapes and sizes at the time of harvest (day 5), however, and it appeared that flow, either from seeding or from perfusion culture, was distorting the channel shape. While a variable channel diameter would may not be incredibly damaging to the success of this method, it does hinder the delivery of a consistent shear stress throughout the channel, which has been shown to affect sprouting from endothelialized channels.[95]

In attempts to prevent microchannel distortion, samples were allowed to culture without perfusion for the first 5 days prior to detachment and compaction.

It was discovered that the wires that formed the microchannels were very difficult to remove once the samples had been detached and started to compact. This eliminated late-seeding options, and meant that wire removal and microchannel seeding had to take place on day 0 through day 5 before detachment and compaction.

A new seeding method (the “direct pipet” method) was also developed that did not require connecting the glass capillary tubes to the perfusion tubing, and used much smaller seeding volumes, with a similar seeding flow rate. It was thought that the “perfusion seeding” method may have been responsible for the microchannel distension observed in early experiments because it required large volumes of medium to be flushed through the microchannels at fairly high flow rates in order to deliver the cells to the microchannels. Experiments using the new “direct pipet” seeding method and a “late perfusion” regimen showed less microchannel distension while still achieving endothelialization and sprouting. Some microchannels, however, were occluded with aggregated BOECs, and perfused microbeads were not found in any of the microchannels. The BOEC aggregation could be a result of seeding an excess of BOECs or it could also be a result of gel compaction. The “direct pipet” seeding method was developed during the time of widespread cell death, so it was not able to be tested on

uncompacted gels or early perfusion gels, making it difficult to determine the cause for the microchannel occlusion.

An unexpected outcome of these experiments was that the unseeded control samples with wires removed on day 0 were still endothelialized by BOECs recruited from the surrounding fibrin. When samples with unseeded microchannels were exposed to perfusion and compaction, however, the unseeded microchannels were not maintained. In these cases, the wires were not removed until just prior to detachment, when compaction is initiated. It is likely that the compaction of the gel (most of which occurs within 24 hours) caused the newly formed microchannels to collapse, as there was not time for BOECs to be recruited from the existing microvascular network in order to endothelialized the microchannel and strengthen it by depositing extracellular matrix.

More experimentation implementing the conditions found optimal for sprouting and inosculation in Chapter 3 was attempted, specifically introducing a hybrid medium culture approach, but attempts were wasted by the ongoing cell-death issues, described previously. Future experimentation (when cell viability from experiment to experiment is more stable) should include a hybrid medium culture approach.

Future studies should also investigate the success of the “direct pipet” seeding method on day 0 with perfusion culture beginning within the first 24 hours and continuing through day 5 as well as through day 8, as detachment and compaction of early perfusion samples was never investigated. If the microchannels are already endothelialized and being perfused at the time of compaction, it would likely help keep the channels from collapsing or becoming occluded as the gel compacts, remodels, and aligns.

Another option with this perfusion strategy and bioreactor is the possibility of reversing the flow direction throughout culture. While this was not tested in these experiments, it could be useful if it is discovered that flow plays a role in the anastomoses of sprouts and microvessels. The flow direction could be reversed to induce sprouting and anastomosis from the opposite microchannel, increasing the likelihood of creating a continuous network of perfusable microvessels from one microchannel to the other.

In these studies, fibrin gels with entrapped BOECs and PCs were formed with microchannels inside them that connected to glass capillary tubes where flow was delivered. These channels were endothelialized with BOECs under a variety of conditions and were perfused when flow was initiated in the first 24 hours. Angiogenic sprouts were observed extending from the endothelialized microchannels and many microvessels were present in the surrounding tissue.

Inosculation of these sprouts and microvessels could potentially yield a continuous microvascular network connected to the perfused microchannels, thus enabling perfusion of the lumens of the microvascular network.

While this method was not tested to completion, many advances were made. The microchannels were endothelialized and perfusable. Sprouting was observed from the microchannel wall in many of the perfusion regimens tested, including early perfusion and early seeding + late perfusion. Samples were able to be compacted and aligned, yielding many aligned lumen-containing microvessels surrounding the sprouting endothelialized microchannels. Further work optimizing this perfusion culture strategy could very likely lead to the perfusion of these microvascular tissues.

## 4.5 Figures

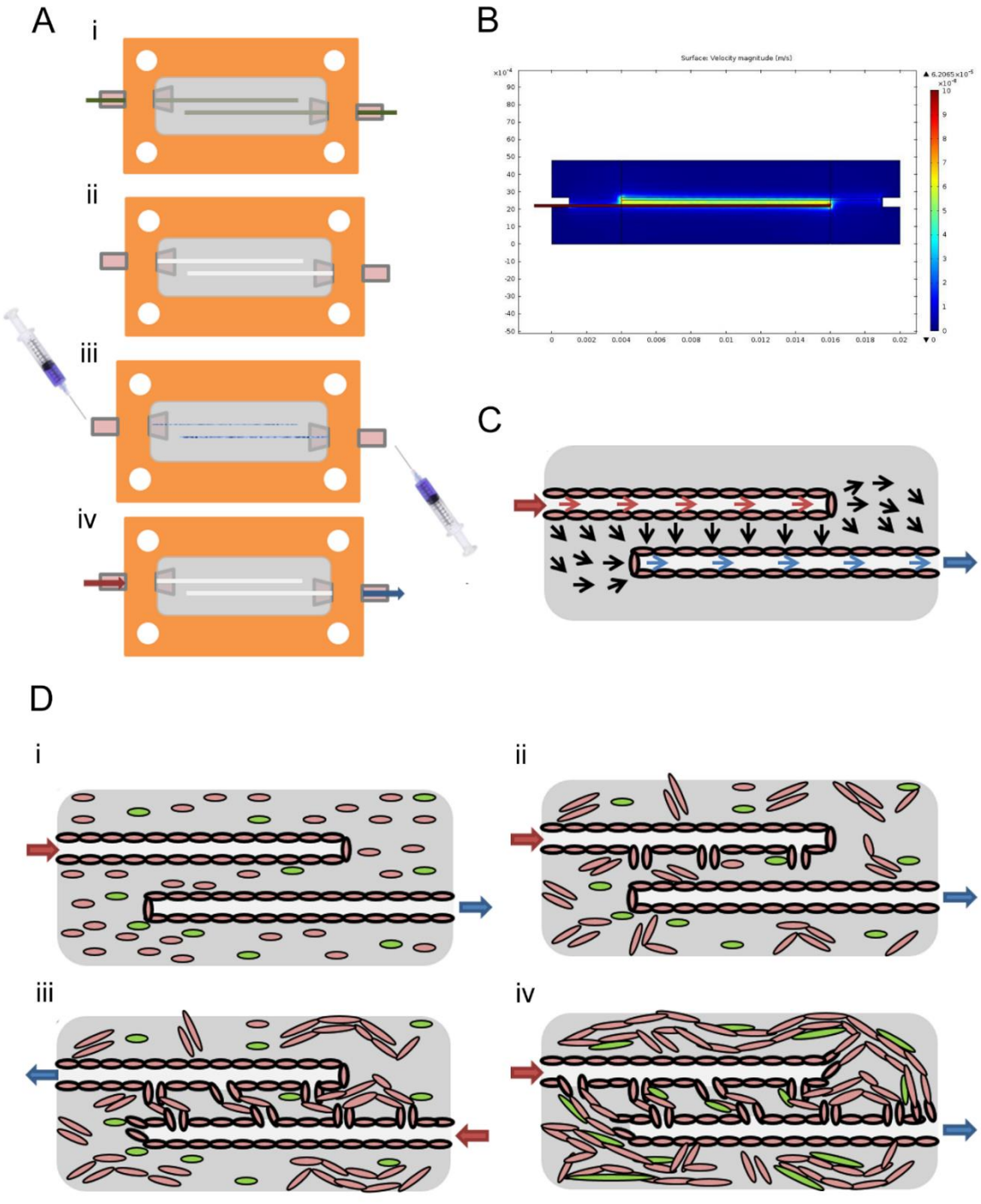
A
i
ii
iii
iv
B
Surface: Velocity magnitude (m/s)
C
D
i
ii
iii
iv

**Figure 4-1.** Sample Preparation and Perfusion Flow Path.

A. Perfusion chamber and sample preparation technique. (i) Fibrin gel-forming solution with suspended BOECs and PCs is cast in the well of an ultem perfusion mold containing an inlet and outlet glass capillary tube with 150 μm wires extending into the gel. (ii) The wires are removed to reveal microchannels in the fibrin gel. (iii) Microchannels are seeded by injecting a BOEC suspension into the inlet and outlet capillary tubes and allowing cells to adhere to the channel walls. (iv) The microchannels and the gel in-between are perfused by pumping culture medium into the inlet capillary tube. B. Flow field modeled in COMSOL (printed with permission from Michelle Lenz) showing that the majority of fluid flow in this configuration occurs between the two microchannels. C. Cartoon of the flow field between two BOEC-seeded (pink) microchannels, with channel perfusion depicted by inlet arrows (red) and outlet arrows (blue) and interstitial flow depicted by black arrows. D. Strategy for perfusing microvascular tissues. (i) BOECs (pink) and PCs (green) are entrapped in fibrin gel with BOEC-seeded microchannels. (ii) Angiogenic sprouting induced by interstitial flow occurs in the inlet microchannel while microvessels begin to form in the bulk gel. (iii) Flow direction can be reversed, if necessary, to encourage sprouting in the outlet microchannel. Microvessels continue to develop in the bulk gel and begin to connect with the sprouts. (iv) Eventually sprouts from each channel anastomose

with microvessels spanning the gel between the channels, perfusing the microvessels in the fibrin gel.

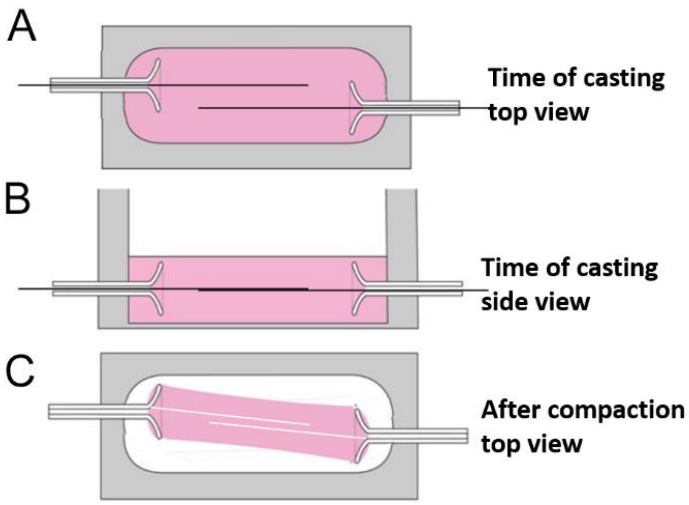


**Figure 4-2.** Perfusion Chamber Schematic.

A. Top-down view and B. Side-view of a fibrin gel (pink) in the ultem perfusion chamber (grey) with inlet and outlet glass capillary tubes (the offset of the capillary tubes is exaggerated) and microchannel-forming wires. C. Top-down view of a fibrin gel after the wires have been removed, the gel has been detached from the chamber walls, and compaction has occurred.

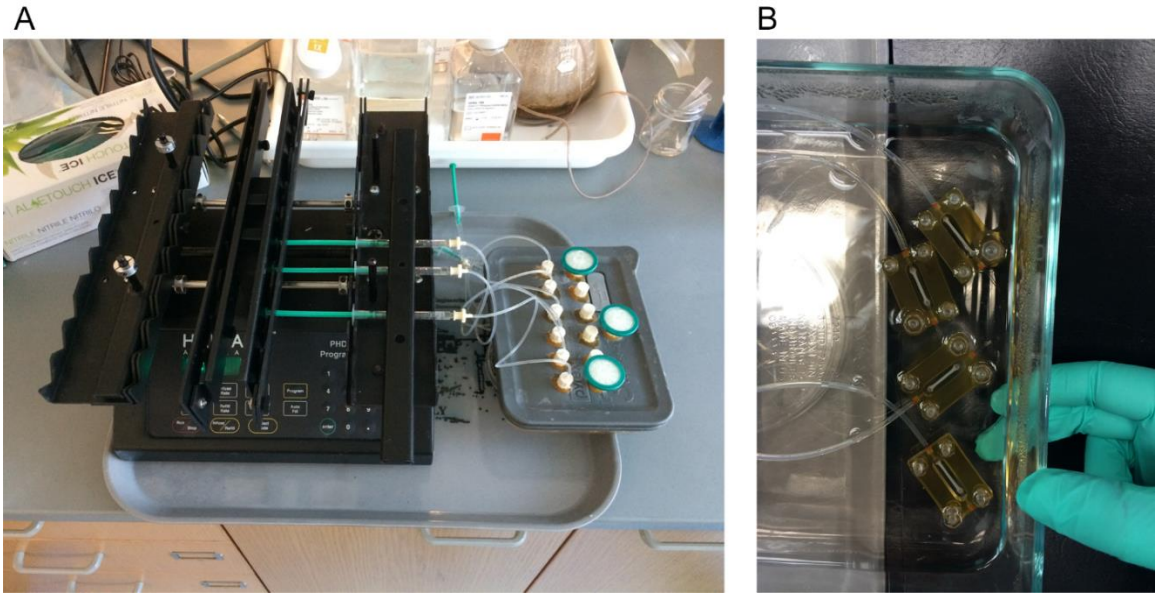


**Figure 4-3.** Perfusion Bioreactor.

A. Bioreactor set up consisting of a syringe pump, 1 mL syringes, 3/16” silastic tubing, luer connectors, a Pyrex™ baking dish with a modified lid and 3 syringe filters for air transfer. B. Inside of the bioreactor culture dish showing four perfusion chambers connected to flow tubing with compacted gels (white) suspended between the inlet and outlet capillary tubes.

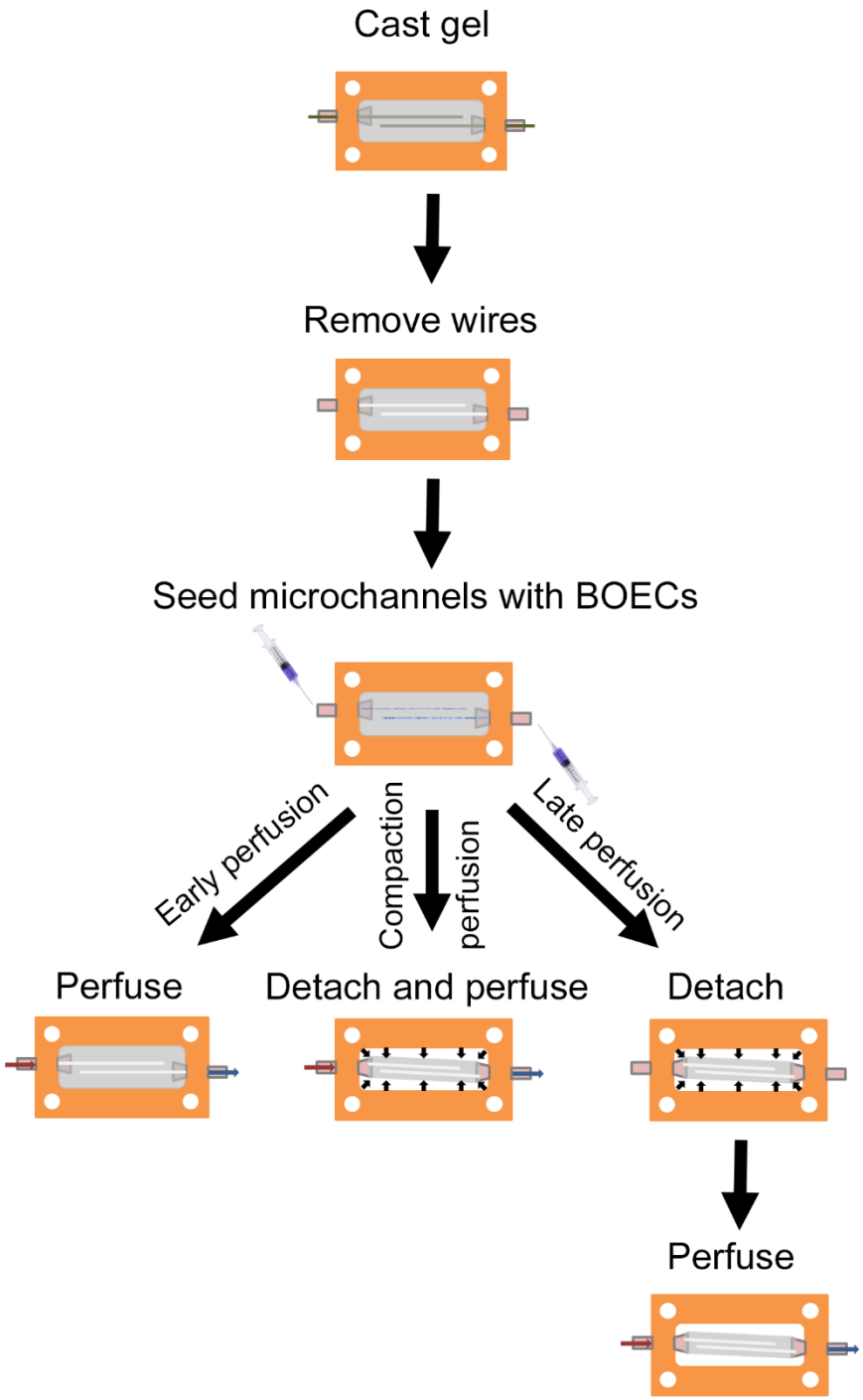
Cast gel
Remove wires
Seed microchannels with BOECs
Early perfusion
Compaction
perfusion
Late perfusion
Perfuse
Detach and perfuse
Detach
Perfuse

**Figure 4-4.** Perfusion Regimens.

Each regimen begins with casting of a fibrin gel with entrapped wires. The wires are removed to reveal microchannels, which are then seeded with BOECs to endothelialized the microchannels. Then either the “early perfusion”, “compaction perfusion”, or “late perfusion” regimen is initiated. In “early perfusion, the samples perfused within the first 24 hours of culture. In “compaction perfusion”, the samples are perfused during and after compaction, which occurs on day 5. With “late perfusion”, samples are detached and allowed to compact, and then once compaction has occurred for at least 1 day, perfusion is initiated.

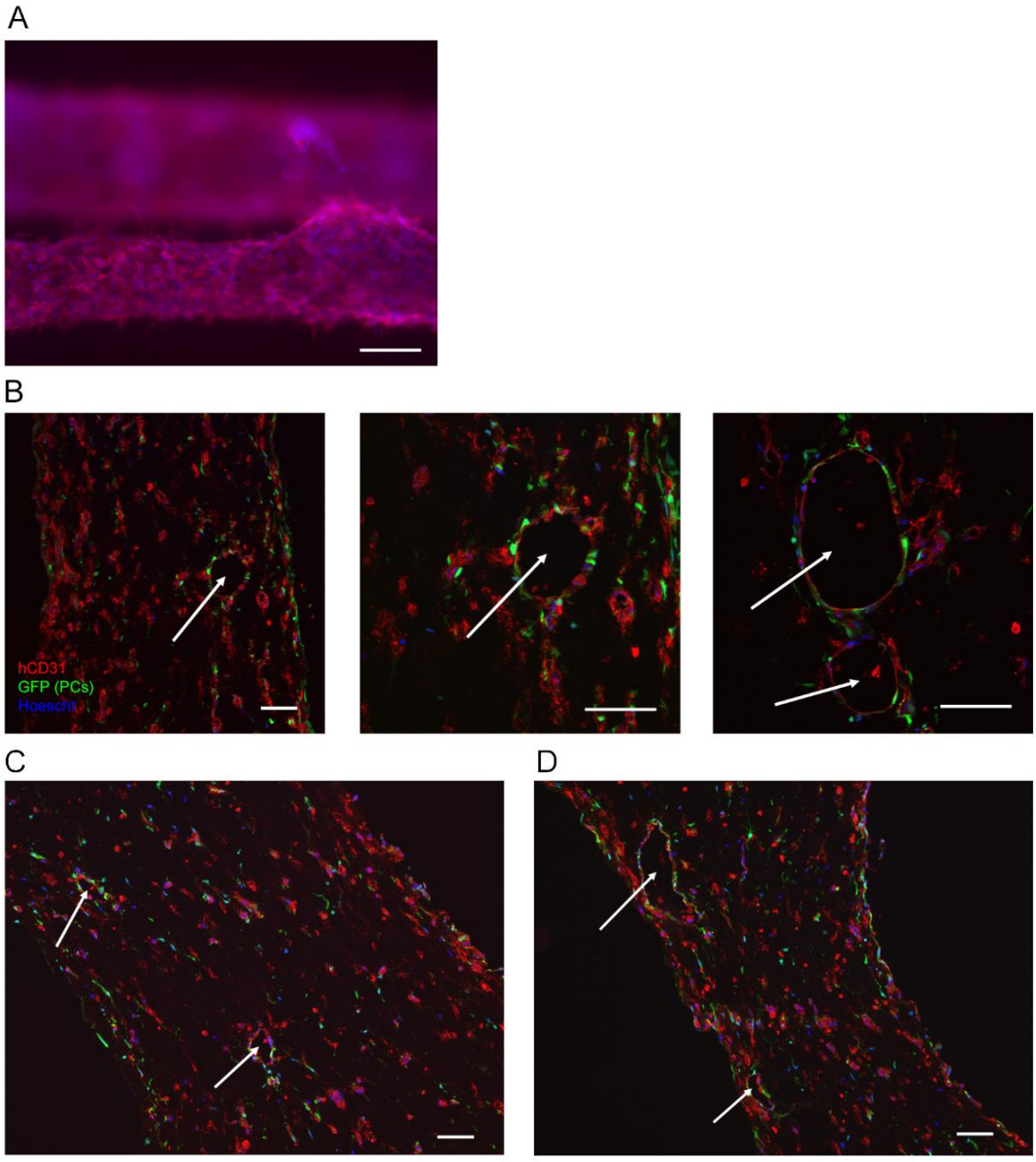


**Figure 4-5.** Endothelialization in Static Culture.

A. Whole-stain image of a cell-free fibrin gel with microchannels seeded with HUVECs using the “pipet + tubing” seeding method. Complete endothelialization

occurred after 2 days and small sprouts were visible, but deformations in the channel were also observed. B. BOEC/PC gels with microchannels “perfusion seeded” at 120 µl/min on day 0, then cultured statically for 5 days. Microchannels were completely endothelialized with recruited PCs and sprouts extending from the microchannels. C. Microchannels that were “perfusion seeded” at 60 µl/min then cultured statically for 5 days and D. Microchannels that were left unseeded and cultured statically for 5 days both were endothelialized. Scale bar = 100 µm.

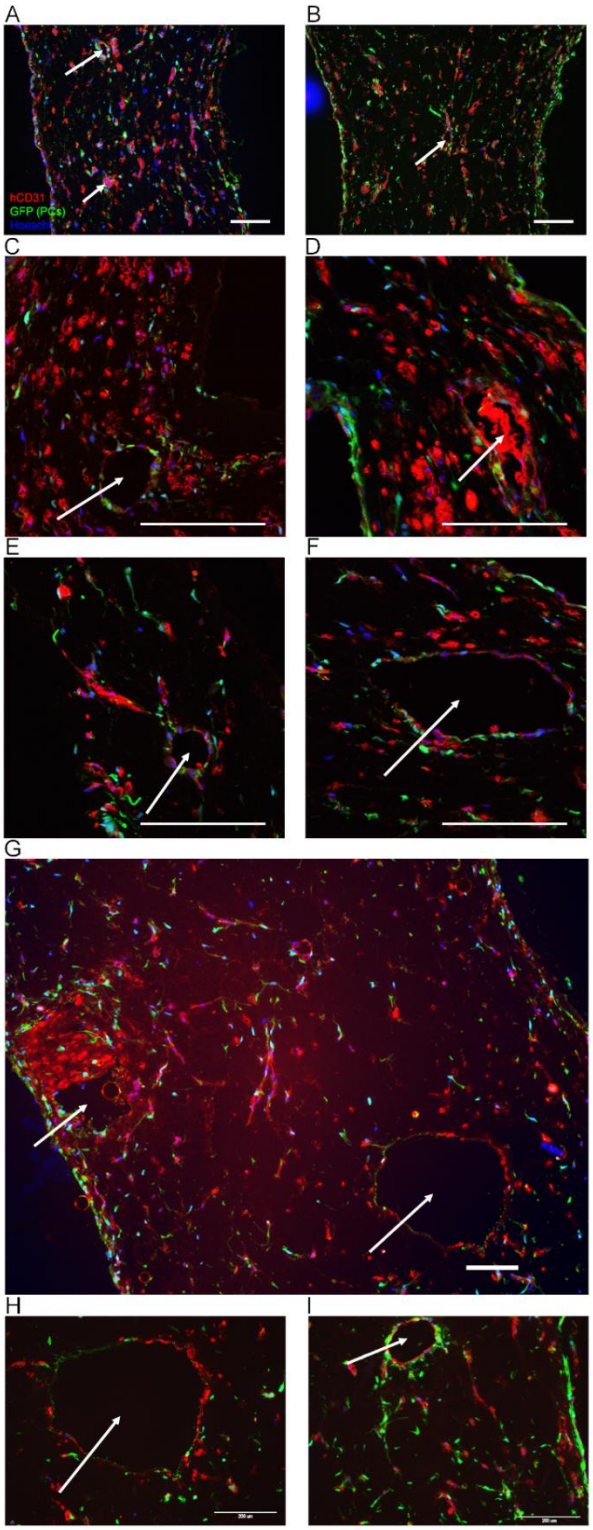
A
B
hCD31
GFP (PCs)
C
D
E
F
G
H
I

**Figure 4-6.** Early Perfusion Results.

Arrows indicate the presence of a microchannel. A,B. Microchannels perfusion seeded at ultra-low flow rates (0.043µl/min) were endothelialized and sprouting was seen from the microchannels. C,D. Microchannels seeded at 60 µl/min then perfused for 5 days at 0.043 µl/min showed complete endothelialization of the microchannels with some aggregated BOECs in the channels and many sprouts. E,F. Unseeded microchannels cultured statically for 5 days were mostly endothelialized and contained sprouts. G,H,I. Microchannel seeding delayed 1 day. Perfusion-seeded at 60 µl/min and perfused from day 1 – 5 at 0.072 µl/min. Inlet microchannels (H) and outlet microchannels (I) were mostly endothelialized with sprouts and contained perfused microbeads (1µm green dots), but neither the sprouts nor the microvessel lumens contained microbeads. Scale bar = 200 µm.

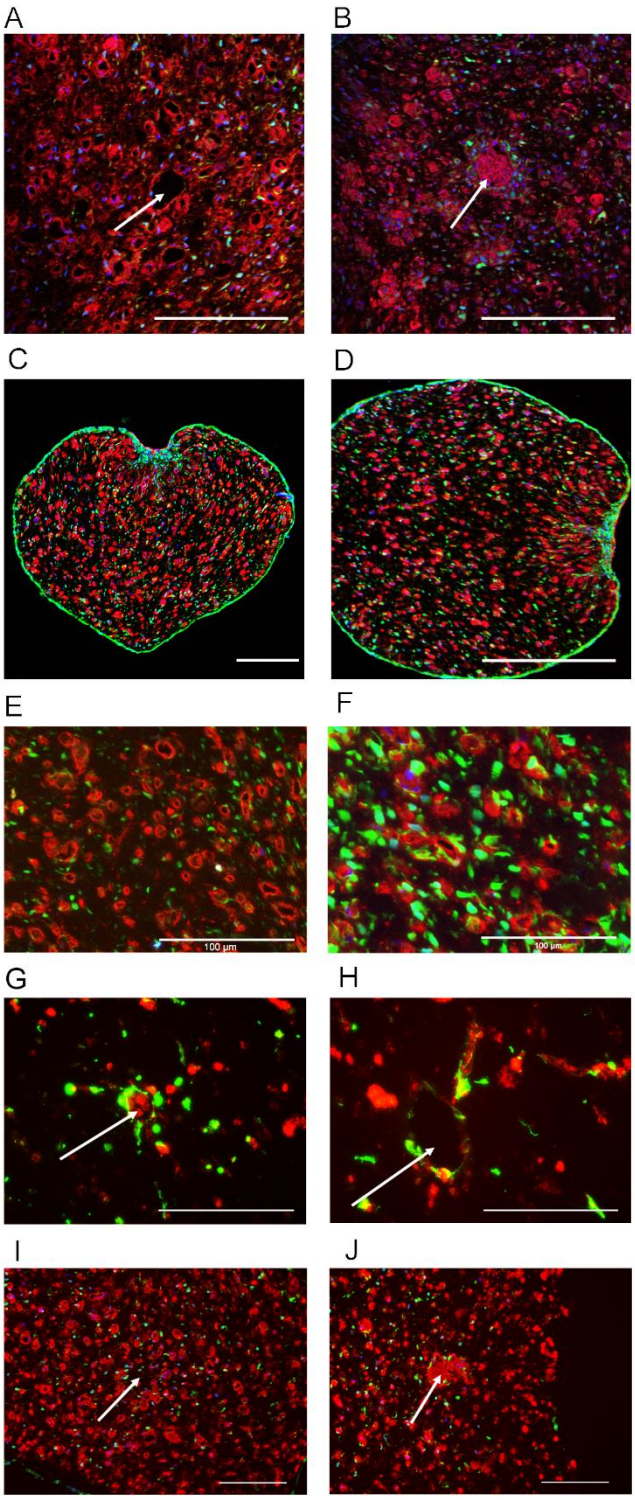
A
B
C
D
E
F
100 µm
100 µm
G
H
I
J

**Figure 4-7.** Compaction Perfusion and Late Perfusion Results.

A. Microchannels perfusion seeded on day 6 at 60 µl/min, perfused day 6-7 at 0.072 µl/min, then static culture day 7-11. Microchannels were endothelialized and contained many sprouts but did not contain any perfused microbeads. B. Unseeded microchannels cultured statically contained microchannels that were occluded with aggregated BOECs. C, D. Unseeded microchannels perfused from day 5 - day 10 did not retain their microchannels. The indentations suggest their wires were too close to the outer edge of the tissue. E,F. Unseeded microchannels were perfused from day 7-10, but again the microchannels did not survive. G, H. Microchannels seeded via direct pipet method on day 0, and perfused day 5-10 during compaction. Samples contained reduced lumen-containing microvessels, but microchannels were maintained throughout compaction and perfusion, and were partially endothelialized, with some sprouts. Some microchannels were filled with aggregated BOECs (G). I,J. Microchannels seeded via direct pipet method on day 0, perfused day 6-10, similar to G,H. Samples demonstrated normal microvessel properties, and microchannels were present, partially endothelialized (I), and contained sprouts. Some were filled with aggregated BOECs (J). Perfused microbeads were not found in any microchannels or microvessel lumens for any samples perfused during or after compaction. Scale bar = 200 µm unless marked otherwise.

# Chapter 5. Conclusions and Future Directions

## 5.1 Major Contributions

This PhD research has impacted the field of microvascular tissue engineering through a published study in *Biomaterials* on "Inosculation and Perfusion of Pre-Vascularized Tissue Patches Containing Aligned Human Microvessels after Myocardial Infarction" (Chapter 2).[47] This work has also contributed to field through the development of a high-throughput assay enabling the simultaneous study of angiogenic sprouting, microvessel formation in 3D matrices, and inosculation of sprouts and microvessels. Finally, this work has developed an in vitro perfusion strategy and bioreactor for perfusion of large engineered microvascular tissues. These contributions highlight the challenges and advances made toward the development of large-scale microvascular engineered tissues containing aligned and perfusable microvessels.

### 5.1.1 Pre-vascularized tissues developed for implantation with a high density of aligned microvessels

Microvascular tissues were developed for implantation with the highest density of engineered human microvessels reported to date, and approximately half the capillary density found in human adult myocardium. Over 75% of the pericytes in the tissues were recruited to the microvessels, and microvessel

lumen diameters were in the range of healthy human capillaries. These microvessels were able to be aligned or they could be left anisotropic, and both tissue types were implanted in a rat myocardial infarct model.

### 5.1.2 Pre-vascularized tissues inosculated and were perfused when implanted over myocardial infarcts

This was the first report of pre-formed human microvessels being implanted and perfused in a myocardial infarct model. Studies involving implantation of cell-containing patches in the cardiac infarct environment are of high interest due to the challenging nature of cell retention and survival in this diseased tissue environment. When these pre-vascularized microvascular tissue patches were implanted over acute myocardial infarcts for 6 days, the transplanted microvessels anastomosed with host vessels and were perfused. The implications for future tissue engineering strategies that could implement such a microvascular network are especially promising, as these microvascular tissues were able to rapidly deliver nutrients to the surrounding tissue. This could enable the implantation of thicker, denser, or more metabolically active engineered tissues for regenerative therapies.

### 5.1.3 Combined angiogenic/vasculogenic assay developed for high throughput testing

A high-throughput assay was developed that enabled the study of angiogenic sprouting, vasculogenic tubule formation, and a combined approach with sprouting and tubulogenesis occurring in the same system. In the angiogenic assay, ECs were seeded on top of fibrin gels to form a monolayer. This monolayer simulated the endothelial lining of a vessel, and angiogenic sprouting could be observed extending into the fibrin gel. The vasculogenic assay contained ECs and PCs entrapped in the fibrin gel, and vasculogenic tubule formation led to the development of a microvascular network. The combined angiogenic/vasculogenic assay contained fibrin gels with entrapped ECs and PCs and a surface monolayer of ECs that were pre-labeled with a cell-tracking stain. This enabled the tracking of angiogenic sprouts into the fibrin gel, where inosculation points could be discovered.

### 5.1.4 Hybrid medium culture enabled inosculation of sprouts and microvessels

Hybrid medium culture (1 day of defined medium, 4 days of BOEC medium) was shown to increases angiogenic sprouting, support microvessel formation, and enable inosculation of sprouts and microvessels in 3D fibrin gels containing VEGF and FGF. Angiogenic assays formed without VEGF and FGF

lacked the extensive and deep sprouting that was observed in assays containing VEGF and FGF. Both defined medium and the hybrid medium culture regimens led to numerous sprouts in angiogenic assays, but defined medium, alone, did not lead to the formation of a robust microvascular network in vasculogenic assays. Both BOEC medium and the hybrid medium culture regimens led to well-developed microvascular networks in vasculogenic assays, but BOEC medium, alone, did not lead to extensive angiogenic sprouting.

### 5.1.5 Bioreactor and culture strategy developed for the in vitro perfusion of microvascular tissues.

A perfusion bioreactor and engineering strategy was developed for the *in vitro* perfusion of microvascular tissues. This bioreactor made use of a previous design that enabled the compaction and alignment of fibrin gels, leading to a dense and aligned network of microvessels. These microvascular tissues were modified to contain offset, parallel microchannels with closed ends that could be seeded with ECs to form endothelialized channels. These microchannels could be perfused sending interstitial flow across the channel wall between the two channels to promote angiogenic sprouting and encourage anastomoses to form with the surrounding microvascular network.

Six samples could be perfused simultaneously in this bioreactor, with the ability to alternate the flow direction as desired. Samples were able to be fully

immersed in culture medium during perfusion rather than typical methods which embed tissues in agarose. This enabled the use of ultra-low perfusion flow rates optimal for angiogenic sprouting, as the delivery of nutrients was primarily through the surrounding culture medium. Perfusion flow could be initiated at any time point starting on day 0 and samples could be perfused before, during, or after gel compaction and alignment.

### 5.1.6 Microchannels in fibrin gels were endothelialized, formed sprouts, and were perfused

Microchannels were endothelialized under a number of conditions including static culture, early perfusion culture, and early seeding + late perfusion culture. Even unseeded microchannels were often endothelialized in static and early perfusion culture. These endothelialized microchannels contained sprouts extending from the channel walls, an encouraging result for the future perfusion of the nearby microvessels. In early perfused samples, microchannels were completely endothelialized, contained sprouts, and perfused microbeads were found inside the microchannels, verifying that these microchannels could be perfused.

### 5.1.7 Early seeding of microchannels promoted microchannel survival during compaction

Unseeded microchannels and late-seeded microchannels were not maintained during compaction, but when microchannels were seeded within the first 24 hours of culture, they formed partially endothelialized microchannels with sprouts in compacted gels. Some of these microchannels, however, were occluded with aggregated BOECs, likely preventing perfusion of the channels. Future efforts should attempt to continue with early seeding, but efforts will need to be made to prevent microchannel occlusion to ensure that any potential anastomoses of sprouts and microvessels will result in microvessel perfusion.

## 5.2 Future Directions

### 5.2.1 Integrate cardiomyocytes with pre-vascularized tissue patches for implantation.

Pre-vascularized tissue patches containing microvessels and pericytes have been successfully implanted and perfused in a myocardial infarct model. The next step would be to integrate these aligned patches with a third cell type, such as cardiomyocytes, to create pre-vascularized heart patches. This work is currently being done by Jeremy Schaefer in the Tranquillo lab.

### 5.2.2 Develop a hierarchical vascular network

This work made some advances toward creating perfusable microvascular tissues, and even made strides toward creating larger-diameter perfusable microchannels that resembled an arteriole and venule with a microvascular network in between. Future work would be enhanced by further development of a more robust hierarchical vascular network containing microvessels, such as those created in this study, connected to larger diameter arteriole and venule-like engineered vessels with similar properties to native arterioles and venules. The addition of robust, larger diameter vessels connected to the microvascular network would allow for direct microsurgical attachment to host vasculature and therefore, immediate perfusion of the entire hierarchical network. This would greatly reduce the time required for anastomosis and perfusion of implanted engineered tissues and could enable the transplantation of larger, highly metabolic tissues that would otherwise not survive implantation without connection to blood flow.

### 5.2.3 Modify perfusion chamber design

While microvascular tissues containing perfusable microchannels were successfully created and aligned, the perfusion chamber design could benefit from some modifications to reduce inconsistencies and potential for leaking. As the perfusion chambers do not make a perfect seal with the bottom piece during

casting, some fibrin gel-forming solution can often leak through the bottom piece. This results in slightly smaller-volume gels and can sometimes even lead to the glass capillary flares protruding above the gel surface. When this occurs, leaks are much more likely to occur between the gel and the flare of the glass capillary tube, and sometimes the wires and resulting microchannels will be so close to the gel surface that the microchannels will collapse, or fluid will channel out of the gel.

Two design changes could reduce these issues greatly. First, the ultem perfusion chamber pieces could be re-machined to fit more snugly and reduce the potential for leaking of the fibrin gel-forming solution. Second, the new glass capillary tubes could be made with smaller flares than the current 2-3 mm size. Smaller flares would increase the thickness of fibrin gel between the flare edge and the gel outer surface, which would reduce the potential for channeling and leaking. Reducing the flare diameter would also narrow the tolerance of the wire placement, leading to more controlled microchannel placement and reducing the potential for the two wires to come into contact during casting.

### 5.2.4 Optimize microchannel seeding method

Future studies could optimize the microchannel seeding method to improve the endothelialization of the microchannels and reduce aggregation of BOECs that were found occluding the channels, and ensure microchannel

survival during gel compaction. Evidence from Chapter 4 suggests that early seeding of the microchannels (within the first 24 hours) is important for ensuring endothelialization and microchannel survival during gel compaction.

The “direct pipet” seeding method outlined in Chapter 4 delivered the same number of cells as the “perfusion seeding” method, but without requiring the perfusion of such a large volume of culture medium. Reducing the volume of fluid perfused at a high flow rate could prevent distortion of the microchannels, so this “direct pipet” method is preferred. However, alternative methods that could deliver cells even more efficiently may offer advantages.

One alternative method that was not yet tested was seeding a lower volume of cell suspension (5 µl or 75% less volume) using an insulin syringe + needle to inject cells directly into the microchannel inlet by inserting the needle in and through the glass capillary tube. Gels could then be very gently and briefly perfused to push the cell suspension down the microchannel. This seeding method would best be tested in cell-free fibrin gels with seeding on day 0 and analysis of endothelial coverage on day 1.

Pre-labeling of microchannel-seeded BOECs with Qtracker 705, as was done in Chapter 2, would be useful for differentiating between the BOECs seeded in the microchannels and those entrapped in the fibrin gel. It would also help identify sprouts that originated from the microchannels. Finally, it would

enable relatively quick and thorough analysis of the endothelialization of microchannels by fluorescence imaging of uncompacted whole-tissue without requiring freezing and immunohistochemical staining.

### 5.2.5 Continue testing of perfusion regimens to achieve sprout and microvessel perfusion

Future testing of the *in vitro* perfusion system should compare BOEC-medium cultured samples (as in Chapter 4) with samples cultured with the hybrid medium regimen, which was shown to increase sprouting and encourage anastomosis of sprouts and microvessels (Chapter 3).

A variety of conditions were already tested and eliminated from testing for achieving sprout and microvessel perfusion. Late seeding (after compaction had begun) followed by perfusion was not successful in retaining microchannels, which is a critical factor for achieving perfusion of the microvascular network. Early seeding + perfusion regimens enabled consistent endothelialization as well as the perfusion of endothelialized microchannels. In these experiments, the microchannels were distorted with widely varying diameters and shapes. It is unknown whether this microchannel distortion was a result of perfusion or simply the rather aggressive seeding method used in those studies.

With the newly developed microchannel seeding methods and the early perfusion regimen, it is likely that these microchannels will show more consistent

diameters and shapes, as the flow rate used in these perfusion studies is extremely low. Beginning perfusion on day 0 (50 minutes after seeding) or day 1 (24 hours after seeding) should both be evaluated. Fluorescent microbead perfusion should be applied on day 5 (once the microvascular network has developed, prior to compaction) and day 6 (1 day after compaction has begun) to investigate when perfusion of the microvessels occurs and whether compaction helps or hinders microvessel perfusability. Additionally, fluorescent microbead perfusion should be applied to more mature samples (day 8 - 14) that have received several days of perfusion after compaction to determine whether continued perfusion culture eventually leads to anastomoses between the sprouts and microvessels and perfusion of the network.

If early perfusion proves unsuccessful, late-perfusion (with microchannels still seeded within the first 24 hours of culture) could be tested, with perfusion being initiated at any time, depending on the circumstances. If perfusion is disrupting the development of the microvascular network, then waiting until day 5 when the microvascular network is fully developed could prevent issues with tubulogenesis. If a more robust tissue is required before perfusion can be initiated (due to leaking or channeling through the fibrin gel, as examples), then waiting 1-3 days after gel compaction could prove more successful.

If perfusion of sprouts and microvessels can be shown, but perfusion of the outlet microchannel is not occurring, then the flow could be reversed by connecting the outlet glass capillary tube to the perfusion lines. This could induce sprouting from the opposite microchannel, encouraging anastomosis with the existing network. Reversal of the flow could be done a number of times, alternating the inlet and outlet microchannels to encourage even sprouting from each, if necessary.

### 5.2.6 Perfusion during compaction to prevent lumen collapse and create physiological lumen densities

The methods described in this dissertation have created dense and aligned microvascular tissues with the highest lumen densities reported to date. However, previous studies with these tissues have shown that many lumens present prior to compaction, are not maintained after compaction, suggesting many of the lumens collapse under the cell traction forces.[30] If these lumens could be prevented from collapsing, it would yield an even higher lumen density than the current 940 lumens/mm$^2$, currently achieved (Chapter 2).

Flow through microvessel lumens may provide enough support to prevent the lumens from collapsing under the traction forces of gel compaction. If the microvessels could be perfused using the methods outlined in this dissertation and their lumens could be prevented from collapsing during gel compaction, this

would dramatically increase the lumen density in these microvascular tissues to near-physiological levels for adult human myocardium.

The *in vitro* perfusion of such a native-like tissue would be a major breakthrough for the field of tissue engineering, and would motivate a wave of future research incorporating these microvascular tissues into the development of other dense, highly metabolic tissues such as engineered liver or heart patches for the treatment of myocardial infarction.

# References


1. Auger FA, Gibot L, Lacroix D. The Pivotal Role of Vascularization in Tissue Engineering. *Annu Rev Biomed Eng*. 2013;**15**:177–200.
2. Phelps E a, García AJ. Engineering more than a cell: vascularization strategies in tissue engineering. *Curr Opin Biotechnol*. 2010;**21**:704–709.
3. Laschke MW, Menger MD. Vascularization in Tissue Engineering: Angiogenesis versus Inosculation. *Eur Surg Res*. 2012;**48**:85–92.
4. Montgomery M, Zhang B, Radisic M. Cardiac Tissue Vascularization: From Angiogenesis to Microfluidic Blood Vessels. *J Cardiovasc Pharmacol Ther*. 2014;**19**:382–393.
5. Moya ML, Hsu Y-H, Lee A, Hughes CCW, George S. In vitro perfused human capillary networks. *Tissue Eng Part C Methods*. 2013;**9**:730–737.
6. Rakusan K, Flanagan MF, Geva T, Southern J, Praagh R Van. Morphometry of human coronary capillaries during normal growth and the effect of age in left ventricular pressure-overload hypertrophy. *Circulation*. 1992;**86**:38–46.
7. Iaizzo PA. Handbook of Cardiac Anatomy, Physiology, and Devices. 2nd ed. Iaizzo PA, editor. Springer; 2009.
8. Davis GE, Stratman AN, Sacharidou A, Koh W. Molecular basis for endothelial lumen formation and tubulogenesis during vasculogenesis and angiogenic sprouting. 1st ed. Int. Rev. Cell Mol. Biol. Elsevier Inc.; 2011.
9. Hanjaya-Putra D, Bose V, Shen Y-I, Yee J, Khetan S, Fox-Talbot K, Steenbergen C, Burdick J a, Gerecht S. Controlled activation of morphogenesis to generate a functional human microvasculature in a synthetic matrix. *Blood*. 2011;**118**:804–815.
10. Nguyen EH, Zanotelli MR, Schwartz MP, Murphy WL. Differential effects of cell adhesion, modulus and VEGFR-2 inhibition on capillary network formation in synthetic hydrogel arrays. *Biomaterials*. 2014;**35**:2149–2161.
11. Caviglia S, Luschnig S. Tube fusion: making connections in branched tubular networks. *Semin Cell Dev Biol*. 2014;**31**:82–90.
12. Davis GE, Kim DJ, Meng C, Norden PR, Speichinger KR, Davis MT, Smith AO, Bowers SLK, Stratman AN. Control of Vascular Tube Morphogenesis and Maturation in 3D Extracellular Matrices by Endothelial Cells and Pericytes. In: Baudino TA, editor. *Cell-Cell Interact Methods Protoc*.

Totowa, NJ: Humana Press; 2013. p. 17–28.

13. Rao RR, Peterson AW, Ceccarelli J, Putnam AJ, Stegemann JP. Matrix composition regulates three-dimensional network formation by endothelial cells and mesenchymal stem cells in collagen / fibrin materials. *Angiogenesis*. 2012;**15**:253–264.

14. Montaño I, Schiestl C, Schneider J, Pontiggia L, Luginbühl J, Biedermann T, Böttcher-Haberzeth S, Braziulis E, Meuli M, Reichmann E. Formation of human capillaries in vitro: the engineering of prevascularized matrices. *Tissue Eng Part A*. 2010;**16**:269–282.

15. Davis GE, Camarillo CW. An alpha 2 beta 1 integrin-dependent pinocytic mechanism involving intracellular vacuole formation and coalescence regulates capillary lumen and tube formation in three-dimensional collagen matrix. *Exp Cell Res*. 1996;**224**:39–51.

16. Stratman AN, Davis MJ, Davis GE. VEGF and FGF prime vascular tube morphogenesis and sprouting directed by hematopoietic stem cell cytokines. *Blood*. 2011;**117**:3709–3719.

17. Morin KT, Tranquillo RT. In vitro models of angiogenesis and vasculogenesis in fibrin gel. *Exp Cell Res*. 2013;**319**:2409–2417.

18. Chan JM, Zervantonakis IK, Rimchala T, Polacheck WJ, Whisler J, Kamm RD. Engineering of In Vitro 3D Capillary Beds by Self- Directed Angiogenic Sprouting. *PLoS One*. 2012;**7**:1–11.

19. Chrobak KM, Potter DR, Tien J. Formation of perfused, functional microvascular tubes in vitro. *Microvasc Res*. 2006;**71**:185–196.

20. Miller JS, Stevens KR, Yang MT, Baker BM, Nguyen D-HT, Cohen DM, Toro E, Chen A a, Galie P a, Yu X, Chaturvedi R, Bhatia SN, Chen CS. Rapid casting of patterned vascular networks for perfusable engineered three-dimensional tissues. *Nat Mater*. Nature Publishing Group; 2012;**11**:768–774.

21. Mishra R, Roux BM, Posukonis M, Bodamer E, Brey EM, Fisher JP, Dean D. Effect of prevascularization on in vivo vascularization of poly(propylene fumarate)/fibrin scaffolds. *Biomaterials*. 2015;**77**:255–266.

22. Takebe T, Koike N, Sekine K, Fujiwara R, Amiya T, Zheng Y-W, Taniguchi H. Engineering of human hepatic tissue with functional vascular networks. *Organogenesis*. 2014;**10**:1–8.

23. Whisler JA, Chen MB, Kamm RD. Control of Perfusable Microvascular Network Morphology Using a Multiculture Microfluidic System. *Tissue Eng*

*Part C Methods*. 2014;**7**:543–552.

24. Aird AL, Nevitt CD, Christian K, Williams SK, Hoying B, Leblanc AJ, Hospital J, Hospital J, Hospital J. Adipose - derived stromal vascular fraction cells isolated from old animals exhibit reduced capacity to support the formation of microvascular networks. *Exp Gerontol*. 2015;**63**:18–26.
25. Lin Y, Weisdorf DJ, Solovey A, Hebbel RP. Origins of circulating endothelial cells and endothelial outgrowth from blood. *J Clin Invest*. 2000;**105**:71–77.
26. Belair DG, Whisler J a, Valdez J, Velazquez J, James A, Vickerman V, Lewis R, Daigh C, Hansen TD, Mann A, Thomson J a, Griffith LG, Kamm RD, Michael P. Human vascular tissue models formed from humann induced pluripotent stem cell derived endothelial cells. *Stem Cell Rev*. 2015;**11**:511–525.
27. Allt G, Lawrenson JG. Pericytes: cell biology and pathology. *Cells Tissues Organs*. 2001;**169**:1–11.
28. Tell D von, Armulik A, Betsholtz C. Pericytes and vascular stability. *Exp Cell Res*. 2006;**312**:623–629.
29. Chang WG, Andrejecsk JW, Kluger MS, Saltzman WM, Pober JS. Pericytes modulate endothelial sprouting. *Cardiovasc Res*. 2013;**100**:492–500.
30. Morin K. The Development and Alignment of Engineered Microvasculature in Fibrin Gel. University of Minnesota; 2012.
31. Stratman AN, Malotte KM, Mahan RD, Davis MJ, Davis GE. Pericyte recruitment during vasculogenic tube assembly stimulates endothelial basement membrane matrix formation. *Blood*. 2009;**114**:5091–5101.
32. Stratman AN, Schwindt AE, Malotte KM, Davis GE. Endothelial-derived PDGF-BB and HB-EGF coordinately regulate pericyte recruitment during vasculogenic tube assembly and stabilization. *Blood*. 2010;**116**:4720–4730.
33. Vapniarsky N, Arzi B, Hu JC, Nolta JA, Athanasiou KA. Concise Review: Human Dermis as an Autologous Source of Stem Cells for Tissue Engineering and Regenerative Medicine. *Stem Cells Transl Med*. 2015;**4**:1187–1198.
34. Grainger SJ, Putnam AJ. Assessing the permeability of engineered capillary networks in a 3D culture. *PLoS One*. 2011;**6**:e22086.
35. Rane A a, Christman KL. Biomaterials for the treatment of myocardial

infarction a 5-year update. *J Am Coll Cardiol*. Elsevier Inc.; 2011;**58**:2615–2629.

36. Holnthoner W, Hohenegger K, Husa A, Muehleder S, Meinl A, Peterbauer-scherb A, Redl H. Adipose-derived stem cells induce vascular tube formation of outgrowth endothelial cells in a fi brin matrix. *J Tissue Eng Regen Med*. 2012;**9**:127–136.

37. Nakatsu MN, Sainson RC a., Aoto JN, Taylor KL, Aitkenhead M, Pérez-del-Pulgar S, Carpenter PM, Hughes CCW. Angiogenic sprouting and capillary lumen formation modeled by human umbilical vein endothelial cells (HUVEC) in fibrin gels: the role of fibroblasts and Angiopoietin-1. *Microvasc Res*. 2003;**66**:102–112.

38. Chen XF, Aledia a S, Popson S a, Him L, Hughes CCW, George SC. Rapid Anastomosis of Endothelial Progenitor Cell-Derived Vessels with Host Vasculature Is Promoted by a High Density of Cotransplanted Fibroblasts. *Tissue Eng Part A*. 2010;**16**:585–594.

39. Koh W, Stratman AN, Sacharidou A, Davis GE. In vitro three dimensional collagen matrix models of endothelial lumen formation during vasculogenesis and angiogenesis. *Methods Enzymol*. 2008;**443**:83–101.

40. White S, Pittman C, Hingorani R. Implanted Cell-Dense Prevascularized Tissues Develop Functional Vasculature that Supports Reoxygenation Following Thrombosis. *Tissue …*. 2014;**00**:1–13.

41. Wendel JS, Ye L, Tao R, Zhang J, Zhang J, Kamp TJ, Tranquillo RT. Functional Effects of a Tissue-Engineered Cardiac Patch From Human Induced Pluripotent Stem Cell-Derived Cardiomyocytes in a Rat Infarct Model. *Stem Cells Transl Med*. 2015;**11**:1324–1332.

42. Tranquillo RT. Self-organization of tissue-equivalents: the nature and role of contact guidance. *Biochem Soc Symp*. ENGLAND; 1999;**65**:27–42.

43. Morin KT, Dries-Devlin JL, Tranquillo RT. Engineered Microvessels with Strong Alignment and High Lumen Density Via Cell-Induced Fibrin Gel Compaction and Interstitial Flow. *Tissue Eng Part A*. 2013;**20**:553–565.

44. Bjork JW, Tranquillo RT. Transmural flow bioreactor for vascular tissue engineering. *Biotechnol Bioeng*. 2009;**104**:1197–1206.

45. Syedain ZH, Weinberg JS, Tranquillo RT. Cyclic distension of fibrin-based tissue constructs: evidence of adaptation during growth of engineered connective tissue. *Proc Natl Acad Sci U S A*. 2008;**105**:6537–6542.

46. Wendel JS, Ye L, Zhang P, Tranquillo RT, Zhang JJ. Functional

Consequences of a Tissue-Engineered Myocardial Patch for Cardiac Repair in a Rat Infarct Model. *Tissue Eng Part A*. 2014;**20**:1325–1335.

47. Riemenschneider SB, Mattia DJ, Wendel JS, Schaefer JA, Ye L, Guzman PA, Tranquillo RT. Inosculation and perfusion of pre-vascularized tissue patches containing aligned human microvessels after myocardial infarction. *Biomaterials*. Elsevier Ltd; 2016;**97**:51–61.

48. Wong C, Inman E, Spaethe R, Helgerson S. Fibrin-based biomaterials to deliver human growth factors. *Thromb Haemost*. Germany; 2003;**89**:573–582.

49. Leung AD, Wong KHK, Tien J. Plasma expanders stabilize human microvessels in microfluidic scaffolds. *J Biomed Mater Res A*. 2012;**100**:1815–1822.

50. Zheng Y, Chen J, Craven M, Choi NW, Totorica S, Diaz-Santana A, Kermani P, Hempstead B, Fischbach-Teschl C, López J a, Stroock AD. In vitro microvessels for the study of angiogenesis and thrombosis. *Proc Natl Acad Sci U S A*. 2012;**109**:9342–9347.

51. Hernández Vera R, Genové E, Alvarez L, Borrós S, Kamm R, Lauffenburger D, Semino CE. Interstitial fluid flow intensity modulates endothelial sprouting in restricted Src-activated cell clusters during capillary morphogenesis. *Tissue Eng Part A*. 2009;**15**:175–185.

52. Semino C, Kamm R, Lauffenburger D. Autocrine EGF receptor activation mediates endothelial cell migration and vascular morphogenesis induced by VEGF under interstitial flow. *Exp Cell Res*. 2005;**312**:289–298.

53. Shin Y, Jeon JS, Han S, Jung G-S, Shin S, Lee S-H, Sudo R, Kamm RD, Chung S. In vitro 3D collective sprouting angiogenesis under orchestrated ANG-1 and VEGF gradients. *Lab Chip*. 2011;**11**:2175–2181.

54. Hudon V, Berthod F, Black AF, Damour O, Germain L, Auger FA. Cutaneous Biology A tissue-engineered endothelialized dermis to study the modulation of angiogenic and angiostatic molecules on capillary-like tube formation in vitro. *Br J Dermatol*. 2003;**148**:1094–1104.

55. Nakatsu MN, Hughes CCW. An optimized three-dimensional in vitro model for the analysis of angiogenesis. *Methods Enzymol*. 2008;**443**:65–82.

56. Song JW, Munn LL. Fluid forces control endothelial sprouting. *Proc Natl Acad Sci U S A*. 2011;**108**:15342–15347.

57. Helm CE, Fleury ME, Zisch AH, Boschetti F, Swartz MA. Synergy between interstitial flow and VEGF directs capillary morphogenesis in vitro through a

gradient amplification mechanism. *PNAS*. 2005;**102**:15779–15784.

58. Ng CP, Helm C-LE, Swartz M a. Interstitial flow differentially stimulates blood and lymphatic endothelial cell morphogenesis in vitro. *Microvasc Res*. 2004;**68**:258–264.

59. Hsu Y-H, Moya ML, Abiri P, Hughes CCW, George SC, Lee AP. Full range physiological mass transport control in 3D tissue cultures. *Lab Chip*. 2013;**13**:81–89.

60. Helm CE, Zisch A, Swartz MA. Engineered Blood and Lymphatic Capillaries in 3-D VEGF-Fibrin-Collagen Matrices With Interstitial Flow. *Biotechnol Bioeng*. 2007;**96**:167–176.

61. Chen X, Aledia AS, Ghajar CM, Griffith CK, Putnam AJ, Hughes CCW, George SC. Prevascularization of a fibrin-based tissue construct accelerates the formation of functional anastomosis with host vasculature. *Tissue Eng Part A*. 2009;**15**:1363–1371.

62. Sekine H, Shimizu T, Hobo K, Sekiya S, Yang J, Yamato M, Kurosawa H, Kobayashi E, Okano T. Endothelial cell coculture within tissue-engineered cardiomyocyte sheets enhances neovascularization and improves cardiac function of ischemic hearts. *Circulation*. 2008;**118**:S145–S152.

63. Sakaguchi K, Shimizu T, Horaguchi S, Sekine H, Yamato M, Umezu M, Okano T. In Vitro Engineering of Vascularized Tissue Surrogates. *Sci Reports - Nat*. 2013;**3**:1–7.

64. Moya ML, Alonzo LF, George SC. Microfluidic Device to Culture 3D In Vitro Human Capillary Networks. *Methods Mol Biol*. 2014;**1202**:21–27.

65. Lee E, Song HHG, Chen CS. Biomimetic on-a-chip platforms for studying cancer metastasis. *Curr Opin Chem Eng*. 2016;**11**:20–27.

66. Wang X, Phan DTT, Sobrino A, George SC, Hughes CCW, Lee AP. Engineering anastomosis between living capillary networks and endothelial cell-lined microfluidic channels. *Lab Chip*. Royal Society of Chemistry; 2016;**16**:282–290.

67. Kim J, Chung M, Kim S, Jo DH, Kim JH, Jeon NL. Engineering of a biomimetic pericyte-covered 3D microvascular network. *PLoS One*. 2015;**10**:1–15.

68. Jeon JS, Bersini S, Whisler JA, Chen MB, Dubini G, Charest JL, Moretti M, Kamm RD. Generation of 3D functional microvascular networks with mural cell-differentiated human mesenchymal stem cells in microfluidic vasculogenesis systems. *Integr Biol*. 2014;**6**:555–563.

69. Moya M, Tran D, George SC. An integrated in vitro model of perfused tumor and cardiac tissue. *Stem Cell Res Ther*. 2013;**4 Suppl 1**:S15.

70. Venugopal JR, Prabhakaran MP, Mukherjee S, Ravichandran R, Dan K, Ramakrishna S. Biomaterial strategies for alleviation of myocardial infarction. *J R Soc Interface*. 2012;**9**:1–19.

71. Coulombe KLK, Bajpai VK, Andreadis ST, Murry CE. Heart regeneration with engineered myocardial tissue. *Annu Rev Biomed Eng*. United States; 2014;**16**:1–28.

72. Muscari C, Giordano E, Bonafè F, Govoni M, Guarnieri C. Strategies Affording Prevascularized Cell-Based Constructs for Myocardial Tissue Engineering. *Stem Cells Int*. 2014;**2014**:1–8.

73. Grainger SJ, Carrion B, Ceccarelli J, Putnam AJ. Stromal Cell Identity Influences the In Vivo Functionality of Engineered Capillary Networks Formed by Co-delivery of Endothelial Cells and Stromal Cells. *Tissue Eng Part A*. 2013;**19**:1209–1222.

74. Morin KT, Smith AO, Davis GE, Tranquillo RT. Aligned Human Microvessels Formed in 3D Fibrin Gel by Constraint of Gel Contraction. *Microvasc Res*. 2013;**90**:12–22.

75. Sakaguchi K, Shimizu T, Okano T. Construction of three-dimensional vascularized cardiac tissue with cell sheet engineering. *J Control Release*. Elsevier B.V.; 2015;**205**:83–88.

76. Rao RR, Vigen ML, Peterson AW, Caldwell DJ, Putnam AJ, Stegemann JP. Dual-Phase Osteogenic and Vasculogenic Engineered Tissue for Bone Formation. *Tissue Eng Part A*. 2015;**21**:530–540.

77. Riegler J, Tiburcy M, Ebert A, Tzatzalos E, Raaz U, Abilez OJ, Shen Q, Kooreman NG, Neofytou E, Chen VC, Wang M, Meyer T, Tsao PS, Connolly AJ, Couture L a, Gold JD, Zimmermann WH, Wu JC. Human Engineered Heart Muscles Engraft and Survive Long Term in a Rodent Myocardial Infarction Model. *Circ Res*. 2015;**117**:720–730.

78. Rakusan K. Quantitative morphology of capillaries of the heart. Number of capillaries in animal and human hearts under normal and pathological conditions. *Methods Achiev Exp Pathol*. SWITZERLAND; 1971;**5**:272–286.

79. Kajiya F, Goto M. Integrative Physiology of Coronary Microcirculation. *Jpn J Physiol*. 1999;**49**:229–241.

80. Chang CC, Nunes SS, Sibole SC, Krishnan L, Williams SK, Weiss JA, Hoying JB. Angiogenesis in a Microvascular Construct for Transplantation

Depends on the Method. *Tissue Eng Part A*. 2010;**16**:795–805.

81. Ghanaati S, Fuchs S, Webber MJ, Orth C, Barbeck M, Gomes ME, Reis RL, Kirkpatrick CJ. Rapid vascularization of starch – poly ( caprolactone ) in vivo by outgrowth endothelial cells in co-culture with primary osteoblasts. *J Tissue Eng Regen Med*. 2011;**5**:e136–e143.

82. Shepherd BR, Hoying JB, Williams SK. Microvascular transplantation after acute myocardial infarction. *Tissue Eng*. 2007;**13**:2871–2879.

83. Chaturvedi RR, Stevens KR, Solorzano RD, Schwartz RE, Eyckmans J, Baranski JD, Stapleton SC, Bhatia SN, Chen CS. Patterning Vascular Networks In Vivo for Tissue Engineering Applications. *Tissue Eng Part C Methods*. 2015;**21**:509–517.

84. Gavin TP, Stallings HW, Zwetsloot KA, Westerkamp LM, Ryan NA, Moore RA, Pofahl WE, Hickner RC. Lower capillary density but no difference in VEGF expression in obese vs. lean young skeletal muscle in humans. *J Appl Physiol*. 2004;**98**:315–321.

85. Ferrara N, Gerber H, Lecouter J. The biology of VEGF and its receptors. *Nat Med*. 2003;**9**:669–676.

86. Cross MJ, Claesson-welsh L, Cross MJ, Claesson-welsh L. FGF and VEGF function in angiogenesis : signalling pathways , biological responses and therapeutic inhibition. *Trends Pharmacol Sci*. 2001;**22**:201–207.

87. Smith AO, Bowers SLK, Stratman AN, Davis GE. Hematopoietic Stem Cell Cytokines and Fibroblast Growth factor-2 Stimulate Human Endothelial Cell-Pericyte Tube Co-Assembly in 3D Fibrin Matrices under Serum-Free Defined Conditions. *PLoS One*. 2013;**8**:e85147.

88. Wilkins JR, Pike DB, Gibson CC, Kubota A, Shiu Y-T. Differential effects of cyclic stretch on bFGF- and VEGF-induced sprouting angiogenesis. *Biotechnol Prog*. 2014;1–10.

89. Radisic M, Christman KL. Materials science and tissue engineering: repairing the heart. *Mayo Clin Proc*. 2013;**88**:884–898.

90. Syedain ZH, Meier LA, Bjork JW, Lee A, Tranquillo RT. Implantable arterial grafts from human fibroblasts and fibrin using a multi-graft pulsed flow-stretch bioreactor with noninvasive strength monitoring. *Biomaterials*. 2011;**32**:714–722.

91. Schüller-Ravoo S, Zant E, Feijen J, Grijpma DW. Preparation of a Designed Poly(trimethylene carbonate) Microvascular Network by Stereolithography. *Adv Healthc Mater*. 2014;**3**:2004–2011.

92. Chaturvedi RR, Stevens KR, Solorzano RD, Schwartz RE, Eyckmans J, Baranski JD, Stapleton SC, Bhatia SN, Chen CS. Patterning Vascular Networks In Vivo for Tissue Engineering Applications. *Tissue Eng Part C Methods*. 2015;**21**:509–517.

93. Mironov V, Kasyanov V, Drake C, Markwald RR. Organ printing: promises and challenges Vladimir Mironov, Vladimir Kasyanov, Christopher Drake and Roger R Markwald. *Regen Med*. 2008;**3**:93+.

94. Jain RK. Transport of molecules, particles, and cells in solid tumors. *Annu Rev Biomed Eng*. 1999;**1**:241–263.

95. Galie P a, Nguyen D-HT, Choi CK, Cohen DM, Janmey P a, Chen CS. Fluid shear stress threshold regulates angiogenic sprouting. *Proc Natl Acad Sci U S A*. 2014;**111**:7968–7973.